

**I. INFECTION CONTROL: EXPLORATION OF SILICEOUS ZEOLITE MFI FILMS
AS COATINGS FOR IMPLANTABLE DEVICES**

**II. ALTERNATIVE APPROACHES FOR POST-OPERATIVE INFECTION CONTROL
USING PRE- AND PRO- BIOTICS: A META-ANALYSIS**

Thesis by

Keisha Latrice Avery

In Partial Fulfillment of the Requirements for the

Degree of

Doctor of Philosophy

UNIVERSITY OF MISSOURI

Columbia, Missouri

April 2022

© 2022

Keisha Latrice Avery

All Rights Reserve

The undersign, appointed by the dean of the Graduate School, have examined the dissertation
entitled

**I. INFECTION CONTROL: EXPLORATION OF SILICEOUS ZEOLITE MFI FILMS
AS COATINGS FOR IMPLANTABLE DEVICES**

**II. ALTERNATIVE APPROACHES FOR POST-OPERATIVE INFECTION CONTROL
USING PRE- AND PRO- BIOTICS: A META-ANALYSIS**

Presented by Keisha Latrice Avery, A candidate for the degree of
Doctor of Philosophy in Bioengineering

And hereby certify that, in their opinion, it is worthy of acceptance.

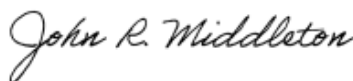
Associate Professor Heather K. Hunt (Chairperson of the Committee)



Professor Sheila Grant



Professor John Middleton



Assistant Professor Kiruba Krishnaswamy


...

ACKNOWLEDGMENTS

First, I would like to express my sincere gratitude to the National GEM Consortium, the Gus T. Ridgels fellowships, the College of Engineering Inclusion, Diversity, and Equity Center (Dr. Tojan Rahhal, Victor Bradford, and Nick Balsler), Dr. Elisa Glick from the Institute of Inclusive Teaching, and the Campus Writing Program (Dr. Amy Lannin, Dr. Christy Goldsmith, Dr. Julie Birt, and Jacqueline Thomas) for providing career and professional advice as well as financial support without which this research would not have been possible.

I would like to express my special appreciation and thanks to my advisor Dr. Heather K. Hunt, you have been a tremendous mentor me and for your patience, guidance, and support. I would like to thank you for encouraging my research and for allowing me to grow as a research scientist. Your advice on my research, my career and life have been invaluable. I have benefited greatly from your wealth of knowledge and meticulous editing. I am extremely grateful that you took me on as a student nine years ago as an undergraduate and continued to have faith in me over the years. Your insightful feedback pushed me to sharpen my thinking and brought my work to a higher level.

Thank you to my committee members, Dr. Sheila Grant, Dr. John Middleton, and Dr. Kiruba Krishnaswamy. Your encouraging words and thoughtful, detailed feedback have been very important to me. I knew you would be the one to help me sort out my thinking on my topic. Your suggestions brought in threads of thought that made my research so much richer, and my dissertation something I can be proud of having written. You've also inspired me with your own body of research and the gift of helping me visualize a similar trajectory for myself.

I would like to acknowledge my colleagues from my internship at Los Alamos National Laboratory for their wonderful collaboration. I would particularly like to single out my supervisors and mentors, John Dunbar, and Michaeline Albright. Having the opportunity to learn from you has made a substantial change in my career. I can confidently say I wouldn't have grown as much as I have over the past three years without your detailed feedback and unwavering support.

Several organizations support my efforts throughout my graduate career, I would like to thank the mentorship and the relationships I gained with my peers, in programs of the First – Year Fellowship, Graduation Scholars of Excellence, Graduate Professional council, the National Society of Black Engineers, the Society of Women Engineers, and Mystical 7. These organizations and relationships helped me find my place at the University of Missouri. All the kind words and assistance help provide me guidance on navigated the resources available on campus to help me succeed.

It is important to strike a balance with life outside the dark depths of the lab. As such I cannot stress enough about the importance of my supportive friends. Thank you, Janae Bradley, Cydini Robertson, Zenia Norman, Rose Hamilton, and Ashanti Bryant who have been my rock and there for every mental breakdown. You help me see my potential and held me accountable through my success.

Most importantly, I am grateful for my family's unconditional, unequivocal, and loving support. Thank you to my mom, Karen Avery, for your endless support. You have always stood behind me, and this was no exception. Mom, thank you for fielding a ridiculous number of phone calls, for calming me down, for listening to me talk out my research (even though you had no clue what I was talking about at times), for you all your love, and for always reminding me of the end goal. Thank you to my brother and sister-in-law, who provided stimulating discussions as well as happy distractions to rest my mind outside of my research.

Thank you to my partner, Lawrence Neely, for constantly listening to me rant and talk things out, for proofreading over and over (even after long days at work and during difficult times), for cracking jokes when things became too serious, and for the sacrifices you made for me to pursue my doctorate, while helping to care for our beautiful daughter.

Lastly, for my family, your love and understanding helped me through dark times. Without you believing in me, I never would have made it. This dissertation stands as a testament to your unconditional love and encouragement. It is time to celebrate; you earned this degree right along with me.

ABSTRACT

The prevention and control of infections associated with indwelling medical implants has remained a top goal for biomedical researchers and clinicians in associated fields. Multiple routes have been explored for this purpose, including drug-based approaches, materials-based approaches, non-drug biological approaches, etc. Although drug-based approaches have long been the mainstay of clinical applications, alternative approaches that use the materials of the implanted devices themselves, or that use non-drug based biologicals, such as pre- and probiotics, offer interesting and potentially useful alternatives, particularly with the rise of antibiotic-resistant bacteria, as well as our increasing understanding of the potential negative, long-term consequences that arise with the use of drugs that fight infections.

For instance, materials that can be used as antimicrobial agents have been investigated as coatings for indwelling devices, which could allow for post-operative local infection control without the need for further interventions. Because of their unique interactions with biomolecules and biological surroundings, nanostructured, porous materials, like zeolites, have been suggested as suitable materials for such applications, as well as many others in tissue engineering, and drug delivery systems. The focus of Part (a) of this dissertation is explore a unique material system, pure-silica zeolite **MFI**, which has only recently begun to be explored for its potential utility in this area due to its unique, three-dimensional pore architecture, high surface area, high thermal and chemical stability, and other unique physicochemical properties that could make it particularly useful in terms of biocompatibility. Here, we synthesize and

characterize these pure-silica zeolite **MFI** in film form through X-ray diffraction, electron microscopy, and common biocompatibility analyses (Enzyme-linked Immunosorbent Assay (ELISA), Bicinchoninic Acid Assay (BCA), and WST – 1 Cell Proliferation Assay) to explore their potential utility as coatings for implantable devices, particularly towards infection control. The synthetic films successfully demonstrated an ability to be biocompatible and to be a candidate for further studies on biofilm reduction.

Part (b) of this dissertation focuses on the characteristics of the target habitat, properties of the probiotic species, and how the probiotic is given are all factors that may impact the effectiveness of probiotic establishment in preexisting microbial communities. However, a significant information gap that impedes microbiome engineering is the relative relevance of variables. We conducted a review and meta-analysis of existing research that looked at the effects of probiotic introductions in human and animal stomachs to fill this information gap. The results of this work showed that, due to the recent improvements in analytical techniques that enable researchers to understand the process of establishment more fully in various biomes, the exploration of pre- and pro-biotics has ample room for more detailed, exhaustive establishment studies. While this remains a gap in the current literature, it points to a clear opportunity for researchers to further explore this non-drug-based approach to infection control.

Table of Contents

ACKNOWLEDGMENTS	iv
ABSTRACT.....	vii
LISTS OF FIGURES.....	xi
LISTS OF TABLES.....	xvii
ABBREVIATIONS.....	xix
Chapter – 1: Introduction and Organization of dissertation Presentation	1
1.1 Introduction	1
1.1.1 Methods of Conventional Infection Control.....	10
1.1.2 Probiotics.....	13
1.1.3 Antimicrobial Coating and Medical Devices	17
1.2 Dissertation Organization.....	18
1.3 References	21
Part I: Infection Control: Exploration of Siliceous Zeolite MFI Films as Coatings for Implantable Devices.....	27
Chapter – 2: Introduction of Silicate – 1 Zeolite Material and Synthesis	28
2.1 Introduction	28
2.2 Introduction of Zeolites and Molecular Sieves	30
2.3 Synthesis Protocol: Silicate-1 (MFI) Films.....	38
2.3.2 Substrate Choice and Modifications.....	40
2.3.3 Characterization Techniques	40
2.3.4 Strategies for Defect Elimination in Films.....	41
Chapter – 3: Lysozyme Sorption of Pure – Silica (MFI) Films	46
3.1 Abstract	46
3.2 Introduction	47
3.3 Materials and Methods	53
3.3.1 Synthesis of Pure – Silica (MFI) Films	53
3.3.2 Characterization.....	53
3.3.3 Enzyme-linked Immunosorbent Assay (ELISA).....	54
3.3.4 Bicinchoninic Acid Assay	55
3.4 Results and Discussion.....	56
3.4.1 Film Characteristics.....	56

3.4.2 Lysozyme Surface Adsorption	60
3.4.3 Total Lysozyme Sorption	64
Chapter – 4: Infection Control: Study of b – oriented pure-silica zeolite MFI films as a biocompatible device coating to reduce surgical site infections after implantation	73
4.1 Abstract	73
4.2 Introduction	74
4.3 Materials and Methods	77
4.3.1 Design of experiment	77
4.3.2 Materials	80
4.3.3 Synthesis of b-oriented, pure-silica zeolite MFI Thin Films	80
4.3.4 Film Characterization	81
4.3.5 Film Characterization	82
4.3.6 Cell Viability (WST-1).....	83
4.4 Results and Discussion	84
4.4.1 Film Characterization	84
4.4.2 Lysozyme Sorption.....	87
4.4.3 Cell Viability	88
4.5 Conclusion.....	90
4.6 References	90
Part II: Alternative Approaches for Post – Operative Infection Control Using Pre- and Pro- Biotics: A Meta – Analysis.....	95
Chapter – 5: Meta-analysis of factors affecting probiotic establishment in pre-existing microbiomes.....	96
5.1 Abstract	96
5.2 Introduction	96
5.3 Methods	99
5.4 Results and Discussion.....	100
5.4.1 What is the current focus of gut probiotics studies?.....	100
5.4.2 Do probiotics impact ecosystem function and community composition of the gut?	108
5.5 Conclusions	115
5.6 References	115
Chapter – 6: Summary and Conclusion.....	119
6.1 Summary and Conclusion	119

LISTS OF FIGURES

Chapter 1

Figure 1-1. Bacteria cluster together in microcolonies because of intercellular contacts mediated by adhesins cell wall proteins.....2

Figure 1-2. Biofilm formation is caused by a collective of one or more types of microorganism that can grow on many different surfaces; 65% - 80% of all microbial and chronic infections are associated with biofilm formation.....3

Figure 1-3. The four common infections caused by implantable medical devices include CAUTIs, CLABSIs, SSIs, and VAPs; each results in high economic burdens and mortalities.....4

Figure 1-4. Between US\$28 – 45 billion are spent annually on HAIs; this results in a tremendous economic burden to both patients and our healthcare systems.....5

Figure 1-5. Beta-lactams type antibiotics include (A) methicillin, (B) oxacillin, (C) penicillin, and (D) amoxicillin; the MRSA, MSSA, VISA, and VRSA strains of *Staphylococcus aureus* are known to have resistances to these drugs.....6

Figure 1-6. The schematic represents the standardize protocols put in place to control the risks of infection that could result in human error and the correlation to one another.....12

Figure 1-7. Harmful bacteria strains that are toxic to the human body and can lead to infectious disease.....14

Figure 1-8. Bacteria strains, of (A) Lactobacillus, (B) Bifidobacterium, (C) Enterococcus, (D) Streptococcus, and (E) Escherichia commonly use probiotic supplements.....15

Figure 1-9. Schematic of the 3 methods of intaking probiotics: ingestion via fermented foods, dairy products, and pills/chewables.....15

Chapter 2

Figure 2-1. Pore like structure of zeolite, ZSM – V. This organized structure is created by an alternating silicon or aluminum (blue) to oxygen (red) bond framework.....28

Figure 2-2. Chemists, technicians, and mineralogists are all fascinated with zeolites. Specific features of zeolites reveal a wide range of uses for this kind of material and demonstrate the usefulness of zeolites in a variety of fields.....30

Figure 2-3. The ZSM-5 (MFI) structure. (A) The pentasil unit. (B) Chains of pentasil units. (C) Layers of these chains. (D) Layers linked.....33

Figure 2-4. The main stages of zeolite synthesis by the hydrothermal method.....36

Figure 2-5. Schematic representation of the steps of the silicate-1 (MFI) synthesis.....40

Chapter 3

Figure 3-1. Representative SEM micrographs of pure – silica **MFI** films; randomly – oriented films are shown on the left column, *b*-oriented films on the right column. Surface views (top and middle rows) show characteristic, coffin-like crystals (5 – 8 μm), providing a secondary indication that **MFI** was successfully synthesized. In addition, it is evident that *b*-oriented films possess less compacted domains while randomly-oriented films do not. Cross-section micrographs show a representative measure of film thickness (randomly oriented: $170 \pm 3 \mu\text{m}$ and *b*-oriented: $100 \pm 5 \mu\text{m}$). It is apparent from these images that the top layer of crystals has macroporosity due to spacing among crystals.....**58**

Figure 3-2. Representative X-ray diffraction patterns of *b*-oriented (top) and randomly-oriented **MFI** films (bottom) show that the synthesis was capable of producing the expected zeolite structure.....**59**

Figure 3-3. Influence of film orientation on lysozyme adsorption onto pure-silica **MFI** films incubated for different times and different volumes of lysozyme solution. Results are presented as the mean normalized absorbance from three independent experiments ($n = 3$) and the error bars represent the propagated experimental error. A * indicates a p-value < 0.05 between the samples indicated.....**61**

Figure 3-4. Influence of incubation time and volume on lysozyme adsorption onto *b*-oriented **MFI** films. The results are presented as the mean absorbance from three independent

experiments ($n = 3$) and the error bars represent the propagated experimental error. A * indicates a p-value < 0.05 between the samples indicated.....64

Figure 3-5. Lysozyme concentration in the supernatant solution following **MFI** incubation. No statistically significant differences were seen in these data, indicating that approximately 35% of the initial protein (400 μg) remains in solution after lysozyme sorption regardless of incubation conditions.....65

Chapter 4

Figure 4-1. Representative X-ray diffraction patterns of *b*-oriented MFI films synthesized under 6 h aging time and 12 h crystallization time (top) and 1 h aging time and 3 h crystallization time (bottom) circumstances show that the syntheses produced the desired zeolite structure.....85

Figure 4-2. Representative SEM micrographs of *b* – oriented **MFI** films, (A) 1h – 3h – Short, (B) 1h – 3h – Long, (C) 6h – 12h – Short, and (D) 6h – 12h – Long. Surface views show characteristic, coffin-like crystals (5 – 8 μm), providing a second indication that **MFI** was successfully synthesized.....86

Figure 4-3. The effects of aging, crystallization, and incubation time on lysozyme adsorption on *b*-oriented, pure-silica **MFI** films. The data are presented as the average of four independent experiments' normalized absorbance.....88

Figure 4-4. The normalized absorbance of 3 and 7 – day WST – 1 assay analyzing cellular viability of L929 fibroblast murine cells with *b*-oriented, pure-silica **MFI** films showed to increase the cell proliferation over time.....**89**

Chapter 5

Figure 5-1. The vast majority of studies reviewed (43.7%) focused on comparing treatments with or without a probiotic, rather than factors that impact probiotic success. For studies that did assess other factors, the type and dose of probiotics were commonly explored, as well as the use of prebiotics.....**101**

Figure 5-2. (a) Among the studies we reviewed, a dose of 10^9 CFU/g was the most frequently administered dosage, closely followed by 10^7 and 10^8 CFU/g, **(b)** with the doses predominantly delivered in liquid form, followed by food form, and then capsule form, **(c)** typically administered over a 14-day period. **(d)** Most studies then performed measurements daily, **(e)** sampling from both feces and the gut.**104**

Figure 5-3a. The types of taxa used at the domain used in the probiotic mixture; bacteria were primarily used, rather than fungi.....**105**

Figure 5-3b. Over 95% of studies included in our analysis included bacteria in the administered probiotics.....**106**

Figure 5-4. Despite a large number of available bacteria genera to be studied, most studies reviewed in our analysis focused on only 1 taxa as the inoculant. This is an interesting gap that could be explored in more detail to enrich the data set available to researchers.....**107**

Figure 5-5a. The functional outcomes of treatments and conditions were evaluated for each study. Disease suppression and pathogen regression were the top functional outcomes observed.

.....110

Figure 5-5b. While most studies focused on the presence/absence of probiotics, almost 85% also evaluated changes in function after the administration of probiotics. Less common was the measurement of the composition, richness, and diversity after administration. Of these factors, it is interesting that probiotic administration yielded changes in composition and function in most of the studies that evaluated these factors.111

Figure 5-5c. Of the studies that we analyzed, 16.5% of studies showed establishment, 14.4% of studies did not show establishment, and 69.1% of studies did not report establishment.....112

Figure 5-6a. The total number of studies vs. the studies that measure establishment and the number of studies; that had quantitative raw data that could be extracted from studies for comparison using statistical analysis.113

Figure 5-6b. The establishment magnitude of the data extracted to perform statistical analysis on the species used in the probiotic ($n=13$114

LISTS OF TABLES

Chapter 1

Table 1-1. Three of the most common factors that put patients in risk of developing a *Staphylococcus aureus* causing infection include their communities, their hospitals, and other healthcare facilities.7

Table 1-2. Medical devices that are colonized by *Staphylococcus aureus* are typically Class II and III medical devices.....9

Table 1-3. Probiotics have been shown to effective in treating the medical conditions listed below.....16

Chapter 2

Table 2-1. Summarizes the various parameters used to synthesize silicate (MFI) zeolite films..39

Table 2-2. Characterization techniques used to characterize and study the properties of silicate-1 (MFI) films.....41

Chapter 3

Table 3-1. Summary of experimental conditions used to synthesize pure-silica **MFI** films on silicon wafer substrates. The substrates were placed either slightly angled or horizontally in the reaction container to encourage the formation of *b*-oriented or randomly – oriented **MFI** films, respectively.....52

Table 3-2. Carbon-to-silicon ratio of pure-silica **MFI** films measured using EDS. After calcination, the presence of carbon was not detected, indicating successful structure-directing agent removal.....**59**

Chapter 4

Table 4-1. The summary is a list of the experimental conditions used to make b-oriented MFI films on silicon wafer substrates. The substrates were slightly tilted in the reaction (the angle varied depending on the size of the substrate) to favor the development of b – oriented MFI films.....**79**

ABBREVIATIONS

Abbreviation	Meaning	Page
HAI	Healthcare associated infections	5
CAUTI	Catheter-associated Urinary Tract Infections	5
CLABS	Central Line-associated Bloodstream Infection	5
SSI	Surgical Site Infection	5
VAP	Ventilator-associated Pneumonia	5
MRSA	Methicillin-resistant <i>staphylococcus aureus</i>	7
MSSA	Methicillin-susceptible <i>staphylococcus aureus</i>	7
VISA	Vancomycin-intermediate <i>Staphylococcus aureus</i>	7
VRSA	Vancomycin-resistant <i>Staphylococcus aureus</i>	7
FDA	Food and Drug Administration	11
MFI	Zeolite Socony Mobil-5	30
IZA	International Zeolite Association	30
CMC	Critical Micelle Concentration	33
CAC	Critical Aggregation Concentration	33
SDA	Structure-directing agent	34
TEOS	Tetrapropylammonium hydroxide	37
TPAOH	Tetraethylorthosilicate	37
DI	Deionized	37
XRD	X-ray Diffraction	39
SEM	Scanning Electron Microscope	39
EDS	Energy Dispersive Spectroscopy	39
ELISA	Enzyme-linked Immunosorbent Assay	44
BCA	Bicinchoninic Acid Assay	44
LYZ	Lysozyme	52
PBS	Phosphate Buffered Saline	52
TCPS	tissue culture polystyrene	52
LTL	Nanozeolite L	60
NIH	National Institutes of Health	67
MOR	Mordenite zeolite	68
FAU	Faujasite Zeolite	68
OPD	O-Phenylenediamine	74
anti-LYZ	Lysozyme antibody	74
WST-1	Cell Proliferation Reagent	75
ROS	Reactive Oxygen Species	113

Chapter – 1: Introduction and Organization of dissertation Presentation

1.1 Introduction

Bacterial adhesion to surfaces has posed a consistent threat in the healthcare industry, resulting in intensive research to understand the process of how bacterial adhesion and bacteria biofilm growth occur, as shown in **Figure 1-1**. [1] Biofilms are collectives of one or more types of microorganisms that can grow on many different surfaces; microorganisms that form biofilms include not just bacteria, but also fungi and protists. [2] The growth of these biofilms can cause an environment surrounding implantable devices in the human body that is resistant to antimicrobial agents and that can cause infection in the surrounding tissue. [3, 4] Infections due to biofilms can be categorized as either *primary* or *secondary* infections, as shown in **Figure 1-2**. [4, 5] *Primary* infections occur in the presence of intravenous catheters, urinary catheters, and implantable devices. *Secondary* infections are infections that travel through the blood stream and can affect the brain, kidneys, joints, and interverbal spaces.

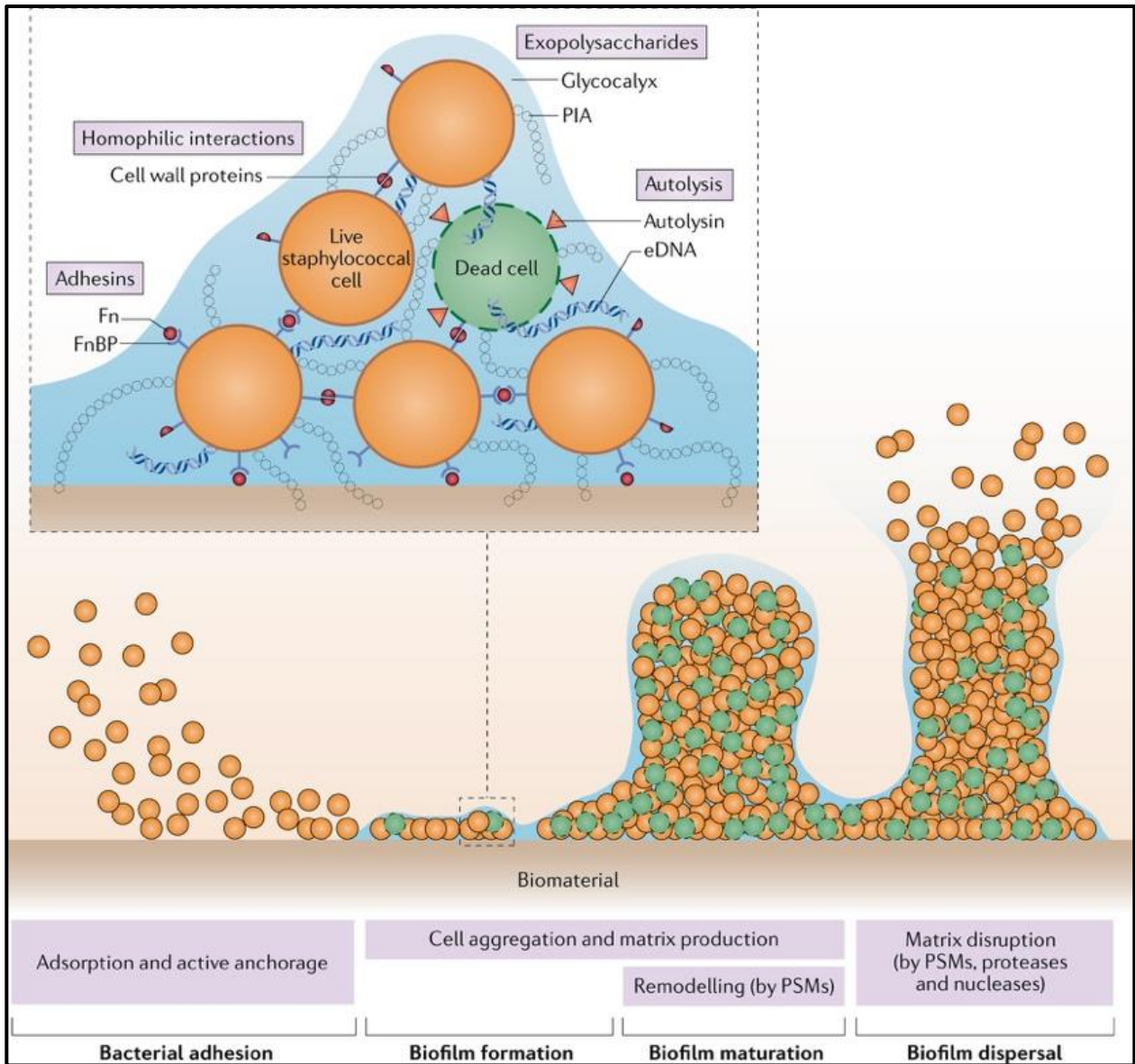


Figure 1-1. Bacteria cluster together in microcolonies because of intercellular contacts mediated by adhesins and cell wall proteins. [6]

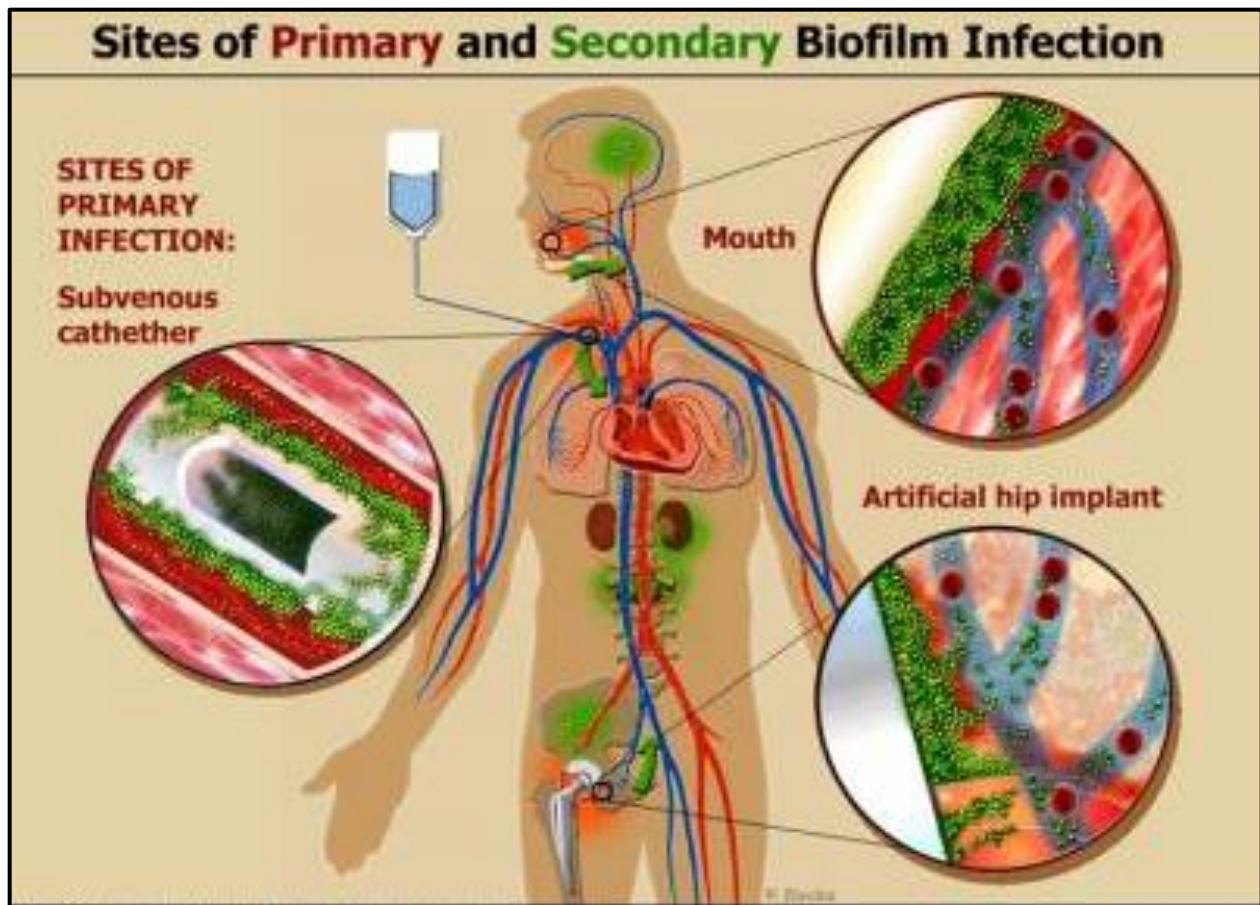


Figure 1-2. Biofilm formation is caused by a collective of one or more types of microorganism that can grow on many different surfaces; 65% - 80% of all microbial and chronic infections are associated with biofilm formation. [4]

Infections associated with the implantable device can decrease the devices' longevity, create life-threatening conditions for the patient, and increase cost. [7] For instance, each year, approximately 2 million nosocomial infections will cost our healthcare systems nearly \$11 billion in the United States alone, with 50-70% of these infections estimated to be the result of indwelling or invasive medical devices, as summarized in **Figure 1-3.** [8-10] The factors

contributing to the risk of infections in patients include patient age and medical history, the implant location, and how the device was manufactured. [11] Beyond these factors, the risk of infection becomes more concerning with increasing antibacterial resistance, which reduces the chances of recovery after infection occurs. **Therefore, the development of alternative approaches to post-operative infection control that do not rely *solely* on antibiotics is urgently needed to treat biofilm formation on implantable devices, or more broadly, infections in the tissue surrounding implantable devices.** It is essential to develop anti-infection implantable devices that are not based on antibiotics (which target specifically target bacteria) but instead on antimicrobial agents (which encompass a broader range of products that act on microbes in general). [12]

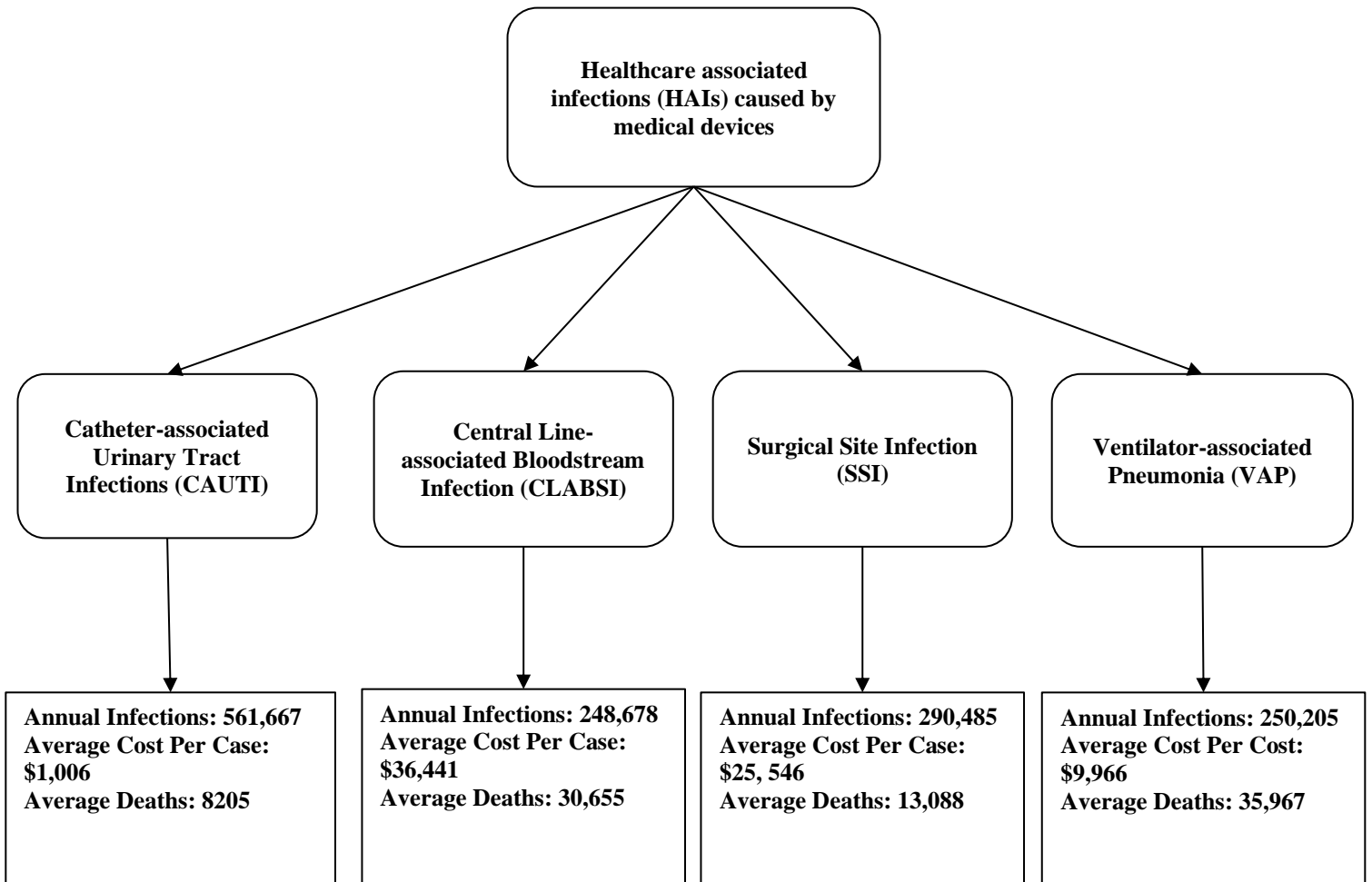


Figure 1-3. The four common infections caused by implantable medical devices include CAUTIs, CLABSIs, SSIs, and VAPs; each results in high economic burdens and mortalities.

Figure 1-4 summarizes the impact of healthcare-associated infections (HAIs) caused by invasive medical devices. [13] Approximately 50% of the 2 million HAIs are associated with indwelling or invasive medical devices, [14] with 30% of patients being hospitalized, [13] and approximately 90,000 patients dying globally each year [4] from the infection or conditions associated with the infection. In some cases, infections also can cause injuries, and some might require invasive treatment, such as restoration or replacement of the device, due to failure. According to the to the FDA, there are roughly 4,000 medical devices on the market; on average in the United States, approximately 80,000 deaths have occurred since 2008 due to medical device-related infections. [15] The economic burden of HAIs costs hospitals between US\$28 billion to 45 billion, annually in the US. [13] Catheters, heart, joint, and brain implants are the most common medical devices associated with medical device-related infections. Studies have shown that around “30% of patients are hospitalized after receiving a urinary catheter, and 45% of implantable devices cause all nosocomial infections.” [16]

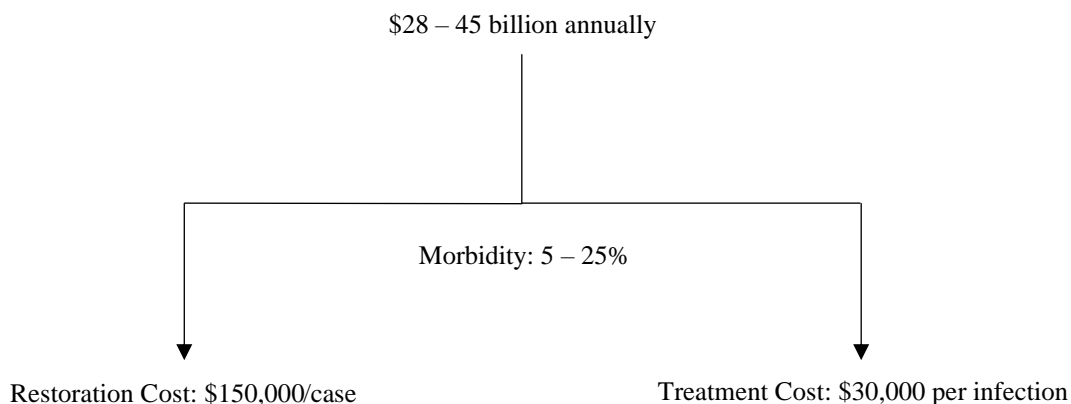


Figure 1-4. Between US\$28 – 45 billion are spent annually on HAIs; this results in a tremendous economic burden to both patients and our healthcare systems

The most common HAI is caused by *Staphylococcus aureus* (staph) [17], a Gram-positive, round-shaped bacterium typically found on human skin in the nose, armpit, and other areas. Different types of staph cause staph infections, including methicillin-resistant *staphylococcus aureus* (MRSA), methicillin-susceptible *staphylococcus aureus* (MSSA), vancomycin-intermediate *Staphylococcus aureus* (VISA), and vancomycin-resistant *Staphylococcus aureus* (VRSA). MRSA and MSSA typically spread by direct contact with an infected wound, from the contaminated hands of healthcare workers, [18] or from individuals who carry MRSA but do not show signs of infection. These staph bacteria are known to mostly be resistant to the type of antibiotics called beta-lactams, which include methicillin, oxacillin, penicillin, and amoxicillin, shown in **Figure 1-5**. [19] VISA, VRSA, AND MRSA are antimicrobial-resistant bacteria. Those who develop these types of staph infections often have underlying health conditions (such as diabetes and kidney disease) and tubes inserted in the body (such as catheters).

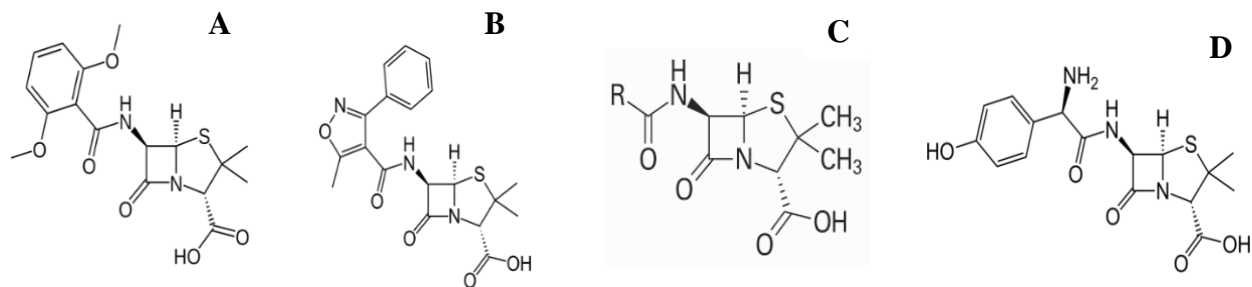


Figure 1-5. Beta-lactams type antibiotics include (A) methicillin, (B) oxacillin, (C) penicillin, and (D) amoxicillin among others; the MRSA, MSSA, VISA, and VRSA strains of *Staphylococcus aureus* are known to have resistances to these drugs.

Staph-related infections in healthcare can be severe and potentially fatal. [20] Firstly, staph can cause bacteremia or sepsis, which causes bacteria to spread to the bloodstream. Secondly, staph can lead to pneumonia, which commonly occurs in patients with underlying lung diseases. [21] Thirdly, staph can cause endocarditis, an infection of the heart valves, which can lead to heart failure or stroke.[22] Fourthly, staph can cause soft tissue infection at the surgical site and can kill the surrounding tissue. [23] Lastly, staph can result in osteomyelitis, a bone infection caused by staph bacteria in the bloodstream, trauma caused by a puncture wound of the foot, or drug abuse caused by intravenous (IV) insertion. [24] Those at greater risk of developing a staph infection include patients with chronic illnesses, such as diabetes, cancer, vascular disease, eczema, and lung disease, and those who inject drugs. [25] Hospitals, clinics, nursing homes, intensive care units (ICU), and other healthcare facilities also pose a risk for patients to develop staph-related infections due to compromised immune systems. [26] The three most common factors that put individuals at risk for staph infection are (1) the patient's communities, (2) hospitals, and (3) other healthcare facilities and the sources of those factors that cause risk are listed below in **Table 1-1**.

Table 1-1. Three of the most common factors that put patients at risk of developing a *Staphylococcus aureus* infection include community, hospitals, and other healthcare facilities.

Community Risk Factors
- Open or draining wounds
- Sharing personal items
- Recent stays in healthcare facilities
- Injectable drug use

Hospital Risk Factors

- Hospital stays or surgery
- Exposure to patients/staff carrying staph
- Exposure to patients who have been infected with staph
- Medical devices in the body, such as IV catheters

Other Healthcare Facility Risk Factors

- Outpatient surgeries and procedures
- Nursing homes
- Medical devices in the body

Although MSSA, MSRA, VRSA are typically the cause of HAIs, there has recently been more investigation of the group of coagulase-negative staphylococci, called *Staphylococcus epidermidis*. [27] This strain usually colonizes skin mucous membranes of the human body and is found in the body's normal bacterial flora. The cause of the *S. epidermidis* infections can be due to the presence of foreign bodies, such as implantable devices. The success of *S. epidermidis* and *S. aureus* infections can be due to their ability to adhere to the device's surface and remain there. According to the Food and Drug Administration (FDA), there are three established regulatory classes for medical devices necessary to assure the devices' safety and effectiveness. [28] Class I medical devices are classified as devices that are not intended to help support or sustain life or be substantially important in preventing impairment to human health and may not present an unreasonable risk of illness or injury. [29] Class II medical devices are classified as moderately high-risk devices to the patient and/or user; require more FDA regulations to assure safety and effectiveness. [30] Class III medical devices are classified as devices used to support or sustain human life and/or present a potentially high risk of illness or injury to patients. [31]

Most of all medical-device-related infections colonized by staphylococci are classified as Class II and III medical devices, as shown below in **Table 1-2**.

Table 1-2. Medical devices that are colonized by *Staphylococcus aureus* are typically when Class II and III medical devices are used.

Medical Device	Device Classification
- Contact Lens	II & III
- Central venous catheters	II
- Endotracheal tubes	II
- Intra-uterine devices	II
- Heart valves	III
- Pacemakers	III
- Peritoneal dialysis catheters	II
- Protistic joints	II & III
- Tympanostomy tubes	II
- Urinary catheters	II
- Voice prostheses	II

Surgical site infections (SSIs) are one of the most common causes of HAIs [32] and are usually preventable, but there are two main factors that have made treating SSIs complicated: (1) high antibiotic usage for prolong stay in the hospital post-operative, which leads to more antibiotic-resistant bacteria and antimicrobial agents, and (2) another surgery might need to be done to treat the infections, which can cause more infections to occur.

1.1.1 Methods of Conventional Infection Control

The implantable devices that tend to have a high rate of infection (types II and III) include electric device implants, orthopedic and metal implants, plastic implants, and dental implants.

Each device has risk factors associated with the chance of infection at the implant site.

According to Kok *et al.*, the risk factors for early implant-related SSIs include both patient-related and surgical-related factors. [33] Patient-related risk factors include, but are limited to, (1) the patient's age, (2) if they are a smoker, (3) if they have diabetes mellitus, (4) if they are overweight, (5) if they have a pre-existing infection, and (6) if they have liver disease. Surgical-related risk factors include, (1) scoring > 2 by the American Society of Anesthesiology, (2) no prophylactic antibiotics, (3) emergency surgeries, (4) surgical duration, (5) microbial contamination, and (6) surgical type.

Current methods of control are performed at three different stages (preoperatively, intraoperatively, and postoperatively) to address primarily *surgical*-related factors, as represented in **Figure 1-6**, and are typically non-technological methods, but there are also more complicated approaches to prevent SSIs, such as antimicrobial device coating. Technological methods, for which recommendations have been made [34], typically include physicochemical modifications, the use of antimicrobial agents incorporated onto or into medical devices, the use of antibiotic-containing materials, and the use of materials that contain antiseptic and metallic metals. These technological methods are typically prevention strategies aiming to, for instance, inhibit the adhesion, accumulation, and biofilm formation of pathogenic bacterial species. Von Eiff *et al.* suggest that the strategies to target each of these technological preventions include

polymer surface modification, antimicrobial devices that inhibit specific factors involved in accumulation, and electrical current and ultrasound plus antimicrobials.

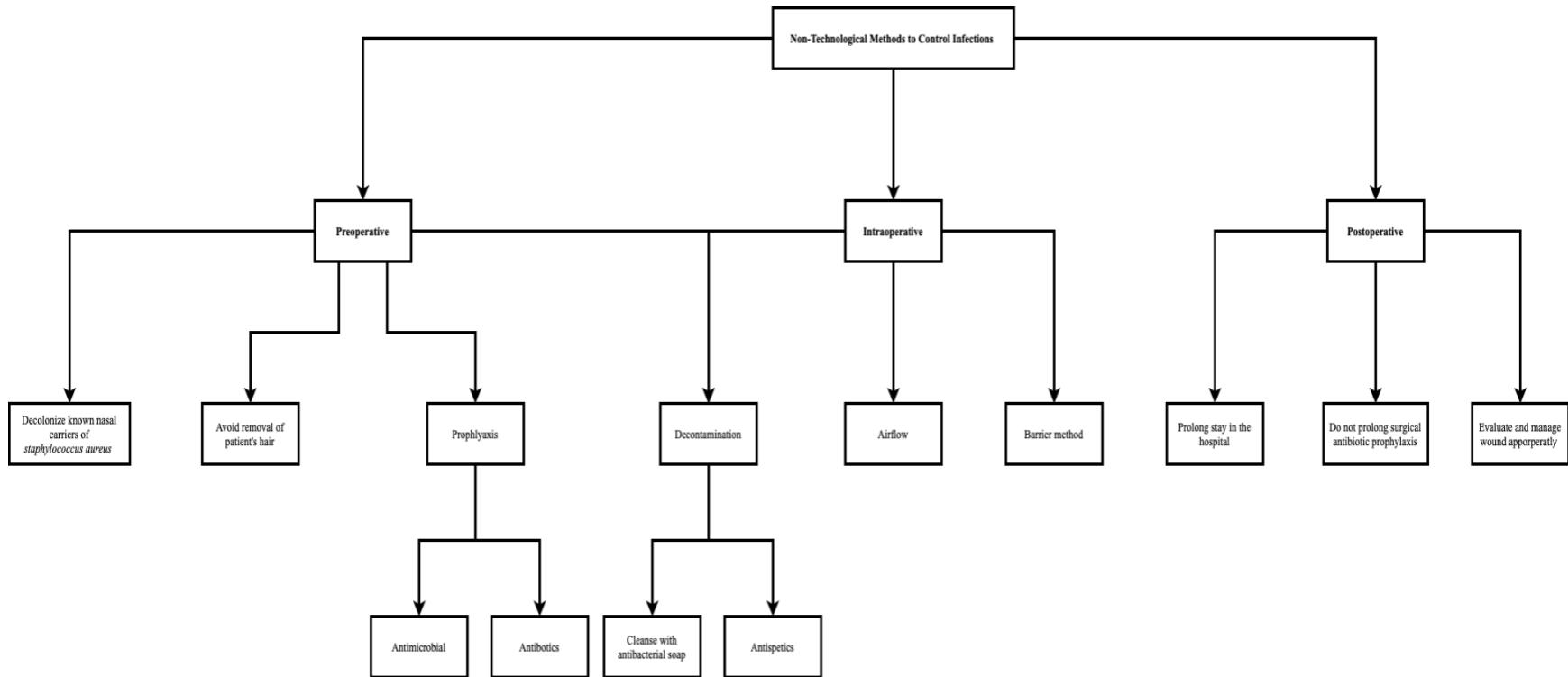


Figure 1-6. The schematic represents the standardized protocols put in place to control the risks of infection that could result in human error and the correlation to one another.

1.1.2 Probiotics

Beyond the use of materials-based approaches, probiotics are also being explored within the realm of infection control, although this field is relatively new in comparison to the existing body of literature on materials approaches. It is now widely accepted that probiotics are *not* a one-size-fits-all solution due to the complexity of the individual gut flora. [35, 36] Some researchers have found no effect using particular strain preparations, while others discovered large results using other strain preparations. [37] There is a need to explore the processes by which probiotics work and the role they play in infection control, alongside developing antimicrobial compounds to fight pathogens and materials to coat implantable devices to help prevent infection.

As the rise of antibiotic resistance continues, there has been a push for alternative approaches to treating infection-related diseases, caused by various bacterial strains, such as those shown in **Figure 1-7**. [38, 39] Probiotics can help to decrease the occurrence of certain infections and alleviate their symptoms. [40] Antibiotic use may be minimized or delayed by taking probiotics, which may lead to a reduction or delay in the formation of multi-resistant bacteria. [41] However, the process or processes by which probiotics function are largely unknown, and many research questions remain unanswered. [35] Probiotics, are known to help to regulate gut pH, fight pathogens by creating antimicrobial compounds, compete for pathogen binding and receptors sites, as well as available nutrients and growth factors, stimulate immunomodulatory cells, and produce lactase. [42]

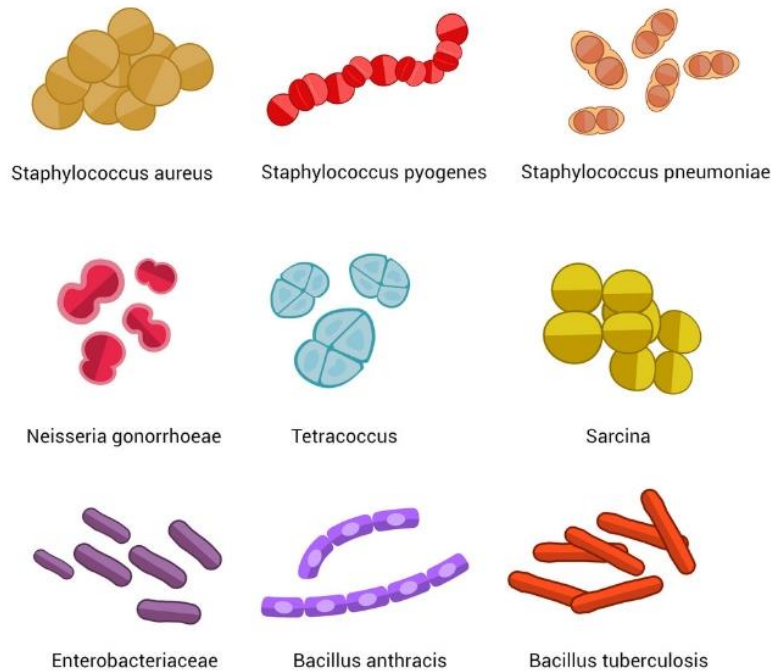


Figure 1-7. Harmful bacteria strains that may be toxic to the human body and can lead to infectious disease. [38]

Lactobacillus and *Bifidobacterium* (gram-positive, lactic acid-producing bacteria commonly found in the intestinal tract) are among the microorganisms marketed as probiotic agents, though some dietary supplements may contain strains of *Enterococcus*, *Bacillus*, and *Streptococcus*, which are less commonly found in the intestinal tract. [43] **Figure 1-8** shows the various types of bacteria strains used in probiotic supplements, while **Figure 1-9** shows the most common of the probiotic supplements on the market. Probiotics are most effective in preventing or treating five conditions: necrotizing enterocolitis, acute infectious diarrhea, acute respiratory tract infections, antibiotic-associated diarrhea, and infant colic. [44] There are several other conditions that are treated with the use of probiotics listed in **Table 1-3**.

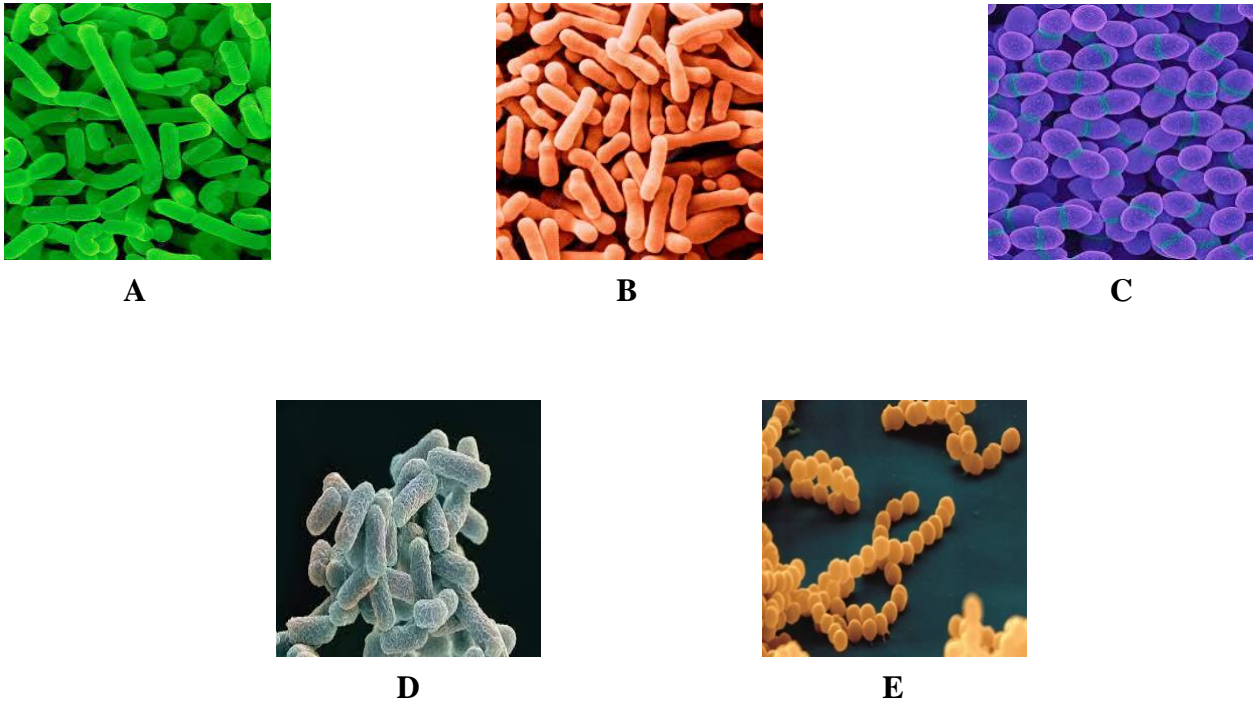


Figure 1-8. Bacteria genera, of (A) Lactobacillus, (B) Bifidobacterium, (C) Enterococcus, (D) Streptococcus, and (E) Escherichia commonly used in probiotic supplements.

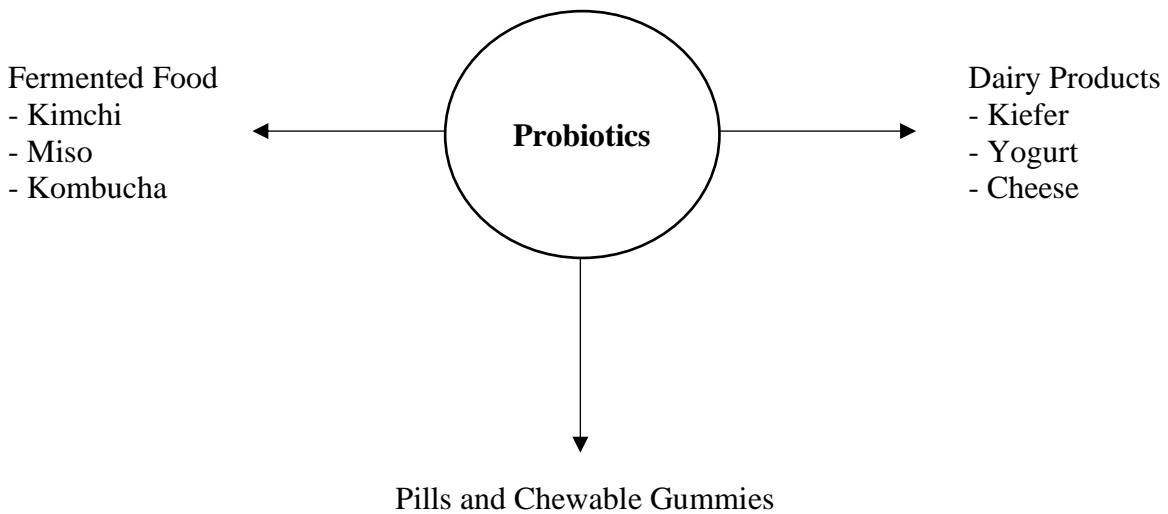


Figure 1-9. Schematic of the 3 methods of intaking probiotics: ingestion via fermented foods, dairy products, and pills/chewables.

Table 1-3. Probiotics have been shown to effective in treating the medical conditions listed

below. [44]

Medical Condition
Abdominal pain in children
Antibiotic-associated diarrhea (children)
Blood glucose and A _{1C} levels in type II diabetes mellitus
Constipation
Halitosis
<i>Helicobacter pylori</i> eradication
Hepatic encephalopathy
Infant colic
Infection risk in the critically ill
Irritable bowel syndrome
Late-onset sepsis in preterm infants
Prevention of <i>C. difficile</i> in hospitalized infants
Prevention of radiation-associated diarrhea
Small intestinal bacterial overgrowth
Surgical site infections
Total cholesterol and low – density lipoprotein
Ulcerative colitis

Probiotics have also shown to have benefit preoperative and postoperative surgical use. [45] Postoperative surgical site infection is a major cause of morbidity and mortality, accounting for one-third of all cases of post-operative sepsis. [46] Nutritional adjuncts, such as probiotics, prebiotics (Food ingredients that promote the development or activity of beneficial microorganisms like bacteria and fungus), and synbiotics (preparations that combine probiotics and prebiotics), are emerging as new therapeutic methods for avoiding postoperative infections. [47] Surgical trauma and prophylactic antibiotics affect the gut's microbial balance and barrier function, amplifying the inflammatory response and further depressing the immune system. [45] Probiotics have been shown to aid in the improvement of the gut barrier and immunomodulation. [48] The use of antibiotics post-surgery has shown that 3 in 5 patients will experience a complication, 2 in 5 patients will experience a post-operative complication after discharge, and 1 in 4 patients will be readmitted within 30 days. [37] Due to antibiotics causing harm to the body's microbiome, probiotics are needed to help support replacing those "good bacteria" [49] in the microbiome that may have been reduced using perioperative antibiotics.

1.1.3 Antimicrobial Coating and Medical Devices

Recently, there has been an emerging field of long-term, antimicrobial device coatings to help combat device-related infections. While there are various new upcoming technologies, there are limitations to these approaches, such as:

1. Some coatings rely on the use of antibiotics to inhibit the formation of biofilms. The long-term use of antibiotics use can lead to drug-resistant bacteria. Antibiotics can also be unsuccessful, due to impaired penetration to the infected area and a compromised immune system. [50]

2. Metal coatings can continuously leach metal ions throughout the body in high concentrations, which can be cytotoxic. [51]
3. Polymeric coatings repel the bacteria from the surface of the material, rather than being antimicrobial, causing bacteria to still form around the material's site. [52, 53]

Therefore, more research is needed to explore the development of coatings with enhancements to improve antimicrobial activity duration and minimize the risk of developing antibiotic-resistant bacteria. As the need for infection prevention increases, more materials research advances are needed to create a long-lasting antimicrobial coating, to reduce the occurrence post-operative infections.

1.2 Dissertation Organization

In this dissertation, our research goal was twofold: (1) to explore pure-silica zeolite **MFI** films for their biocompatibility and (2) to explore the factors that are associated with the establishment of probiotics in specific microbiomes. Both projects could have significant impacts on the field of infection control.

Our first research goal had three aims: (1) to optimize the synthesis conditions of pure-silica zeolite **MFI** films by performing biocompatibility studies to determine which set of synthesis conditions is more beneficial for the biomedical applications we are interested in enhancing, including potential use as a coating for infection prevention or control; (2) to explore the lysozyme sorption of *b* – oriented pure-silica zeolite **MFI** films; and (3) to explore the metabolic activity of L929 murine fibroblast cells when in contact with *b* – oriented pure-silica zeolite **MFI**

films. The successful completion of these aims did help to determine if **MFI** films could be potentially used as device coatings that could enhance medical devices, for instance, by reducing biofilm adhesion and implant site infections.

Our second research goal had 3 aims: (1) determine the type of probiotic that is most used for studies; (2) probiotic establishment in the gut, the magnitude of establishment and how long do probiotics stay in the gut; (3) evaluating the resident microbial community diversity and composition, to determine if probiotics alter the ecosystem and the dependency of the number and types of bacteria used in probiotics.

Chapter 2 provides a general introduction to pure-silica zeolite **MFI** films and their synthesis. In this chapter, we discuss in detail zeolite synthesis. This chapter contains information on how **MFI** films are created, including substrate choice and modifications, coating and synthesis strategies, characterizations, defect elimination in films, and a short discussion of selecting film synthesis methods based on the intended application.

Chapter 3 discusses in detail the interaction of lysozyme sorption of pure-silica zeolite **MFI** films. We include a brief introduction to the applications of zeolites used for biomedical applications. This chapter discusses the specific synthesis strategies we used for pure-silica zeolite **MFI** films, characterization to study the surface properties of zeolites, and the biological techniques used (ELISA and BCA) to quantify the amount of lysozyme sorption into the pores and surface of **MFI** films.

Chapter 4 evaluates the interaction of L929 fibroblast cells with pure-silica zeolite **MFI** films. We include a brief introduction to zeolites in biological environments. We discuss the importance of using fibroblast cells in this study and how the cells are cultured. **Chapter 4** uses the methodology and strategies developed in **Chapter 3** to demonstrate the pure-silica zeolite **MFI** films synthesis and the characterization techniques to study the surface properties of the films. Using these films, we investigate the cell viability of fibroblast *in vitro*.

Chapter 5 provides a comprehensive meta-analysis of factors affecting probiotic establishment in preexisting microbiomes. This chapter expands on the introduction but focuses on finding the exact quantitative and qualitative data that is missing when studying the factors of bacteria migration and the establishment of probiotics in the gut microbiome. We also provide a brief introduction of the experimental process to conduct a meta-analysis. This chapter also discusses extracting experimental and statistical data that was obtained from 239 studies.

Chapter 6 concludes this dissertation and discusses future opportunities of using the pure-silica zeolite **MFI** films as a coating for biomedical applications. The effects of changing synthesis conditions (synthesis gel aging time, and crystallization time), the further investigation of film properties (film thickness, topography, hydrophilic and hydrophobic interactions) using characterization techniques studying the interaction of biological species, such as bacteria on the surface of **MFI** films. The chapter then concludes with a short discussion exploring multi-prolonged approaches to infection control that could be created by combining antimicrobial coatings and probiotics.

1.3 References

1. Garrett, T.R., M. Bhakoo, and Z. Zhang, *Bacterial adhesion and biofilms on surfaces*. Progress in Natural Science, 2008. **18**(9): p. 1049-1056.
2. Vidyasagar, A. *What Are Biofilms*. 2016 [cited 2022; Available from: <https://www.livescience.com/57295-biofilms.html>].
3. Yeo, I.S., et al., *Implant surface factors and bacterial adhesion: a review of the literature*. Int J Artif Organs, 2012. **35**(10): p. 762-72.
4. Khatoon, Z., et al., *Bacterial biofilm formation on implantable devices and approaches to its treatment and prevention*. Heliyon, 2018. **4**(12): p. e01067-e01067.
5. Salleg. *Biofilm bacteria*. 2020 [cited 2022; Available from: mpkb.org/home/pathogenesis/microbiota/biofilm].
6. Arciola, C.R., D. Campoccia, and L. Montanaro, *Implant infections: adhesion, biofilm formation and immune evasion*. Nature Reviews Microbiology, 2018. **16**(7): p. 397-409.
7. Olofsson, A.-C., M. Hermansson, and H. Elwing, *N-Acetyl-L-Cysteine Affects Growth, Extracellular Polysaccharide Production, and Bacterial Biofilm Formation on Solid Surfaces*. Applied and Environmental Microbiology, 2003. **69**(8): p. 4814-4822.
8. Schierholz, J.M. and J. Beuth, *Implant infections: a haven for opportunistic bacteria*. Journal of Hospital Infection, 2001. **49**(2): p. 87-93.
9. Xu, Y.-Q., et al., *Implant-related infection in the tibia: surgical revision strategy with vancomycin cement*. TheScientificWorldJournal, 2014. **2014**: p. 124864-124864.
10. Stone, P.W., *Economic burden of healthcare-associated infections: an American perspective*. Expert review of pharmacoeconomics & outcomes research, 2009. **9**(5): p. 417-422.

11. Ribeiro, M., F.J. Monteiro, and M.P. Ferraz, *Infection of orthopedic implants with emphasis on bacterial adhesion process and techniques used in studying bacterial-material interactions*. Biomatter, 2012. **2**(4): p. 176-194.
12. Liu, P., et al., *Fabrication and Characterization of Composite Meshes Loaded with Antimicrobial Peptides*. ACS Appl Mater Interfaces, 2019. **11**(27): p. 24609-24617.
13. Prevention, C.o.D.C.a. *Current HAI Progress Report*. Available from: <https://www.cdc.gov/hai/data/portal/progress-report.html>.
14. Darouiche, R.O., *Treatment of Infections Associated with Surgical Implants*. New England Journal of Medicine, 2004. **350**(14): p. 1422-1429.
15. Press, A. *Medical devices for pain, other conditions have caused more than 80,000 deaths since 2008*. 2018; Available from: <https://www.statnews.com/2018/11/25/medical-devices-pain-other-conditions-more-than-80000-deaths-since-2008/>.
16. Percival, S.L., et al., *Healthcare-associated infections, medical devices and biofilms: risk, tolerance and control*. J Med Microbiol, 2015. **64**(Pt 4): p. 323-334.
17. *Strategies to Prevent Hospital - onset Staphylococcus aureus bloodstream infections in Acute Care Facilities*. 2019 December 16, 2019 2022]; Available from: Prevention, C.o.D.C.a., Staphylococcus aureus in Healthcare Settings.
18. Prevention, C.o.D.C.a., *Methicillin-resistant Staphylococcus aureus (MRSA)*.
19. Prevention, C.o.D.C.a., *Healthcare-associated Infections*.
20. Prevention, C.o.D.C.a. *General Information about Staphylococcus aureus*. Available from: <https://www.cdc.gov/hai/organisms/staph.html>.
21. Clinic, M., *Staph infections*.

22. Sinai, C. *Bacterial Endocarditis*. Available from: <https://www.cedars-sinai.org/health-library/diseases-and-conditions/b/bacterial-endocarditis-adult.html>.
23. *Necrotizing Soft Tissue Infection*. Available from: <https://www.hopkinsmedicine.org/health/conditions-and-diseases/necrotizing-soft-tissue-infection>.
24. Disorders, N.O.f.R. *Osteomyelitis*. Available from: <https://rarediseases.org/rare-diseases/osteomyelitis/>.
25. Prevention, C.o.D.C.a., *Staphylococcus aureus in Healthcare Settings*.
26. Chamchod, F. and P. Palittapongarnpim, *Effects of the proportion of high-risk patients and control strategies on the prevalence of methicillin-resistant Staphylococcus aureus in an intensive care unit*. BMC infectious diseases, 2019. **19**(1): p. 1026-1026.
27. Vuong, C. and M. Otto, *Staphylococcus epidermidis infections*. Microbes and Infection, 2002. **4**(4): p. 481-489.
28. Administration, T.F.a.D. *Classify Your Medical Device*. Available from: <https://www.fda.gov/medical-devices/overview-device-regulation/classify-your-medical-device>.
29. *FDA Medical Devices: Definition and Classifications*. Available from: <https://www.in2being.com/fda-medical-devices-definition-and-classifications>.
30. Association, T.F.a.D. *Learn if a Medical Device Has Been Cleared by FDA for Marketing*. Available from: <https://www.fda.gov/medical-devices/consumers-medical-devices/learn-if-medical-device-has-been-cleared-fda-marketing>.

31. Wassmann, T., et al., *The influence of surface texture and wettability on initial bacterial adhesion on titanium and zirconium oxide dental implants*. International Journal of Implant Dentistry, 2017. **3**(1): p. 32.
32. Deverick J Anderson, M., MPH, Daniel J Sexton, MD. *Overview of control measures for prevention of surgical site infection in adults*. Available from: <https://www.uptodate.com/contents/overview-of-control-measures-for-prevention-of-surgical-site-infection-in-adults#H4019022927>.
33. Kok, T.W., et al., *Risk factors for early implant-related surgical site infection*. J Orthop Surg (Hong Kong), 2016. **24**(1): p. 72-6.
34. Von Eiff, C., et al., *Modern Strategies in the Prevention of Implant-Associated Infections*. The International Journal of Artificial Organs, 2005. **28**(11): p. 1146-1156.
35. Kechagia, M., et al., *Health benefits of probiotics: a review*. ISRN nutrition, 2013. **2013**: p. 481651-481651.
36. de Simone, C., *The Unregulated Probiotic Market*. Clinical Gastroenterology and Hepatology, 2019. **17**(5): p. 809-817.
37. HealFast. *Probiotic After Surgery - A Stronger Recovery* 2022; Available from: <https://healfastproducts.com/blogs/posts/probiotics-after-surgery-a-stronger-recovery>.
38. *Top 11 Probiotic Strains + Why They're So Important to Your Health* March 30, 2022; Available from: <https://1md.org/health-guide/digestive/ingredients/probiotics>.
39. George Kerry, R., et al., *Benefaction of probiotics for human health: A review*. Journal of Food and Drug Analysis, 2018. **26**(3): p. 927-939.

40. Hungin, A.P.S., et al., *Systematic review: probiotics in the management of lower gastrointestinal symptoms - an updated evidence-based international consensus*. *Alimentary pharmacology & therapeutics*, 2018. **47**(8): p. 1054-1070.
41. *Probiotics for infection control*. *Hospital Infection Control* [cited 2022 April 7]; Available from: <https://www.infectiousdiseaseadvisor.com/home/decision-support-in-medicine/hospital-infection-control/probiotics-for-infection-control/>.
42. Amara, A.A. and A. Shibl, *Role of Probiotics in health improvement, infection control and disease treatment and management*. *Saudi pharmaceutical journal : SPJ : the official publication of the Saudi Pharmaceutical Society*, 2015. **23**(2): p. 107-114.
43. Dorval, E. *Probiotics as a Treatment for Infectious Diseases*. 2015 [cited 2022; Available from: <https://www.uspharmacist.com/article/probiotics-as-a-treatment-for-infectious-diseases>.
44. Liu, Y., D.Q. Tran, and J.M. Rhoads, *Probiotics in Disease Prevention and Treatment*. *Journal of clinical pharmacology*, 2018. **58 Suppl 10**(Suppl 10): p. S164-S179.
45. Jeppsson, B., P. Mangell, and H. Thorlacius, *Use of probiotics as prophylaxis for postoperative infections*. *Nutrients*, 2011. **3**(5): p. 604-612.
46. Chen, P.-Y., et al., *Epidemiological Characteristics of Postoperative Sepsis*. *Open medicine (Warsaw, Poland)*, 2019. **14**: p. 928-938.
47. Chowdhury, A.H., et al., *Perioperative Probiotics or Synbiotics in Adults Undergoing Elective Abdominal Surgery: A Systematic Review and Meta-analysis of Randomized Controlled Trials*. *Annals of Surgery*, 2020. **271**(6).
48. Ward, T., M. Nichols, and J. Nutter, *Can Probiotics Improve Your Surgical Outcomes?* *Plast Surg Nurs*, 2016. **36**(2): p. 74-7.

49. Gagliardi, A., et al., *Rebuilding the Gut Microbiota Ecosystem*. International journal of environmental research and public health, 2018. **15**(8): p. 1679.
50. Li, X., et al., *Antimicrobial nanoparticle coatings for medical implants: Design challenges and prospects*. Biointerphases, 2020. **15**(6): p. 060801.
51. Lee, S., et al., *Surface engineering of titanium alloy using metal-polyphenol network coating with magnesium ions for improved osseointegration*. Biomaterials Science, 2020. **8**(12): p. 3404-3417.
52. Cyphert, E.L. and H.A. von Recum, *Emerging technologies for long-term antimicrobial device coatings: advantages and limitations*. Experimental biology and medicine (Maywood, N.J.), 2017. **242**(8): p. 788-798.
53. Elumalai, A., et al., *3D Printed Ceramic-Polymer Composites for Treating Bone Infection*. 2020. p. 613-635.

Part I: Infection Control: Exploration of Siliceous Zeolite MFI Films as Coatings for Implantable Devices

Chapter – 2: Introduction of Silicate – 1 Zeolite Material and Synthesis

2.1 Introduction

Zeolites, as a group of natural minerals, were first discovered in 1765. Their name arises from the Greek words “zeo” and “lithos” meaning “boil” and “stone,” because when heated, the minerals would emit water. [54] Because of the unique structures of these materials (for example, **Figure 1**), among other interesting physicochemical properties, zeolites are used as shape-selective catalysts, ion-exchangers, and adsorbents all over the world. [55]

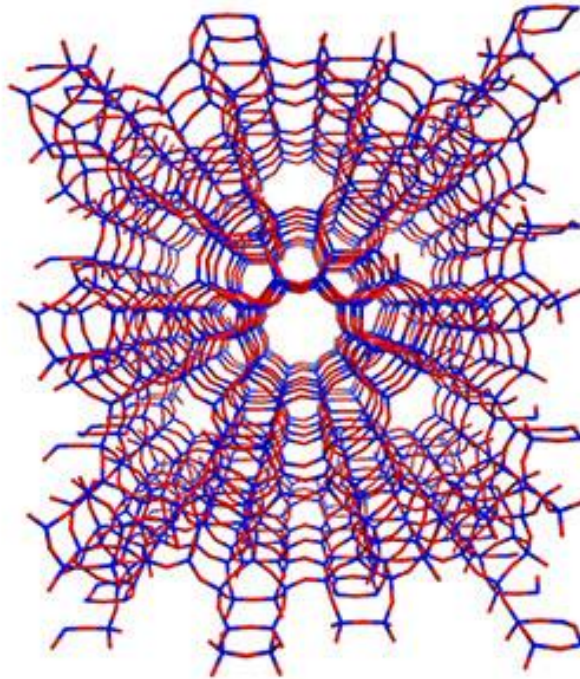


Figure 2-1. Pore like structure of zeolite, ZSM – V. This organized structure is created by an alternating silicon or aluminum (blue) to oxygen (red) bond framework. [56]

Despite this interesting, and somewhat unique behavior, zeolites were originally regarded as inert materials with no practical value. [57] Rather, mineralogists were almost entirely focused in understanding the surroundings and crystallization conditions, as well as their crystal structures, rather than their properties and possible practical applications.

The initial definition of zeolites was proposed by J.V. Smith as, “*an aluminosilicate with a framework structure enclosing cavities occupied by large ions and water molecules, both of which have considerable freedom of movement, permitting ion-exchange and reversible dehydration.*” [58] This definition hints at the myriad possible applications for which zeolites and zeolitic materials could be envisioned. It wasn't, however, until the 1940s when R.M. Barrer validated the crystalline, microporous materials' molecular sieving characteristics that would cause these materials to be reconsidered for practical applications. [59] In the 1950s, Milton and Breck at Union Carbide reached some of the most important early synthesis milestones from an industrial standpoint; in 1954, the company first entered the market and, beginning in the 1960s, the company began producing a profit on an annual basis, with an initial investment of just over \$7 million. [60] Of these milestones, arguably the most important is the discovery of reactive gel crystallization, which is now the industry standard for zeolite production. [61] Once researchers had a better understanding of the processes involved in the nucleation and growth of zeolite crystals during synthesis, *synthetic* zeolites (as opposed to natural zeolite minerals which are mined) became frequently employed as catalysts and carriers in a wide range of chemical reactions and refining processes. [55] For example, today zeolites are used in the oil refining industry, in such processes as catalytic cracking, hydrocracking, hydrodimerization of short and

long paraffins, and isomerization of n-butenes. [62] Those incredible materials are still the world's largest catalysts for industrial use. [63] (**Figure 2-2.**)

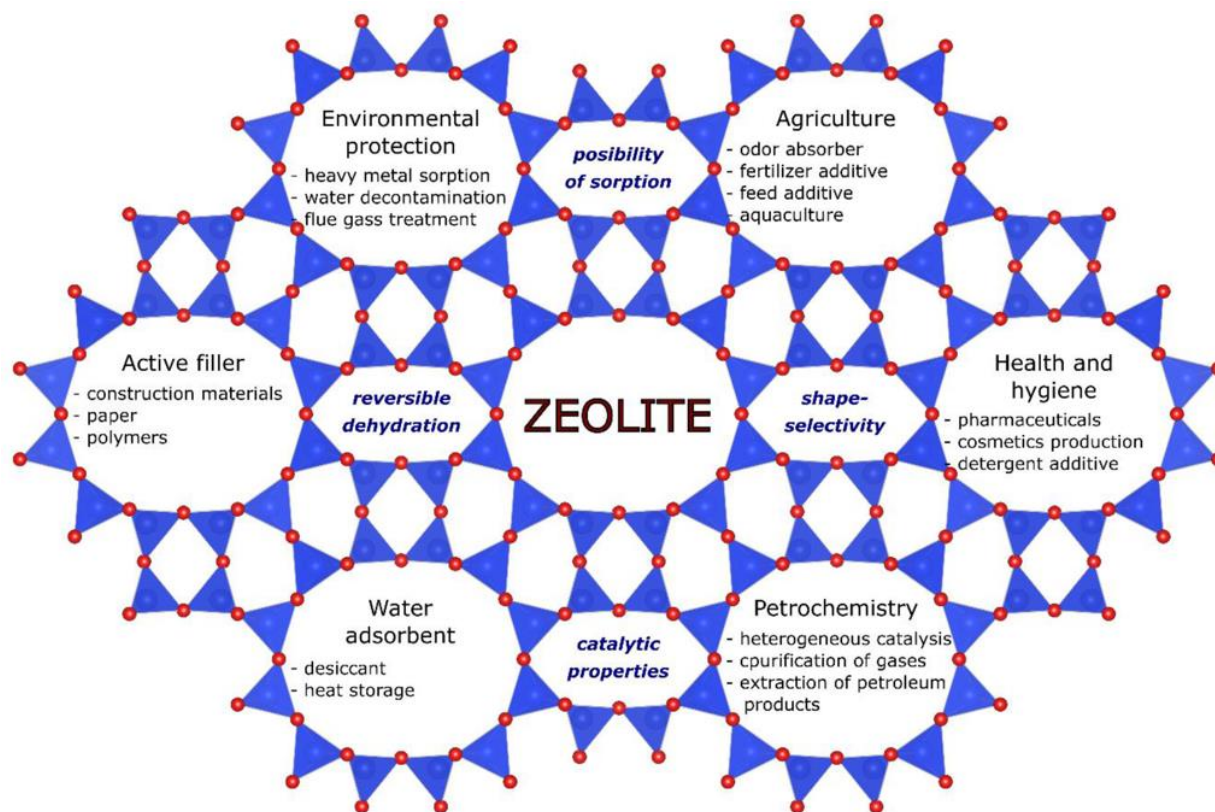


Figure 2-2. Chemists, technicians, and mineralogists are all fascinated with zeolites. Specific features of zeolites reveal a wide range of uses for this kind of material and demonstrate the usefulness of zeolites in a variety of fields. [64]

2.2 Introduction of Zeolites and Molecular Sieves

Zeolites are nanostructured, microporous materials that have been intensively explored due to their ultra-high surface-to-volume ratio, which is typical of nanomaterials. [65] These porous materials have organized, interconnected, microporous channels that range in diameter from 0.2 to 2 nm, which corresponds to the size of numerous organic molecules. [66] The crystalline

structure of zeolite comprises a three-dimensional network of atoms, such as Si and Al, as the backbone. [67] These atoms (also known as T-atoms) are tetrahedrally bonded to four oxygen atoms, and to their neighboring T-atoms by these shared oxygen atoms, keeping the oxygen to T-atoms framework ratio at 2. [68] Because of this, zeolites have substantial acid activity with shape-selective characteristics as compared to compositionally comparable amorphous materials. Elements iso-electronic with Al^{+3} or Si^{+4} have been proposed to substitute into the framework lattice during synthesis including B^{+3} , Ga^{+3} , Fe^{+3} and Cr^{+3} in place of Al^{+3} , and Ge^{+4} and Ti^{+4} in place of Si^{+4} , etc. [69] The incorporation of transition elements such as Fe^{+3} for framework Al^{+3} cations change the acidity of the materials. [70]

The general empirical formula for a zeolite's composition is $\text{Al}_2\text{O}_3 \cdot x \text{SiO}_2 \cdot y \text{H}_2\text{O} \cdot \text{M}_{2/n}\text{O}$, where M is a cation; the cation will often “sit” within the cage structure or pores of the zeolite to act as a charge-compensator, as the presence of the aluminum ions requires an additional framework cation to balance the net charge on the framework. (Pure-silica compositions have a neutral electronic structure and therefore no need of the cation.) Note that the cation is not bound within the structure of the framework. The ratio of silica (SiO_2) to alumina (Al_2O_3) varies, but it is always equal to or larger than 2, because aluminum tetrahedra do not sit in adjacent positions due to the bond angle strain that would be imposed.

One-, two-, and/or three-dimensional structures are produced from these tetrahedral building blocks, which may then be joined to form the microporous cages and channels for which zeolites are famous. [71, 72] Zeolites are named based on three-letter structure codes representing their specific framework type (structure). There are 217 distinct zeolite framework types that have

been successfully synthesized, many with multiple compositions, with many more theoretically expected. [73]

Each type of framework is given a three-letter code by the International Zeolite Association (IZA). The codes are based on how fundamental units, such as atoms in a tetrahedral arrangement, are connected, regardless of atom type, chemical content, or unit cell size. [71, 72] However, many zeolites are still referred to by several different names, often based on their structure codes, composition, and creators. Typically, distinct names are given to different chemical compositions with the same topology. For instance, ZSM-5 (**MFI**) is used for aluminosilicate compositions with varied Si/Al ratios, while silicalite-1 (**MFI**) is utilized for pure-silica polymorphs [specified in a Mobil patent]. [74]

As an example, the structure of the **MFI** zeolite is made up of double five-ring secondary building units (SBUs), which can be assembled to form a "pentasil" (**Figure 2-3**) structure with compositions ranging from purely silicate to aluminosilicate, phosphosilicate, and so on, but the crystal structure remains constant. A zig-zag pore network along [100] and an intersecting straight cylinder pore system along [010] make up the structure (**Figure 2-3**). The lattice parameters of **MFI** with an aluminosilicate composition are $a = 20.048 \text{ \AA}$, $b = 19.884 \text{ \AA}$, $c = 13.352 \text{ \AA}$, $\alpha, \beta, \gamma = 90^\circ$, but the lattice parameters of silicalite-1 are slightly different to accommodate the different bond angles. The **MFI** structure comprises rather large pores that run in the directions of (100) and (010). The dimensions of the zig-zag pore openings are $5.1 \text{ \AA} \times 5.5 \text{ \AA}$ while those of the straight cylinder are slightly larger and are $5.4 \text{ \AA} \times 5.6 \text{ \AA}$ [1]. Pores within

zeolites are typically classified by size: small (8-member ring), medium (10-member ring) (Figure 2-3) and large (12-member ring).

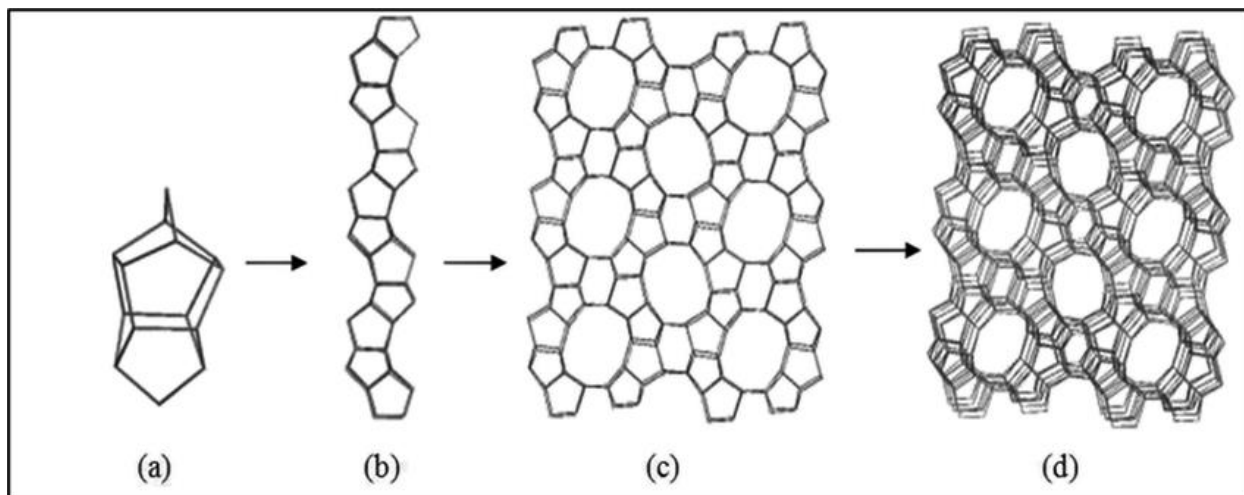


Figure 2-3. The ZSM-5 (MFI) structure. (A) The pentasil unit. (B) Chains of pentasil units. (C) Layers of these chains. (D) Layers linked. [75]

Because of their ability to act as molecular sieves, zeolites have great economic value: they are (1) selective and powerful absorbers, (2) selective ion-exchangers, and (3) suitable solid-state catalysts. The capacity of most zeolites to selectively absorb one component from a mixture is what makes them so valuable in industrial applications. Zeolites have been widely used in various applications, such as separations, catalysis, ion-exchange, and heavy metal adsorption processes, primarily as powders or powder-coatings of structural materials, due to their unique porous, crystalline nanostructure and the molecular sieving properties mentioned previously.

2.3 Introduction to Zeolite Synthesis

One of the most frequently used methods for making nanostructured materials (zeolites or otherwise) is to employ templates, which function as scaffolds within, or around which nucleated material, such as crystals, grow. Nanostructures in zeolites are created using this approach. The nanostructure can develop as either complementary to the substrate, or the template can merely be physically involved in driving growth, in which case it must be selectively eliminated using post-synthetic operations. [72, 73]

Zeolites are typically formed by a mixture of nucleation and growth processes that start with the formation of energetically unstable nuclei and progress to the formation of thermodynamically stable, larger particles as the surface area ratio decreases. [76] As a result, the observable zeolite crystal grows at the expense of numerous tiny crystals that offer crucial content for growth and subsequently disappear. [73] When the concentration of the active ingredient reaches a value known as the critical micelle concentration (CMC) or critical aggregation concentration (CAC), they disperse surfactant molecules and can aggregate and form micelles before proceeding to further growth. This occurrence can be compared to micellar behavior in an aqueous solution. [77]

The nanoparticles/nuclei increase through the Ostwald ripening mechanism because of the applied heat, causing the density of nuclei to decrease significantly. As a result, zeolites are thermodynamically metastable phases of the components, where the first phase created is replaced by the second phase, which is more stable, owing to consumption, and this trend continues until the most stable phase is formed, according to Ostwald's law. [78] From a kinetic

standpoint, if a relatively less stable thermodynamic phase hits a large energy barrier in the process of transcending to a more stable phase and can sometimes continue to exist by crystallizing. [79] Several sources provide information on the gel system and the crystallization kinetics of zeolites. [71, 78] The following factors are part of the basic approach that drives zeolite crystallization and synthesis: (1) gel composition; (2) temperature and time; and (3) nature of the starting material. [59, 71]

When the reagents for synthesis are mixed, they form a gel that is transformed into zeolite crystals after being exposed to autogenous conditions for a period, dividing the gel into two phases: solid and liquid (**Figure 2-4**). The density of the reaction gel increases as the crystallization process progresses, and it begins to settle to the bottom of the vessel used for crystallization, which accounts for successful zeolite crystallization. Specific crystallization containers are used in the hydrothermal synthesis of zeolite. Under synthesis conditions, small stainless-steel autoclaves with Teflon liners are used (temperature above the boiling point of water). In the laboratory, zeolite synthesis involves heating a mixture containing a source of silica, water, usually an organic cation such as a structure-directing agent (SDA), such as carbon and a mineralizing agent at hydrothermal temperatures (70-200 C) under autogenous pressure, which results in the formation of highly crystalline materials with exquisite structures after a few hours to several days.

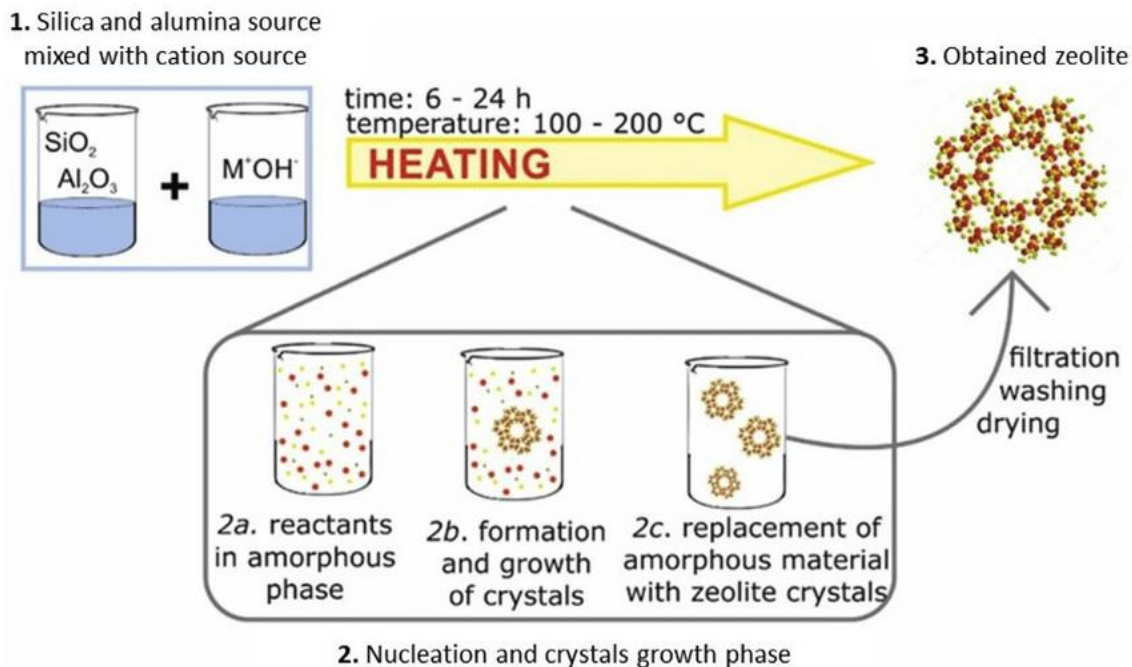


Figure 2-4. The main stages of zeolite synthesis by the hydrothermal method. [80]

During synthesis, the reaction gel is aged by allowing it sit at room temperature for several hours under slow shaking/agitating conditions. This stage seeks to equilibrate and develop seeds/nuclei in the reaction mixture, which will form the desired crystal phase once the temperature is reached, and the crystallization rate is increased. The product distribution has been found to be affected by keeping the reaction gel under static or agitating conditions, as well as the type of movement, such as stirred, rolled, vibrated, or shaken. The $\text{SiO}_2/\text{Al}_2\text{O}_3$ ratio, the gel's hydroxide concentration, the presence of inorganic cation, and organic additives are all factors that influence the final crystalline structure (SDA). The form and crystal size of the final crystalline product are also influenced by the inorganic/organic cation.

The concentration of hydroxide (OH^-) in the molar composition of the reaction gel should be kept as low as possible because a larger OH^- concentration lowers the yield of the crystalline material. The concentration of free OH^- in the reaction gel is affected by the pH of the reaction gel mixture. The reaction mixture is alkaline before crystallization begins; however, there is a significant change in pH when crystallization begins, owing to the incorporation of SiO_2 units into the silicate framework, which is accompanied by the release of free OH^- in the surrounding gel mixture, that grows with crystallization. Water by interacting strongly with the cations in the solution, becomes part of the 'template' for structure-directing. The water content of the reaction gel determines its transport characteristics and viscosity, for example, in MFI synthesis, the water content of the reaction gel determines the synthesis of large-pore MFIs.

The mineralizing agent gives the reactants the necessary alkaline pH for crystallization to proceed at a specified pace (also determined by the molar composition of the reaction gel and the temperature provided). In the gel, OH^- is also employed to solubilize silicate and aluminate species. [81] It has been discovered that when F^- is utilized as a mineralizing agent instead of OH^- for zeolite production, the resulting crystals are both hydrophobic and defect-free.

Once crystallization is complete, the SDA must be removed via calcination or other methods to open the pore network. [82] Zeolites of various geometry have been synthesized using a distinct structure-directing agent and T-atoms such as Ge, Al, B, Be, Zn, and others. [79] Due to the high alkalinity of zeolite synthesis, it is preferable to utilize non-reactive laboratory equipment that does not contaminate the zeolite reaction gel, such as Teflon, plastic, or stainless steel. [83] If a

mixed solvent is used in the production of zeolite nanocrystals, it should be included in the molar composition, for example, ethanol should be added if nanocrystals form. [84]

2.3 Synthesis Protocol: Silicate-1 (MFI) Films

We used a variety of zeolite synthesis procedures to achieve evenly oriented zeolite crystals as a film, shown in **Table 2-1**. Using the above synthesis strategies, we focused on achieving a monolayer of *b – oriented* and *randomly – oriented* silicate-1 (MFI) films on a silicon (Si) substrate. We were able to obtain films with diameters ranging from 200 to 500 nm *in situ*. The normal synthesis steps shown in **Figure 2-5**. are as follows: (1) Prepare a clear reaction gel solution comprised of TEOS (Tetrapropylammonium hydroxide), TPAOH (tetraethylorthosilicate), and deionized (DI) water. TPAOH is first combined with DI water in a clean 125 mL Nalgene bottle, and the solution is mixed on a stir plate for 10 minutes, TEOS is then added to the solution; (2) The reaction gel is aged under stirring with a magnetic stir bar for different amount of time (**Table 2-1.**); (3) Clean substrate is dipped in the reaction gel to produce films at different orientations (**Figure 2-5.**); (4) Crystallization is carried out in a convection oven in a Teflon-lined Parr autoclave (**Table 2-1.**); (5) Substrate is removed from the autoclave and rinsed with deionized water and films air dried for 24 hours; (6) The films are then calcined to remove the structure-directing agent (carbon) (**Table 2-1.**)

Table 2-1. Summarizes the various parameters used to synthesize silicate (MFI) zeolite films.

Molar Ratio	Aging Time (h)	Substrate	Substrate Dimensions	Temperature (°C)	Time (h)	Orientation	Calcination	Ref.
99H ₂ O/0.23TPAOH /0.84TEOS	3	Si	2.0 cm x 0.5 cm	165	6	(b-)	Calcination- 400 °C, 4h, ramping rate 0.5°C/min	Exter - 1997
99H ₂ O/0.23TPAOH /0.84TEOS	3	Si	0.5 cm x 0.5 cm	165	6	Random	Calcination- 400 °C, 4h, ramping rate 0.5°C/min	Exter - 1997
99H ₂ O/0.23TPAOH /0.84TEOS	1	Si	1.5 cm x 0.5 cm	165	3	(b-)	Calcination- 400 °C, 4h, ramping rate 0.5°C/min	Exter - 1997
99H ₂ O/0.23TPAOH /0.84TEOS	1	Si	2.5 cm x 0.5 cm	165	3	(b-)	Calcination- 400 °C, 4h, ramping rate 0.5°C/min	Exter - 1997
99H ₂ O/0.23TPAOH /0.84TEOS	6	Si	1.5 cm x 0.5 cm	165	12	(b-)	Calcination- 400 °C, 4h, ramping rate 0.5°C/min	Exter - 1997
99H ₂ O/0.23TPAOH /0.84TEOS	6	Si	2.5 cm x 0.5 cm	165	12	(b-)	Calcination- 400 °C, 4h, ramping rate 0.5°C/min	Exter - 1997

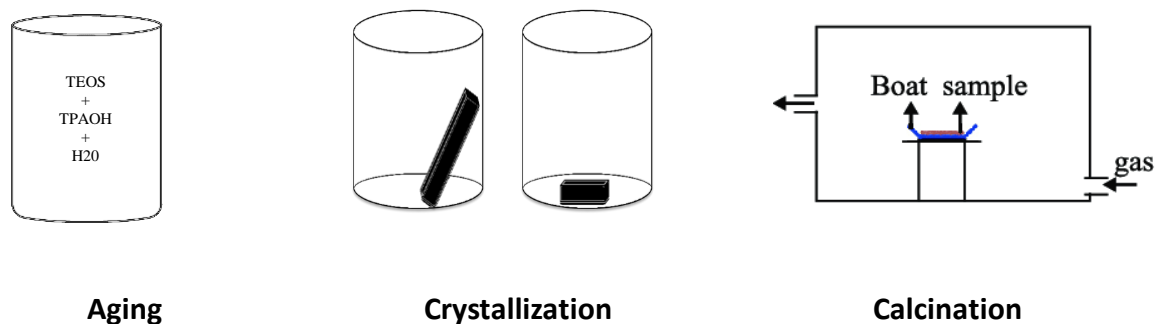


Figure 2-5. Schematic representation of the steps of the silicate-1 (MFI) synthesis

2.3.2 Substrate Choice and Modifications

Various supports, such as silicon, glass, quartz, ceramic, alumina, polymeric membranes, stainless 34 steel, clay, and Teflon, have been used to synthesize zeolite films and membranes.

[85-88] Piranha Solution [volume ratio; 1Hydrogen Peroxide (H₂O₂, 40 wt. percent): 4Sulphuric Acid (H₂SO₄, 98 wt. percent)] is the most frequent procedure for modification of silicon substrates. For the fabrication of silicalite-1 films, clean room grade wafers have also been employed without any further processing. [89]

2.3.3 Characterization Techniques

X-ray diffraction (XRD) is used to check the clarity of the silicalite-1 films produced on Si (100). (Rigaku). Under a scanning electron microscope (SEM), the film thickness, surface coverage, crystal size, crystal habit, degree of intergrowth, morphology, quality, and nature of thin films on Si (100) substrates may be evaluated at the conclusion of coating and *in situ* growth (Hitachi S4700). Energy Dispersive Spectroscopy (EDS) with an FEI Quanta 600 Field Emission Gun, Extended Vacuum is used to validate the elimination of the organic template after the

calcinations. **Table 2-2** summarizes the characterization techniques used in this dissertation to study the properties of silicate-1 (MFI) films.

Table 2-2. Characterization techniques used to characterize and study the properties of silicate-1 (MFI) films.

Characterization Techniques	Properties
X-Ray Diffraction (XRD)	Structure Identification
Scanning Electron Spectroscopy (SEM)	Film thickness and Morphology
Energy Dispersive Spectroscopy (EDS)	Element Composition

2.3.4 Strategies for Defect Elimination in Films

The quality and effectiveness of synthesis techniques, such as deposition techniques where the zeolite layer consists of individual crystals attached to the substrate by physical or chemical bonds, might result in inter-crystalline gaps or membrane defects, which can reduce sieving selectivity. [86] We assume comprehensive coverage of the films across the substrate during synthesis, based on the goal of film synthesis in this study. To obtain comprehensive coverage with intergrowth of films, we may need to tune synthesis parameters (gel composition, aging/crystallization durations, substrate orientation, crystallization temperature). The areas where extra caution and care must be applied to reduce film flaws and maximize yield can be boiled down to the following strategies:

- Using pure precursors that have been preserved in ideal circumstances.
- During aging, uniformly combining the precursors.
- Assuring the usage of clean substrates.
- Assuring that reaction vessels (autoclaves) are clean and free of depositions from previous synthesis.

- Before placing the reaction vessels in the oven, the temperature should be raised to achieve crystallization equilibrium.
- The substrate orientation can be changed to either horizontal or slightly angled depending on the desired film.

Flaking and peeling effects can be avoided by properly storing and managing the films.

2.4 References

54. Mervine, E. *Geology World of the Week: Z is for Zeolite*. 2012 October 28, 2012; Available from: <https://blogs.agu.org/georneys/2012/10/28/geology-word-of-the-week-z-is-for-zeolite/>.
55. *Zeolite Chemistry and Applications*. [cited 2022 April 6]; Available from: <https://www.frontiersin.org/research-topics/9329/zeolite-chemistry-and-applications#overview>.
56. Harrison, K. *Methoxsale, xanthotoxin, Oxsoralen, Deltasoralen, Meladinine*. Available from: <https://www.3dchem.com/molecules.asp?ID=86&ID=86>.
57. Bellussi, R.M.a.G., *Chapter 1: Zeolite Science and Perspectives*. *Zeolites in Catalysis: Properties and Applications*, 2017: p. 1-36.
58. Smith, J.V., *Definition of a zeolite*. *Zeolites*, 1984. **4**(4): p. 309-310.
59. Barrer, R.M. and E.A.D. White, 286. *The hydrothermal chemistry of silicates. Part II. Synthetic crystalline sodium aluminosilicates*. *Journal of The Chemical Society* (resumed), 1952: p. 1561-1571.
60. Milton, R.M., *Molecular Sieve Science and Technology: A Historic Perspective*. American Chemical Society 1989.

61. Flanigen, E.M., *Chapter 2 Zeolites and Molecular Sieves an Historical Perspective*, in *Studies in Surface Science and Catalysis*, H. van Bekkum, E.M. Flanigen, and J.C. Jansen, Editors. 1991, Elsevier. p. 13-34.
62. Choudary, N.V. and B.L. Newalkar, *Use of zeolites in petroleum refining and petrochemical processes: recent advances*. *Journal of Porous Materials*, 2011. **18**(6): p. 685-692.
63. Collins, F., et al., *A critical review of waste resources, synthesis, and applications for Zeolite LTA*. *Microporous and Mesoporous Materials*, 2020. **291**: p. 109667.
64. Król, M., *Natural vs. Synthetic Zeolites*. *Crystals*, 2020. **10**(7): p. 622.
65. Baig, N., I. Kammakakam, and W. Falath, *Nanomaterials: a review of synthesis methods, properties, recent progress, and challenges*. *Materials Advances*, 2021. **2**(6): p. 1821-1871.
66. Jeevanandam, J., et al., *Review on nanoparticles and nanostructured materials: history, sources, toxicity and regulations*. *Beilstein journal of nanotechnology*, 2018. **9**: p. 1050-1074.
67. Yang, S., et al., *Identifying Zeolite Frameworks with a Machine Learning Approach*. *The Journal of Physical Chemistry C*, 2009. **113**(52): p. 21721-21725.
68. Schulman, E., W. Wu, and D. Liu, *Two-Dimensional Zeolite Materials: Structural and Acidity Properties*. *Materials (Basel, Switzerland)*, 2020. **13**(8): p. 1822.
69. Agmon, N., *Isoelectronic Theory for Cationic Radii*. *Journal of the American Chemical Society*, 2017. **139**(42): p. 15068-15073.
70. Kosinov, N., et al., *Engineering of Transition Metal Catalysts Confined in Zeolites*. *Chemistry of Materials*, 2018. **30**(10): p. 3177-3198.

71. Szostak, R., *R. Szostak, Molecular sieves*. R. Szostak, Molecular sieves, Springer1998.
72. Davis, M.E. and R.F. Lobo, *Zeolite and molecular sieve synthesis*. Chemistry of Materials, 1992. **4**(4): p. 756-768.
73. ; Available from: <http://www.iza-online.org>.
74. Foster, T.J., *Antibiotic resistance in Staphylococcus aureus. Current status and future prospects*. FEMS Microbiology Reviews, 2017. **41**(3): p. 430-449.
75. Balasundram, V., et al., *Catalytic upgrading of biomass-derived pyrolysis vapour over metal-modified HZSM-5 into BTX: a comprehensive review*. Biomass Conversion and Biorefinery, 2020.
76. Jain, R., A.J. Mallette, and J.D. Rimer, *Controlling Nucleation Pathways in Zeolite Crystallization: Seeding Conceptual Methodologies for Advanced Materials Design*. Journal of the American Chemical Society, 2021. **143**(51): p. 21446-21460.
77. Jafari, S. and M. Sillanpää, *Chapter 2 - Adsorption of dyes onto modified titanium dioxide*, in *Advanced Water Treatment*, M. Sillanpää, Editor. 2020, Elsevier. p. 85-160.
78. J.D. Wright, N.A.S., *Sol-gel materials: chemistry and applications*. CRC press2000.
79. Rimer, J.D., et al., *Silica self-assembly and synthesis of microporous and mesoporous silicates*. Chemistry, 2006. **12**(11): p. 2926-34.
80. Czarna-Juszkiewicz, D., J. Cader, and M. Wdowin, *From coal ashes to solid sorbents for hydrogen storage*. Journal of Cleaner Production, 2020. **270**: p. 122355.
81. Valtchev, V. and L. Tosheva, *Porous Nanosized Particles: Preparation, Properties, and Applications*. Chemical Reviews, 2013. **113**(8): p. 6734-6760.
82. Ghaedi, H. and M. Zhao, *Review on Template Removal Techniques for Synthesis of Mesoporous Silica Materials*. Energy & Fuels, 2022. **36**(5): p. 2424-2446.

83. Narayanan, S., et al., *Recent advances in the synthesis and applications of mordenite zeolite – review*. RSC Advances, 2021. **11**(1): p. 250-267.
84. Khaleque, A., et al., *Zeolite synthesis from low-cost materials and environmental applications: A review*. Environmental Advances, 2020. **2**: p. 100019.
85. Morales, A.M. and C.M. Lieber, *A Laser Ablation Method for the Synthesis of Crystalline Semiconductor Nanowires*. Science, 1998. **279**(5348): p. 208-211.
86. Wang, X. and G.-R. Han, *Fabrication and characterization of anodic aluminum oxide template*. Microelectron. Eng., 2003. **66**(1–4): p. 166–170.
87. Huang, L., et al., *Fabrication of Ordered Porous Structures by Self-Assembly of Zeolite Nanocrystals*. Journal of the American Chemical Society, 2000. **122**(14): p. 3530-3531.
88. Ha, K., et al., *Aligned monolayer assembly of zeolite crystals on platinum, gold, and indium-tin oxide surfaces with molecular linkages*. Microporous and Mesoporous Materials - MICROPOROUS MESOPOROUS MAT, 2004. **72**.
89. Masuda, H. and K. Fukuda, *Ordered Metal Nanohole Arrays Made by a Two-Step Replication of Honeycomb Structures of Anodic Alumina*. Science, 1995. **268**(5216): p. 1466-1468.

Chapter – 3: Lysozyme Sorption of Pure – Silica (MFI) Films

3.1 Abstract

The management of infections associated with indwelling medical implants and prevention has remain a priority. The utilization of materials as antimicrobial agents has been explored to enhance the performance of implantable devices. Nanostructured, porous materials, like zeolites, have been suggested as possible materials for biomedical applications in implantable device coatings, tissue engineering, and drug delivery systems due to their unique interactions with biomolecules and biological environments. Here, the fundamental sorption interactions between a pure-silica zeolite (**MFI**) with lysozyme, a positively charged enzyme, are discussed.

Lysozyme sorption is considered a model for innate immunological processes in the body; high lysozyme sorption has been correlated with the material being a natural antibiotic and cell guardian. The impact of three different parameters on the sorption of lysozyme was evaluated via enzyme-linked immunosorbent assays (ELISAs) and bicinchoninic acid assays (BCAs), including the orientation of the thin film's crystal structure (b-oriented or randomly-oriented), the lysozyme incubation volume (200 μL , 400 μL , 600 μL , 800 μL), and the lysozyme incubation time (1, 6, and 24 hours). Additionally, the films were characterized via X-ray diffraction, scanning electron microscopy, and energy dispersive spectroscopy. In this work, we demonstrated that **MFI** films are capable of lysozyme sorption. Further, our observations suggested that, while crystal orientation did not play a significant role in the sorption process, incubation volume and time both impact sorption. The highest amounts of sorbed lysozyme were detected when films were incubated at intermediate volumes (400 and 600 μL) and shorter incubation times. The films' ability to sorb differing amounts of lysozyme, depending on uptake

parameters, make **MFI**-lysozyme coatings a tailorable candidate for supports and / or coatings for implantable device application as a material for infection control.

3.2 Introduction

Implants are becoming more common in modern medicine, and they are used in a variety of surgical operations for both functional and cosmetic reasons. The increasing use of implants is linked to a rise in perioperative infections problems, thus infection prevention is always a priority in clinical settings. [90] Implant coatings have been considered as a solution to biofilm formation. Zeolites are a group of nanostructured, microporous materials with crystalline pore structures and uniform pore sizes. They are commonly used in catalysis [91, 92], separations [93, 94], and ion exchange [95, 96] applications due to their high surface area, ability to host guest molecules, and high thermal/chemical stability. Beyond these traditional applications, they have been suggested for pharmaceutical applications as binders, carriers, diluents, and lubricants [97]. Additionally, zeolites have been proposed for external applications in cosmetics and dermatology, due to their ability to protect polymers from ultraviolet degradation [98]. Lastly, zeolites have been proposed for many biomedical applications, ranging from dialysis membranes [97] to image contrast agents [99], due to their high surface area, highly ordered porous network, and chemical stability. For example, zeolite powders, such as the pure-silica composition of ZSM-5 (structure code **MFI**), have been demonstrated to reduce the healing time for some types of wounds and surgical incisions [100, 101].

More recently, zeolite **MFI** nanoparticles have been investigated for their ability to prevent bacterial biofilm formation on implantable devices, which is an increasingly serious clinical

concern [11, 102]. For example, a study by Guo *et al.* [103] suggested that gentamicin-loaded, high-silica, **MFI** nanocrystals inhibit *Staphylococcus epidermis* (ATCC35984) proliferation, while allowing high viability of human bone marrow stromal cells. These particles exhibited three times the drug-loading capacity of hydroxyapatite particles. The researcher attributed this behavior to two main factors: (1) the partial insertion of the antibiotic in **MFI**'s microporous network, and (2) the formation of hydrogen bonds between the zeolitic framework and gentamicin molecules. Another study by Bhattacharya *et al.* [104] reported the non-cytotoxicity of **MFI** nanoparticles to human alveolar cells (A549). However, they warned of the possibility of lung diseases arising from long-term exposure and accumulation of zeolitic nanoparticles in lung tissue based on observed oxidative stress, increased mitochondrial activity, and genotoxic damage correlated to the presence of this material. Similarly, studies by Mitra *et al.* [105] and Beving *et al.* [106] suggested that zeolite **MFI** coatings could be good candidates to enhance the performance of orthopedic and dental implants because of their excellent corrosion resistance. In addition to this highly desirable property, Bedi *et al.* [107-109] demonstrated that **MFI** zeolite coatings promoted the proliferation of human fetal osteoblasts and their differentiation into mature cells when compared to the titanium alloy Ti6Al4V. Additionally, the authors observed higher levels of bone morphogenic protein expression in **MFI**-coated samples compared to uncoated samples. These findings presented evidence that zeolite **MFI** coatings could significantly contribute to the development of next-generation orthopedic implants by reducing patient recovery time and enhancing osseointegration.

For these and other emerging applications of zeolites in medicine, it is necessary to have a fundamental understanding of the response of a given zeolite to biological environments and

biomolecules. In particular, the ability of a given zeolite to sorb or otherwise interact with biomolecules is an important area to explore, as these interactions form the basis for the material's biocompatibility [110-114]. Biocompatibility refers to the material's ability to interact with living systems in such a manner as to not be toxic, injurious, or promote immunological rejection [115]. Common biocompatibility metrics include cytotoxicity studies [116-119], as well as sorption studies [120-128] of proteins or other biomolecules, such as enzymes. Cytotoxicity studies indicate if the material will kill cells through direct interactions with the material or chemicals released by the material, while sorption studies determine if specific biomolecules adhere to the surface of the material, or intercalate into the material's pore structure, providing valuable insight into the potential immunological response of the body to the material [129].

One of the more common sorption studies used in biocompatibility testing involves characterizing the interaction of lysozyme with a material [124-128]. Lysozyme is an enzyme that has a prolate spheroid shape (larger cross section of $3.0 \times 4.5 \text{ nm}^2$ and smaller cross section of $3.0 \times 3.0 \text{ nm}^2$) and a net positive charge at neutral pH [130]. It plays a fundamental role in protecting the human body from bacterial infections and is found in secretions such as mucus, tears, saliva, and milk [131, 132]. Its antibacterial effects arise from its ability to damage bacterial cell walls by catalyzing the hydrolysis of 1,4-beta linkages [133]. Bacterial cell walls contain a peptidoglycan layer, in which alternating molecules form a strong glycan chain that acts as a backbone [134], and lysozyme is able to break this glycan chain, resulting in the death of the bacteria [132]. Consequently, high concentrations of lysozyme in wound beds could potentially mitigate the occurrence of bacterial infections [135]. Furthermore, implantable devices whose surfaces are capable of lysozyme sorption could promote antibacterial activity at the implantation

site, which could reduce infection, inflammation, and the eventual need to replace the implant. Therefore, exploring the sorption of lysozyme into or onto zeolite materials could lead to potentially useful applications of zeolites as supports or coatings for implantable devices. It is hypothesized that these antibacterial properties, inherent to lysozyme molecules, can be enhanced by the microporous structure of zeolites, since immobilizing enzymes appears to improve their performance in harsher environments [136], such as implantation sites. Increased sorption of lysozyme could make the healing process around foreign bodies less susceptible to developing bacterial infections [137].

In this work, pure-silica **MFI** was chosen as a model system for zeolite sorption of enzymes due to its well-understood properties, its broad commercial use, and its potentially low toxicity when synthesized in the pure-silica composition [138]. Because of **MFI**'s small pore sizes (from 0.2 – 2 nm), penetration of lysozyme (3 – 4.5 nm) into the pores is unlikely without enzyme denaturation. However, **MFI** films will allow us to study the concentration of lysozyme that interacts with the material through both adsorption to the surface of the material and absorption into the material. This provides insight into the interactions of lysozyme with porous zeolite materials that can be extended to other similarly sized or functioned enzymes, guiding the adaptation of zeolites in future biomedical applications. This would add and enhance the natural antimicrobial microbial properties of zeolites which could be used as a form of infection control.

In this study, the influence of film orientation, incubation time, and incubation volume on the amount of sorbed lysozyme on **MFI** thin films was explored. The aging time and crystallization time of the zeolite syntheses steps remained constant. A software-aided experimental design was

employed to best capture the effect of each of these variables on lysozyme sorption. JMP12 (SAS) was used to assist in advanced experimental planning to minimize trial and error during experimentation. As determined by JMP12-aided experimental design, the incubation time was varied from 1 to 24 h, and the incubation volume was varied from 200 to 800 μL . Films were grown either on horizontal substrates, to obtain randomly oriented crystals, or slightly angled substrates, to obtain crystals whose lattice parameter b is preferentially perpendicular to the surface. For simplicity, we will refer to this second orientation of films as b -oriented films henceforth. **Table 3-1.** summarizes the experimental conditions used in this study.

Table 3-1. Summary of experimental conditions used to synthesize pure-silica **MFI** films on silicon wafer substrates. The substrates were placed either slightly angled or horizontally in the reaction container to encourage the formation of *b*-oriented or randomly – oriented **MFI** films, respectively.

Substrate Orientation	Slightly Angled												Horizontal					
Incubation Volume (μL)	200			400			600			800			200			400		
Incubation Time (h)	1	6	24	1	6	24	1	6	24	1	6	24	1	6	24	1	6	24

3.3 Materials and Methods

3.3.1 Synthesis of Pure – Silica (MFI) Films

Pure-silica **MFI** thin films were synthesized on silica-on-silicon (100) wafers from a clear reaction gel comprised of tetraethyl orthosilicate (TEOS) (10.2 g), tetrapropyl ammonium hydroxide (TPAOH) (4.06 g), and de-ionized (DI) water (101.94 g) according to the procedure reported by Exter *et al.* [139]. TPAOH was first combined with DI water in a clean, 125 ml Nalgene bottle equipped with a magnetic stir bar and a screw-on cap. After mixing the solution on the stir plate for 10 minutes, TEOS was added to the solution, which was then mixed on a stir plate for 1 hour. Square pieces (1 cm x 1 cm) of polished silicon (100) wafer were cleaned via piranha etch (1:4 by volume H₂O₂:H₂SO₄) for 30 minutes to remove organic contaminants. They were subsequently rinsed with DI water and air-dried. Each cleaned substrate was placed in a Teflon holder inside a 23 mL Teflon-lined Parr Autoclave vertically (to obtain b-oriented films), or horizontally with the polished side facing up (to obtain randomly oriented films). The liner was filled 2/3 full of the clear reaction gel and baked in an oven (Thermo Scientific Heratherm) at 165 °C for 6 hours. The autoclaves were then removed from the oven and quenched with cool, running water. Once cooled, the substrates were removed from the liners and rinsed with DI water, then dried at 80°C overnight. The structure-directing agent removal was done through calcination at 450 °C for 2 hours with a ramp rate of 0.5 °C in a tube furnace (Lindberg Blue) under atmospheric pressure.

3.3.2 Characterization

The structures of the resulting films were analyzed by X-ray diffraction (XRD) (Rigaku, 40 kV, 44 mA, wavelength 0.154 nm, 5-40 degrees two theta, speed of 1 degree/min, step size 0.02) to

assure that the structure was intact after calcination. Energy dispersive spectroscopy (EDS, Bruker Quanta 200 with Xflash6) was used to analyze the chemical composition of the films after calcination, to verify that the structure-directing agent was completely removed. Scanning electron microscopy (SEM, Bruker Quanta 200) was used to evaluate the film integrity, crystal size, and film thickness.

3.3.3 Enzyme-linked Immunosorbent Assay (ELISA)

Enzyme-linked Immunosorbent Assay (ELISA) is a biochemical technique used to detect and quantify substances such as peptides, proteins, antibodies, and hormones. In this work, it was used to measure lysozyme adsorption to the zeolite film surfaces. In a glass vial, 2 mg of lysozyme (LYZ) was dissolved in 2 mL of phosphate buffered saline (PBS) solution. The solution was stirred for approximately 15 minutes. In a 24-well tissue culture polystyrene (TCPS) plate, 150 μ L of the lysozyme solution was pipetted into 3 wells as controls. In addition, varying volumes of lysozyme solution were pipetted into separate vials containing zeolite films, which were subsequently incubated for 1.5 hours. The volumes of lysozyme solution that were tested were 800 μ L, 600 μ L, 400 μ L, and 200 μ L. During the incubation period, 0.2 g of anti-LYZ was dissolved in 20 mL of PBS. When the 1.5 hours incubation time came to an end, the TCPS wells were rinsed 5 times with PBS solution and the well plate was patted dry with a Kimwipe®. The films were also rinsed 5 times with PBS solution in the vial, then the films were removed from the vials and placed in a plastic petri dish where they were rinsed 3 additional times with PBS solution. Each zeolite film was then exposed to 2 mL of anti-LYZ solution while the TCPS control wells were exposed to 150 μ L of the anti-LYZ solution for 1.5 hours. During

antibody exposure, the substrate solution (16 μL of hydrogen peroxide and 0.021 g of urea, in 50 mL of DI water) was mixed with one phosphate-citrate buffer tablet (~1.42 g) and 50 mg of OPD. After the 1.5-hour anti-LYZ exposure, the well plate was again rinsed 5 times with PBS solution and the well plate was patted dry with a Kimwipe®. The films were also rinsed 5 times with PBS solution in the vial, then the films were removed from the vials and rinsed an additional 3 times with PBS solution. Each film was then relocated to an empty well in the TCPS well plate. The substrate solution, containing OPD (800 μL), was then added to all of the wells, including the TCPS control wells. The well plate was immediately placed in a Biotek PowerWave XS2 multi-well plate reader for 30 minutes with a set-point temperature of 25 °C and the absorbance at 492 nm was recorded using Gen5 1.07 software (BioTek). After 30 minutes, the films were removed from the wells and the well plate was reinserted into the plate reader for a single test point absorbance measurement at 492 nm without interference from the zeolite substrate. The absorbance results from the ELISA assay were normalized to the absorbance from the TCPS control wells and the lysozyme sorption for each experimental condition was quantified from a minimum of three independently prepared samples and the results are presented as the average of these trials ($n \geq 3$). Propagation of experimental error was used to represent the repeatability of the results for each condition. Results were compared using pairwise, two-tailed t-tests. P-values smaller than 0.05 were considered statistically significant.

3.3.4 Bicinchoninic Acid Assay

In addition to evaluating the relative amount of lysozyme adsorbed on the surface via ELISAs, we utilized bicinchoninic acid assays to evaluate the amount of protein left in the incubation solution after the films were removed. This would enable an estimation of the amount of

lysozyme that absorbed into the porous framework, in addition to that adsorbing to the surface (measurable by ELISA). After the films had been incubated for 1.5 hours in various volumes of lysozyme solution (200 – 800 μL) and times (1, 6 or 24 h), they were removed from the enzyme solution and the amount of adsorbed lysozyme was evaluated according to the procedures described in subsection 3.3.3. Three aliquots of 25 μL of the remaining lysozyme solution were then pipetted to a 96-well plate. A standard curve of lysozyme solutions was also prepared in the well plate with concentrations ranging from 2000 to 0 $\mu\text{L}/\text{mL}$. The BCA working reagent was prepared according to the manufacturer's instructions, and 200 μL were subsequently pipetted into each well. The well plate was covered and left to rest at 37 °C for 30 minutes, and the absorbance at 562 nm was recorded using a Biotek PowerWave XS2 multi-well plate reader. Using the standard curves, the concentration of lysozyme was calculated from the absorbance readings. BCA results are presented as the average \pm standard deviation of three independent experiments ($n = 3$). Comparing the amount of lysozyme adsorbed on the surface and the amount of lysozyme leftover in the solution allowed us to make inferences about the dynamics of the sorption process, especially regarding pore penetration. Results were compared using a two-way analysis of variance and a Tukey-Kramer *post hoc* test. P-values smaller than 0.05 were considered statistically significant.

3.4 Results and Discussion

3.4.1 Film Characteristics

The **MFI** films were characterized to confirm their structure and film orientation. SEM micrographs of the resulting calcined films (**Figure 3-1.**) showed the typical coffin-like crystal

habit, as well as a surface that was fully covered by interconnected crystals. Typically, the films exhibited a thick, intergrown crystalline film with a layer of partially-intergrown crystals on top of this. The crystals averaged approximately 5-8 μm in length, 2-4 μm in width, and approximately 1 μm in thickness. The film thickness achieved under these processing conditions was $170 \pm 3 \mu\text{m}$ for randomly oriented film, and $100 \pm 5 \mu\text{m}$ for b-oriented films, based on the cross-sectional SEM images also shown in **Figure 3-1**. Further characterization of the films was accomplished using EDS to evaluate the amount of carbon present in the film after calcination and the results are summarized in **Table 3-2**. The data indicated that the structure-directing agent was completely removed from pores of the pure-silica zeolite **MFI** film, creating open pores, based on the lack of detectable carbon. X-ray diffraction patterns for the film samples, seen in **Figure 3-2**, confirm that the as-made and calcined films had the **MFI** structure, either as *b*-oriented or randomly oriented and that the structure of the films remained intact after calcination [48].

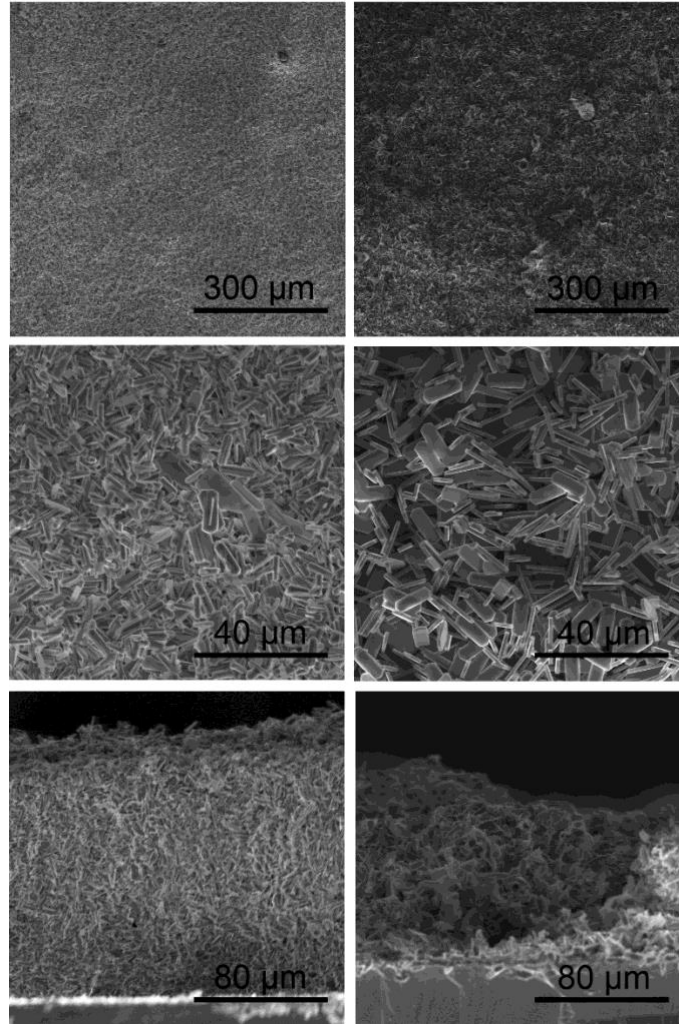


Figure 3-1. Representative SEM micrographs of pure – silica **MFI** films; randomly – oriented films are shown in the left column, *b*-oriented films in the right column. Surface views (top and middle rows) show characteristic, coffin-like crystals (5 – 8 μm), providing a secondary indication that **MFI** was successfully synthesized. In addition, it is evident that *b*-oriented films possess less compacted domains while randomly-oriented films do not. Cross-section micrographs show a representative measure of film thickness (randomly oriented: $170 \pm 3 \mu\text{m}$ and *b*-oriented: $100 \pm 5 \mu\text{m}$) in the bottom row. It is apparent from these images that the top layer of crystals has macroporosity due to spacing among crystals.

Table 3-2. Carbon-to-silicon ratio of pure-silica **MFI** films measured using EDS. After calcination, the presence of carbon was not detected, indicating successful structure-directing agent removal.

Spot Point	Point 1	Point 2	Point 3
C/Si Ratio	0.00	0.00	0.00

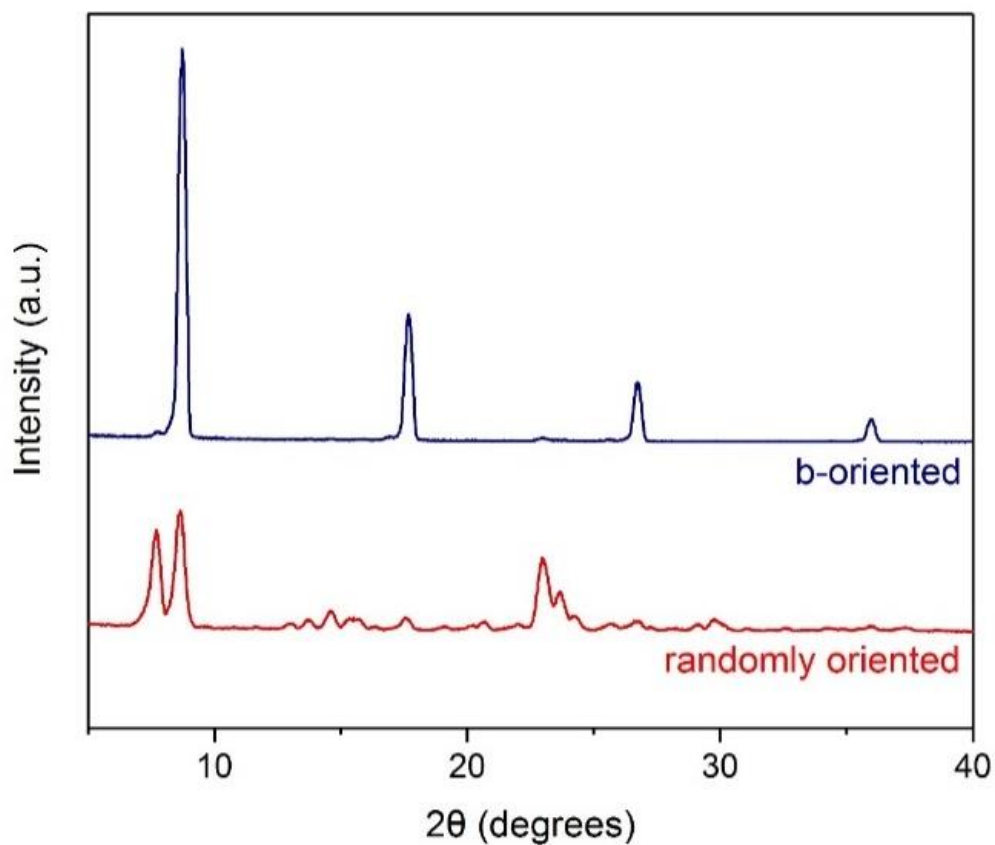


Figure 3-2. Representative X-ray diffraction patterns of *b*-oriented (top) and randomly-oriented **MFI** films (bottom) show that the synthesis was capable of producing the expected zeolite structure.

3.4.2 Lysozyme Surface Adsorption

One of the primary objective of this study was to explore the sorption of lysozyme to **MFI** films in order to gain further insight into the potential for these materials to be used as antibacterial coatings for implantable devices. This was achieved by exploring the influence of crystal orientation, incubation time, and incubation volume using ELISA and BCA. It is important to point out that the use of ELISA allowed for the comparison of lysozyme adsorption between samples, but it is not typically used to provide a *quantitative* analysis of the adsorbed amount. All of the results obtained in this study were normalized to the amount of lysozyme that adsorbed to a TCPS control sample from 150 μL of 1 mg/mL lysozyme in PBS. Moreover, because the ELISA technique is also not capable of directly detecting adsorbed lysozyme molecules, insight into the role of *absorption* in the overall sorption discussion was based on differences in the adsorbed amounts detected and the total lysozyme depletion as measured via BCA.

The first variable that was characterized was the influence of the zeolite crystal orientation on the adsorption of lysozyme. **Figure 3-3** provides comparisons of the amount of lysozyme that adsorbed to either *b*-oriented or randomly-oriented crystals from either 200 μL or 800 μL of solution, following either 1 hour or 24 hours of exposure. Under the majority of the experimental conditions examined here, there were no significant differences in the adsorbed amount of lysozyme as a function of the film orientation. The one exception was seen following twenty-four hours of lysozyme adsorption from both 200 and 800 μL of solution. Under these conditions, there was statistically, significantly lower adsorption on the *b*-oriented film as compared to the randomly-oriented film from 200 μL of solution; the opposite behavior was observed following adsorption from 800 μL of solution. It is possible that the differences in

adsorbed lysozyme following 24 hours of exposure are due to differences in the absorption responses, as discussed in more detail below.

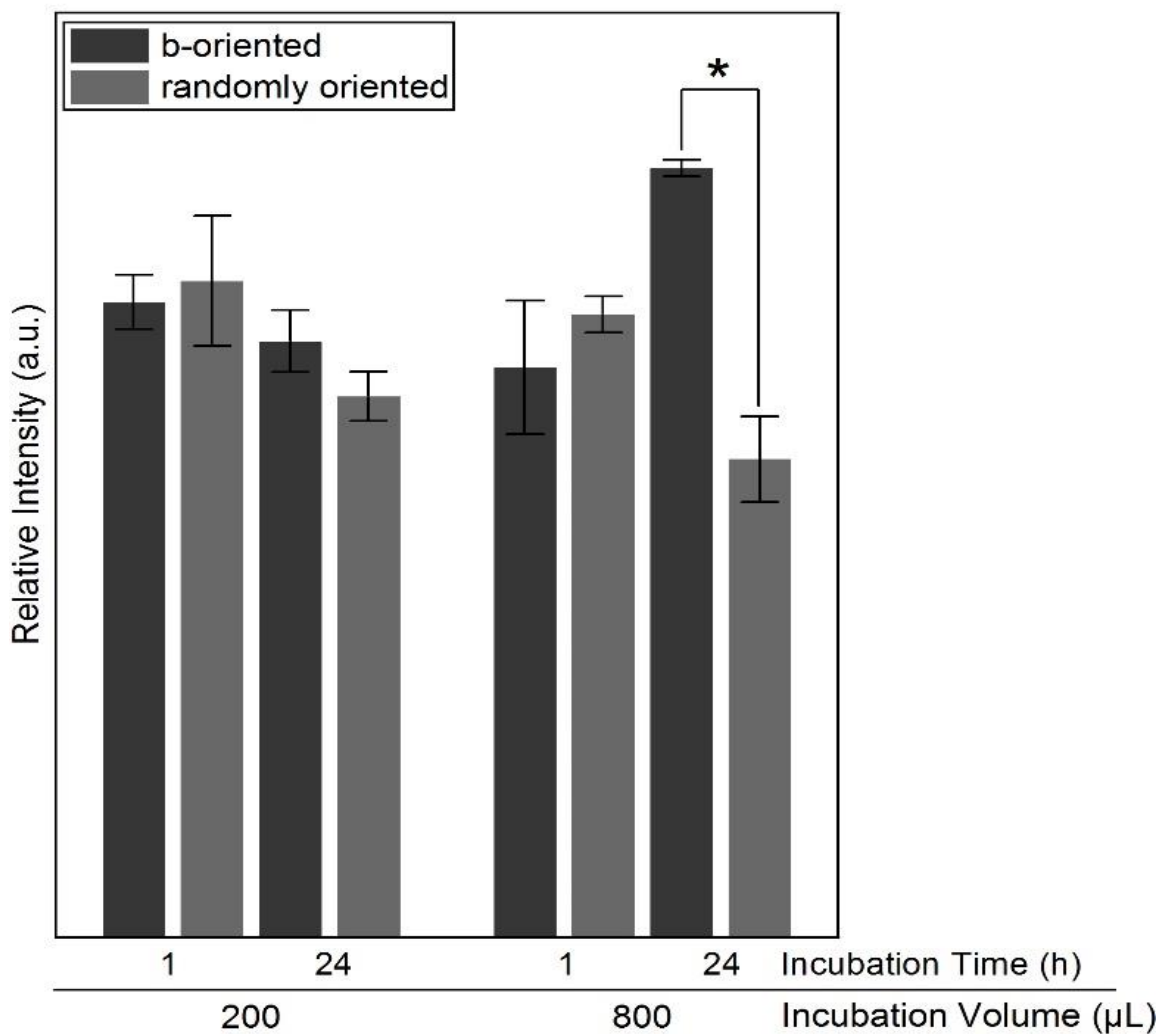


Figure 3-3. Influence of film orientation on lysozyme adsorption onto pure-silica **MFI** films incubated for different times and different volumes of lysozyme solution. Results are presented as the mean normalized absorbance from three independent experiments ($n = 3$) and the error bars represent the propagated experimental error. A * indicates a p -value < 0.05 between the samples indicated.

Hu *et al.* [140] suggested that there is a strong relationship between adsorption capacity and exposed lattice plane on protein-zeolite systems. Particularly, they observed this trend on the adsorption of cytochrome c, myoglobin, and transferrin onto nanozeolite L (**LTL**). By varying **LTL** nanorods length-to-radius ratio, they concluded that abundant exposure of pore openings was the main cause of enhanced protein adsorption capacity for all three proteins studied. Based on their observations, we expected to find differences between the amount of adsorbed lysozyme onto randomly-oriented films and *b*-oriented films, because the broadest channels within the **MFI** framework are parallel to the lattice direction (*b*). Hence, *b*-oriented films have more exposed pore openings than randomly-oriented films, which may lead to enhanced sorption behaviors. For this reason, the subsequent characterizations were focused on the *b*-oriented films alone to reduce the number of experimental variables.

The next variables that were examined were the influence of exposure time and incubation volume on the subsequent level of lysozyme adsorption and the results can be seen in **Figure 3-4**. When the *b*-oriented zeolite films were exposed to 200 μL of lysozyme solution, there was a slight decrease in the adsorbed amount as a function of time, although the results were not statistically significant. One potential explanation for this response is that, over time, the lysozyme penetrated the pore structure of the underlying zeolite structure, causing a reduction in the amount of detectable lysozyme on the surface. Conversely, when *b*-oriented films were exposed to 400 μL and 600 μL of lysozyme solution, the amount of detected lysozyme was greater after 1 hour of incubation than at the other two time points. However, no statistically significant difference was observed between samples incubated for 6 hours and 24 hours.

A different trend was observed when the samples were exposed to 800 μL of lysozyme solution. The lowest levels of surface-bound enzymes were seen following 1 hour of exposure, followed by 6 hours and 24 hours. The amounts of lysozyme on the surface of **MFI** films following these three incubation times were statistically different from each other. While these samples should still promote lysozyme penetration into the pore structure over time, similar to the postulation for the samples exposed to 200 μL , these results suggested an additional phenomenon could be occurring. It is possible that the strongest, surface-bound lysozyme molecules were unfolding, which caused the release of loosely bound lysozyme molecules back into solution. Finally, when the relative adsorption amounts at identical time points were compared among across the volumes studied here, it could be seen that this variable also played a role in the sorption processes. The highest levels of adsorbed species were detected at the intermediate incubation volumes (400 and 600 μL) for all incubation times and the lowest levels of adsorbed species.

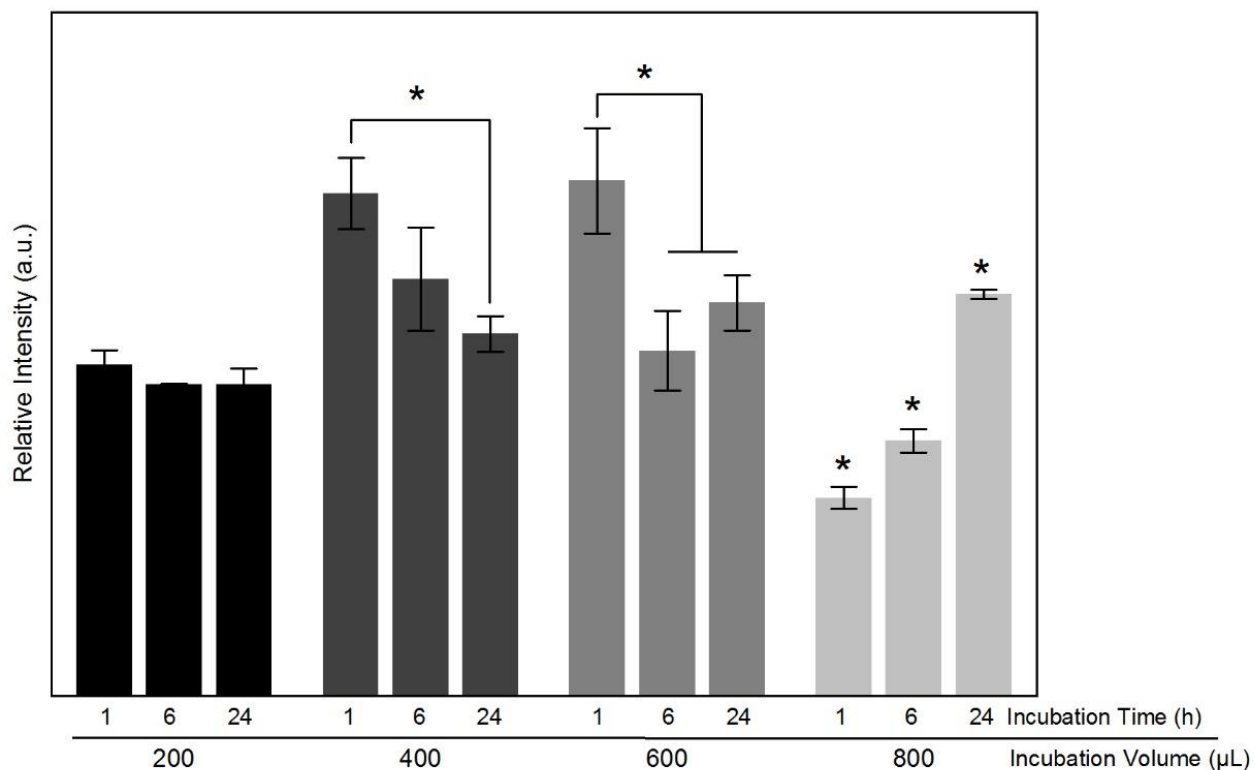


Figure 3-4. Influence of incubation time and volume on lysozyme adsorption onto *b*-oriented MFI films. The results are presented as the mean absorbance from three independent experiments ($n = 3$) and the error bars represent the propagated experimental error. A * indicates a p -value < 0.05 between the samples indicated.

3.4.3 Total Lysozyme Sorption

To further test the hypothesis that there was lysozyme penetration into the pore structure of these samples, a BCA assay was completed to quantify the amount of lysozyme that can be detected in the supernatant solution after incubation. Samples were incubated in a 1 mg/mL lysozyme solution (LYZ), followed by analysis of the supernatant. The data (**Figure 3-5**) indicated that the solution concentration of lysozyme dropped to around 35-40% of the original concentration

following lysozyme sorption. None of the measured solution concentrations were significantly different from each other, suggesting that there is no change in the lysozyme solution concentration following the initial drop upon exposure to the zeolite samples. These results also supported the hypothesis that the surface concentration of lysozyme is decreasing as the enzymes begin to penetrate the pores. If the bound molecules were being released from the surface back into solution, then there would be a corresponding increase in the buffer concentration.

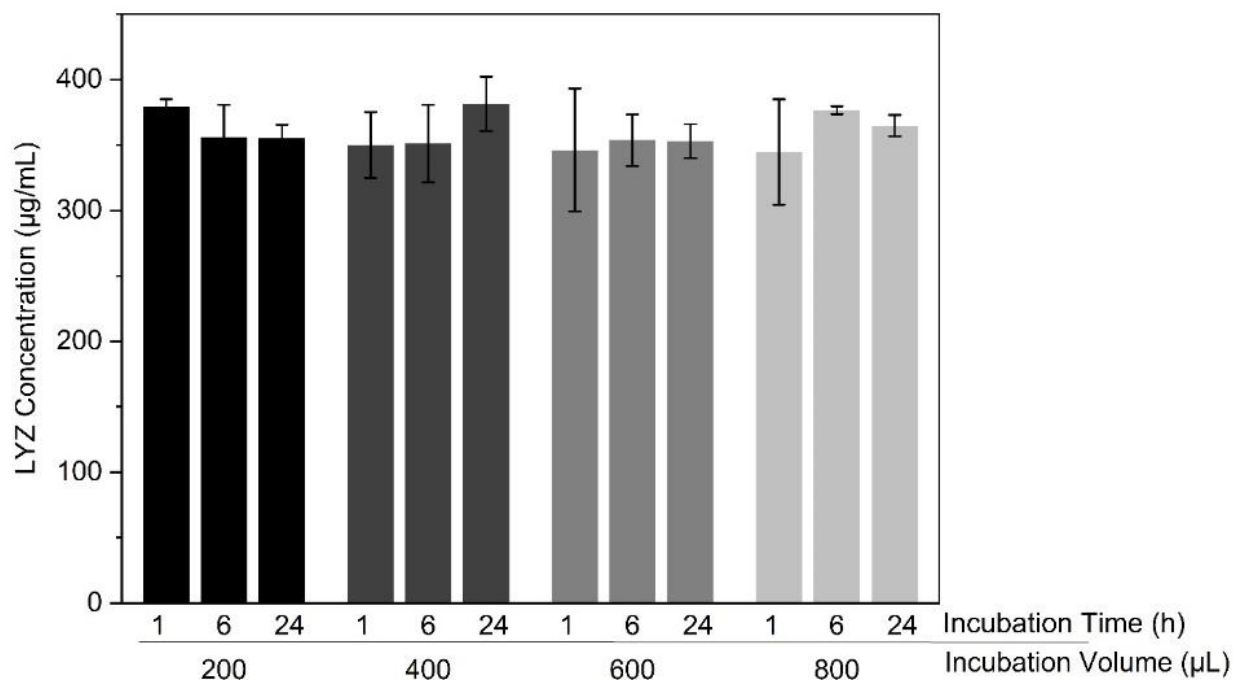


Figure 3-5. Lysozyme concentration in the supernatant solution following **MFI** incubation. No statistically significant differences were seen in these data, indicating that approximately 35% of the initial protein (400 µg) remains in solution after lysozyme sorption regardless of incubation conditions.

3.4 Conclusion

We have demonstrated that siliceous **MFI** thin films are capable of lysozyme sorption, but that sorption occurs in a time- and concentration-dependent manner suspected to be due to the interactions between lysozyme molecules and the underlying film material. The surface adsorption, investigated through ELISAs, appears to be dependent on incubation volume and incubation time. For instance, when incubated at 400 or 600 μL , the surface concentration of lysozyme significantly decreases over time. Conversely, at a higher incubation volume (800 μL), surface concentration increases with time. When contrasted with the total lysozyme sorption, evaluated via BCAs, these results suggest that, at 400 and 600 μL , LYZ molecules are penetrating the porous network and/or inter-crystals spaces in the films, while at 800 μL , this process likely occurs more rapidly followed by a slow, outer-surface adsorption.

Understanding uptake/release process of lysozyme molecules onto inorganic biomaterials, such as pure-silica zeolite **MFI** is fundamental to the application of these systems in next-generation antibacterial coatings for implantable devices, like orthopedic implants and/or implantable sensors. Our results suggest that this process is not significantly influenced by crystal orientation on the substrate. Rather, it appears that it can be tailored via controlling incubation parameters such as volume and time; future work suggests that continued investigation of the effects of this uptake on antibacterial processes for implantable devices could greatly improve the design and development of coatings for implantable devices. The ability of pure-silica zeolite **MFI** films to sorb lysozyme can enhance their antimicrobial properties, can make these films a good candidate for antimicrobial coatings in implantable devices. This can be a potential solution to infection control and reducing the risk of biofilm formation of pathogenic bacterial species.

3.5 References

90. Shahid, A., et al., *The prospects of antimicrobial coated medical implants*. Journal of Applied Biomaterials & Functional Materials, 2021. **19**: p. 22808000211040304.
91. Martin, A., *Zeolite Catalysis*. Catalysts, 2016. **6**(8): p. 118.
92. Weitkamp, J., *Zeolites and catalysis*. Solid State Ionics, 2000. **131**(1–2): p. 175-188.
93. Faruque Hasan, M.M., E.L. First, and C.A. Floudas, *Discovery of novel zeolites and multi-zeolite processes for p-xylene separation using simulated moving bed (SMB) chromatography*. Chemical Engineering Science, 2017. **159**: p. 3-17.
94. Huong, P.T. and B.K. Lee, *Improvement of selective separation of CO₂ over N₂ by transition metal-exchanged nano-zeolite*. Microporous and Mesoporous Materials, 2017. **241**: p. 155-164.
95. Al-Jubouri, S.M. and S.M. Holmes, *Hierarchically porous zeolite X composites for manganese ion-exchange and solidification: Equilibrium isotherms, kinetic and thermodynamic studies*. Chemical Engineering Journal, 2017. **308**: p. 476-491.
96. Król, M., W. Mozgawa, and W. Jastrzębski, *Theoretical and experimental study of ion-exchange process on zeolites from 5-1 structural group*. Journal of Porous Materials, 2016. **23**(1): p. 1-9.
97. Joughehdousta, S. and S. Manafib. *Application of Zeolite in Biomedical Engineering: A Review*. in *Iran International Zeolite Conference*. 2008.
98. Auerbach, S.M., K.A. Carrado, and P.K. Dutta, *Handbook of Zeolite Science and Technology*. 2003: CRC Press.

99. Platas-Iglesias, C., et al., *Zeolite GdNaY nanoparticles with very high relaxivity for application as contrast agents in magnetic resonance imaging*. Chemistry—A European Journal, 2002. **8**(22): p. 5121-5131.
100. Paveli, K.I.a.M.H.I., *Medical Applications of Zeolites*. Handbook of Zeolite Science and Technology 2003.
101. Smith, J.V., *Geology, mineralogy, and human welfare*. Proceedings of the National Academy of Sciences, 1999. **96**(7): p. 3348-3349.
102. Costerton, J., L. Montanaro, and C. Arciola, *Biofilm in implant infections: its production and regulation*. The International journal of artificial organs, 2005. **28**(11): p. 1062-1068.
103. Guo, Y.P., et al., *Hydrothermal fabrication of ZSM-5 zeolites: Biocompatibility, drug delivery property, and bactericidal property*. Journal of Biomedical Materials Research Part B: Applied Biomaterials, 2014. **102**(3): p. 583-591.
104. Bhattacharya, K., et al., *Reactive oxygen species mediated DNA damage in human lung alveolar epithelial (A549) cells from exposure to non-cytotoxic MFI-type zeolite nanoparticles*. Toxicology letters, 2012. **215**(3): p. 151-160.
105. Mitra, A., et al., *Synthesis and corrosion resistance of high-silica zeolite MTW, BEA, and MFI coatings on steel and aluminum*. Journal of the Electrochemical Society, 2002. **149**(10): p. B472-B478.
106. Beving, D.E., et al., *Corrosion resistant high-silica-zeolite MFI coating one general solution formulation for aluminum alloy AA-2024-T3, AA-5052-H32, AA-6061-T4, and AA-7075-T6*. Journal of the Electrochemical Society, 2006. **153**(8): p. B325-B329.

107. Bedi, R.S., L.P. Zanello, and Y. Yan, *Osteoconductive and osteoinductive properties of zeolite MFI coatings on titanium alloys*. *Advanced Functional Materials*, 2009. **19**(24): p. 3856-3861.
108. Bedi, R.S., et al., *Bioactive Materials for Regenerative Medicine: Zeolite-Hydroxyapatite Bone Mimetic Coatings*. *Advanced Engineering Materials*, 2012. **14**(3): p. 200-206.
109. Bedi, R.S., et al., *Biocompatibility of corrosion-resistant zeolite coatings for titanium alloy biomedical implants*. *Acta Biomaterialia*, 2009. **5**(8): p. 3265-3271.
110. Vallet-Regí, M., *Ordered mesoporous materials in the context of drug delivery systems and bone tissue engineering*. *Chemistry—A European Journal*, 2006. **12**(23): p. 5934-5943.
111. Puleo, D.A. and R. Bizios, *Biological Interactions on Materials Surfaces: Understanding and Controlling Protein, Cell, and Tissue Responses*. 2009: Springer New York.
112. Wang, K., et al., *A review of protein adsorption on bioceramics*. *Interface Focus*, 2012. **2**(3): p. 259.
113. Brash, J.L., *Protein Surface Interactions and Biocompatibility: A Forty Year Perspective*, in *Proteins at Interfaces III State of the Art*. 2012, American Chemical Society. p. 277-300.
114. Roach, P., D. Farrar, and C.C. Perry, *Interpretation of Protein Adsorption: Surface-Induced Conformational Changes*. *Journal of the American Chemical Society*, 2005. **127**(22): p. 8168-8173.
115. Ratner, B.D., *The Biocompatibility Manifesto: Biocompatibility for the Twenty-first Century*. *Journal of Cardiovascular Translational Research*, 2011. **4**(5): p. 523-527.

116. Grant, S.A., et al., *Assessment of the biocompatibility and stability of a gold nanoparticle collagen bioscaffold*. Journal of Biomedical Materials Research Part A, 2014. **102**(2): p. 332-339.
117. Zhang, Y., et al., *Effect of size, shape, and surface modification on cytotoxicity of gold nanoparticles to human HEp-2 and canine MDCK cells*. Journal of Nanomaterials, 2012. **2012**: p. 7.
118. Geng, Z., et al., *Incorporation of silver and strontium in hydroxyapatite coating on titanium surface for enhanced antibacterial and biological properties*. Materials Science and Engineering: C, 2017. **71**: p. 852-861.
119. Lacerda-Santos, R., et al., *Citotoxicity of nonlatex elastomeric ligatures of orthodontic use*. Revista Materia, 2015. **20**(1): p. 1-7.
120. Schroeder, M.E., et al., *Multifunctional polyampholyte hydrogels with fouling resistance and protein conjugation capacity*. Biomacromolecules, 2013. **14**(9): p. 3112-3122.
121. Arima, Y. and H. Iwata, *Effect of wettability and surface functional groups on protein adsorption and cell adhesion using well-defined mixed self-assembled monolayers*. Biomaterials, 2007. **28**(20): p. 3074-3082.
122. Barrantes, A., et al., *Poly-l-lysine/heparin multilayer coatings prevent blood protein adsorption*. Journal of Colloid and Interface Science, 2017. **485**: p. 288-295.
123. Dobbins, S.C., D.E. McGrath, and M.T. Bernards, *Nonfouling hydrogels formed from charged monomer subunits*. The Journal of Physical Chemistry B, 2012. **116**(49): p. 14346-14352.
124. Figueiredo, K.C.D.S., et al., *Lysozyme Adsorption onto Different Supports: A Comparative Study*. Adsorption, 2005. **11**(2): p. 131-138.

125. Lei, H., et al., *Control of Lysozyme Adsorption by pH on Surfaces Modified with Polyampholyte Brushes*. Langmuir, 2014. **30**(2): p. 501-508.
126. Wei, T., M.A. Carignano, and I. Szleifer, *Lysozyme Adsorption on Polyethylene Surfaces: Why Are Long Simulations Needed?* Langmuir, 2011. **27**(19): p. 12074-12081.
127. Kubiak-Ossowska, K., et al., *Lysozyme adsorption at a silica surface using simulation and experiment: effects of pH on protein layer structure*. Physical Chemistry Chemical Physics, 2015. **17**(37): p. 24070-24077.
128. Qiao, S.Z., et al., *Synthesis and lysozyme adsorption of rod-like large-pore periodic mesoporous organosilica*. Progress in Solid State Chemistry, 2006. **34**(2-4): p. 249-256.
129. Lewallen, E.A., et al., *Biological strategies for improved osseointegration and osteoinduction of porous metal orthopedic implants*. Tissue Eng Part B Rev, 2015. **21**(2): p. 218-30.
130. Ru-Shi, L., *Controlled Nanofabrication: Advances and Applications*. 2012: Pan Stanford Publishing.
131. Hughey, V.L. and E.A. Johnson, *Antimicrobial activity of lysozyme against bacteria involved in food spoilage and food-borne disease*. Applied and Environmental Microbiology, 1987. **53**(9): p. 2165-2170.
132. Cegielska-Radziejewska, R., G. Lesnierowski, and J. Kijowski, *Antibacterial activity of hen egg white lysozyme modified by thermochemical technique*. European Food Research and Technology, 2009. **228**(5): p. 841-845.
133. Abe, Y., et al., *Effect on catalysis by replacement of catalytic residue from hen egg white lysozyme to *Venerupis philippinarum* lysozyme**. Protein Science, 2016. **25**(9): p. 1637-1647.

134. Brown, L., et al., *Through the wall: extracellular vesicles in Gram-positive bacteria, mycobacteria and fungi*. Nat Rev Micro, 2015. **13**(10): p. 620-630.
135. Johnson, L.N., *The structure and function of lysozyme*. Science Progress (1933-), 1966: p. 367-385.
136. Talebi, M., et al., *Stability improvement of immobilized α -amylase using nano pore zeolite*. Iranian journal of biotechnology, 2016. **14**(1): p. 33.
137. Thangavel, P., B. Ramachandran, and V. Muthuvijayan, *Fabrication of chitosan/gallic acid 3D microporous scaffold for tissue engineering applications*. Journal of Biomedical Materials Research Part B: Applied Biomaterials, 2016. **104**(4): p. 750-760.

Chapter – 4: Infection Control: Study of *b* – oriented pure-silica zeolite MFI films as a biocompatible device coating to reduce surgical site infections after implantation

4.1 Abstract

The pathogens, *Staphylococcus*, *Streptococcus*, and *Pseudomonas* are the prevalent pathogens detected in post-surgical infections following the implantation of a medical device. To reduce the chances of biofilm formation that lead to infection, it is important to consider how the surface of the implant interacts with its environment. For example, a coating may be required to ensure biocompatibility. In this study, we explored the synthesis conditions of aging (1 h and 3 h), crystallization time (3 h and 12 h), and substrate size (1.5 cm x 0.5 cm and 2.5 cm x 0.5 cm) for *b* – oriented, pure-silica zeolite **MFI** films and their interactions with lysozyme (incubations of 1 h and 24 h) to assess aspects of the films' biocompatibility for potential use as a coating for implantable devices. Variable synthesis conditions were explored to determine if films showing higher pore exposure to the surrounding environment resulted in more sorption behavior; higher sorption could enhance the films' anti-microbial properties by using lysozyme as a natural antibiotic against bacterial pathogens. Once the synthesis conditions were optimized based on lysozyme sorption, the films were exposed to L929 fibroblast murine cells for 7 days. Cell metabolic activity was evaluated on days 3 and 7. In this work, we demonstrated that *b* – oriented, pure-silica zeolite **MFI** films with synthesis conditions of 1 h aging time and 3 h crystallization time had high sorption of lysozyme detected. Further analysis showed that, when L929 murine fibroblast cells interacted with the films, a significant increase in metabolic activity compared to the positive control for day 3 and 7 resulted. The films' ability to allow for cell

proliferation indicates that *b* – oriented, pure-silica zeolite **MFI** films may be a potential candidate for implantable device coatings to improve their biocompatibility.

4.2 Introduction

Indwelling medical devices are one of the leading causes of device-associated infections [141] in the U.S. Wound infections occur in 2 - 4% of all patients undergoing surgery [142], resulting in 2 million infections each year in the U.S. [10] To treat an infection properly, the type of infection needs to be known. For instance, the infection could arise due to the presence of a biofilm around the implant site. Biofilms are bacterial colonies that form a matrix of extracellular polymeric substances, resulting in surfaces that are highly resistant to antimicrobial treatments. [143] Microbial cells cling to one another, and to a static surface, forming a biofilm (living or non-living). Biofilms of bacteria are usually harmful and can induce nosocomial illnesses.[144] Moreover, when a biofilm forms, it can be resistant to antimicrobial treatment because it can prevent antimicrobial agents from adhering to the surface of the material [7], resulting in continual infection, even after the initial infection has been treated. According to the National Institutes of Health (NIH), biofilm formation is linked to 65 percent and 80 percent of all microbial and chronic illnesses [145] respectively, resulting in an average of 23,000 deaths a year. [146]

Previous researchers have investigated two key methods for limiting biofilm formation: (1) developing biofilm inhibitors, and (2) changing the materials used in medical devices to minimize biofilm formation. [147]. Additionally, there are three factors to consider when developing an antimicrobial coating for anti-adhesion devices: (1) modifying the chemistry of

the surface; (2) changing the topography of the surface; and (3) applying a surface coating that contains bactericidal agents to make implants more functional.

The interactions of inorganic-based biomaterials within biological systems have shown to be effective in reducing biofilm formation at the surface. [148] Inorganic biomaterials have recently been discovered that can control biological responses, such as cell–cell and cell–matrix interactions. [149] Under a variety of physiological situations, *structured, porous*, inorganic materials demonstrate remarkable chemical and mechanical stability, [150] and can be grafted with bioadhesive and targeting moieties; moreover, their internal pore capacity preserves biological payloads from physiological degradation. [151] Such materials can change the diffusion rate of an adsorbed or encapsulated medicine, gene, or protein due to their hydrophilic nature and porous structure. [152] This organized porosity has been used in drug delivery applications to generate a sustained, regulated, or pulsed release. [153, 154] *Nanostructured* porous inorganic materials, such as microporous materials, are widely employed as drug delivery carriers for cancer therapy [153], gene transfer [155], and other applications.[150] They have the potential to extend the lives of individuals suffering from various diseases. [154]

Microporous inorganic materials, such as molecular sieves, and, in particular, zeolites, are currently of interest to researchers because of their molecular separation capabilities, which include size-dependent filtration or sieving, shape-specific molecular recognition, adsorption, and catalytic activity. [156] Zeolites are “tridimensional crystalline aluminosilicates with pores/cavities of molecular dimensions.” [157] Common zeolite frameworks that have seen great utility in industry include **MOR**, **MFI**, and **FAU**. [158] While technically aluminosilicate

materials, many zeolites are able to be synthesized in a variety of compositions, including the pure-silica composition. For instance, pure-silica zeolite **MFI** nanoparticles have been investigated as a potential surface coating material that can prevent biofilm formation on implantable devices [159]. According to Wang *et al.*, the super hydrophilic character of the zeolite coating gives the material surface additional anti-adhesive properties, inhibiting bacterial proliferation. [160] The exploration of enhancing the environment of the coating *in vitro*, however, was not explored. Beyond these studies, several successfully antifouling techniques and antibacterial techniques have been researched in conjunction with zeolitic materials, such as passive antifouling surface changes, active antimicrobial surface modifications, pre-operative antimicrobial local carriers, and coatings. [161-164] For instance, even at modest Ag loadings and in the presence of large (10⁹ CFU per mL) bacterial concentrations, Ag-containing zeolites are highly effective against *Staphylococcus aureus* (SA) germs. [165] (Silver nanoparticles (AgNPs) have antibacterial activity and are now used as an alternative disinfectant for a variety of applications, including cleaning of aquatic environments and disinfection of medical devices and instrumentation. [166]) Additionally, due to their wound healing, blood coagulation, and antibacterial properties, zeolites appear to be a viable candidate for wound dressing and skin regeneration. [167] Although these methods have proven to show great promise in serving as an antimicrobial *host* to reduce infection and to promote a healing environment, it has been necessary to cross-link zeolites with nanoparticles, such as Ag, to achieve those properties. Moreover, very little work has been done to explore the *fundamental* biocompatibility of the zeolite materials, which is a necessary step, beyond verifying their ability to act as an antimicrobial coating in specific circumstances, in order for these materials to be used as implant coatings to address post-surgical infections around implantable devices.

Here, we investigate pure-silica zeolite **MFI** and observe its biocompatibility behavior *in vitro* to build on existing data about its antimicrobial performance. Zeolites have molecular dimensions: they can selectively allow particle sized compounds into or out of pores. [168] Moreover, they also demonstrate shape selectivity. [169] Due to their uniform pore structure and size, they may be leveraged as antimicrobial coatings and help stop the spread of pathogens that can cause diseases without inadvertently killing cells or “good bacteria” that are needed to maintain healthy function. [170] We have performed assays to detect the quantification of protein in complex mixture and the viability of L929 fibroblast murine cells to demonstrate that *b*-oriented, pure-silica MFI films are biocompatible (and can act as a drug eluting surface by the sorption of lysozyme over time).

4.3 Materials and Methods

4.3.1 Design of experiment

The effect of aging time and crystallization time on *b* – oriented, pure-silica zeolite MFI films were investigated in relation to lysozyme sorption. Changing the synthesis parameters of aging and crystallization [171] time could help obtain comprehensive coverage with intergrowth of films, exposing more pores. In a previous study done [172], *b* – oriented, pure-silica zeolite MFI films showed to have sorption of lysozyme due to more pore exposures, making this a viable candidate to hence the film’s nature antimicrobial properties. The incubation volume (800 μ L) of lysozyme and the incubation time of 1 and 24 h remained constant. Based on a previous study [172], *b* – orientated films showed higher sorption due to the exposure of more pores in the films to the surrounding environment; likely resulting in lysozyme molecules penetrating the

porous network and/or inter-crystal spaces. Varying the synthesis conditions of crystallization time and aging time to expose more pores and optimize the performance of the films. (**Table 4-1.**)

Table 4-1. The summary is a list of the experimental conditions used to make b-oriented MFI films on silicon wafer substrates. The substrates were slightly tilted in the reaction (the angle varied depending on the size of the substrate) to favor the development of b – oriented MFI films.

Sample	Substrate Size	Aging Time (h)	Crystallization Time (h)	Lysozyme Incubation Time (h)
Long	1.5 cm x 0.5 cm	1	3	1, 24
Short	2.5 cm x 0.5 cm	6	12	1, 24
Long	1.5 cm x 0.5 cm	1	3	1, 24
Short	2.5 cm x 0.5 cm	6	12	1, 24

4.3.2 Materials

Silica-on-silicon (100) (680~700 μm SiO_2 layer) wafers were purchased from University Wafers. Tetraethylorthosilicate (98%, TEOS) and tetrapropylammonium hydroxide (40%, TPAOH) were purchased from Sigma – Aldrich. Deionized (DI) water (Elga, Purelab Ultra, 18.2 $\text{M}\Omega/\text{cm}$) was used for all enzyme-linked immunosorbent assays (ELISAs). Lysozyme, from chicken egg white, was obtained from US Biological. Phosphate – Citrate buffer, O-Phenylenediamine (OPD), Urea was obtained from Sigma Aldrich. Hydrogen peroxide (H_2O_2) was obtained from Sigma – Aldrich and prepared in DI water. Tissue culture polystyrene (TCPS) plate (24 wells), with a well volume of 3.5 mL was obtained from Fisher Scientific. Anti-lysozyme antibody with conjugated horseradish peroxidase (anti-LYZ) was obtained from Lifespan Biosciences. L929 murine fibroblast cells, Eagle’s Minimum Essential Media supplemented with 10% (v/v) horse serum and 200 U/mL of Penicillin Streptomycin, Dulbecco’s Phosphate Buffered Saline (DBS), 1X were obtained from ATTC. Phosphate Buffer Saline (Sterile) was obtained from Boston BioProducts. Trypsin/EDTA was obtained from PremaCell. Cell Proliferation Reagent (WST-1), Trypsin Blue Solution was obtained from Sigma – Aldrich. Sterile tissue culture treated by vacuum gas plasma polystyrene non-pyrogenic individually packaged 48 and 96 well plates were obtained from Falcon.

4.3.3 Synthesis of b-oriented, pure-silica zeolite MFI Thin Films

b-oriented, pure-silica zeolite **MFI** films were synthesized on silica-on-silicon (100) wafers from a clear reaction gel comprised of TEOS (10.2 g), TPAOH (4.06 g), and DI water (101.94 g) according to the procedure reported by Exter *et al.* [173] TPAOH was first combined with DI water in a clean, 125 ml Nalgene bottle equipped with a magnetic stir bar and a screw-on cap.

After mixing the solution on the stir plate for 10 minutes, TEOS was added to the solution, which was then mixed on a stir plate for 1 hour or 6 hours. Square pieces (15. cm x 0.5 cm and 2.5 x 0.5 cm) of polished silicon (100) wafer were cleaned via piranha etch (1:4 by volume H₂O₂:H₂SO₄) for 30 minutes to remove organic contaminants. They were subsequently rinsed with DI water and air-dried. Each cleaned substrate was placed in a Teflon holder inside a 23 mL Teflon-lined Parr Autoclave vertically (to obtain b-oriented films). The liner was filled 2/3 full of the clear reaction gel and baked in an oven (Thermo Scientific Heratherm) at 165 °C for 3 hours or 12 hours. The autoclaves were then removed from the oven and quenched with cool, running water. Once cooled, the substrates were removed from the liners and rinsed with DI water, then dried at 80°C overnight. The structure-directing agent removal was done through calcination at 450 °C for 2 hours with a ramp rate of 0.5 °C in a tube furnace (Lindberg Blue) under atmospheric pressure.

4.3.4 Film Characterization

To ensure that the structure of the resultant films was intact after calcination, X-ray diffraction (XRD) (Rigaku, 40 kV, 44 mA, wavelength 0.154 nm, 5-40 degrees two theta, speed of 1 degree/min, step size 0.02) was utilized. The chemical composition of the films after calcination was analyzed using energy dispersive spectroscopy (Bruker Quanta 200 with Xflash6) to ensure that the structure-directing agent was eliminated. The film integrity, crystal size, and film thickness were all evaluated using scanning electron microscopy (SEM, Bruker Quanta 200).

4.3.5 Film Characterization

Peptides, proteins, antibodies, and hormones are detected and quantified using ELISA, a biological technique. It was utilized to measure lysozyme adsorption on zeolite film surfaces in this study. Two mg of lysozyme was dissolved in 2 mL of PBS solution in a glass vial. For around 15 minutes, the solution was swirled. Next, 150 liters of lysozyme solution were pipetted into three wells of a 24-well TCPS plate as controls. Moreover, different quantities of lysozyme solution were pipetted into separate vials containing zeolite films and incubated for 1 hour or 24 hours. The volume of lysozyme solution tested was 800 μ L. 0.2 g of anti-LYZ was dissolved in 20 mL of PBS during the incubation phase. The TCPS wells were rinsed 5 times with PBS solution after 1.5 hours of incubation, and the well plate was patted dry with a Kimwipe®. The films were also rinsed 5 times in the vial with PBS solution, then removed from the vials and placed in a plastic petri plate where they were rinsed 3 more times with PBS solution. After that, each zeolite film was exposed to 2 mL of anti-LYZ solution for 1.5 hours, while the TCPS control wells were subjected to 150 mL of anti-LYZ solution. The substrate solution (16 L hydrogen peroxide and 0.021 g urea in 50 mL DI water) was combined with one phosphate-citrate buffer tablet (1.422 g) and 50 mg of OPD during antibody exposure. The well plate was rinsed 5 times with PBS solution after the 1.5-hour anti-LYZ exposure and then patted dry with a Kimwipe®. The films were also rinsed five times in PBS solution in the vials, then taken from the vials and rinsed three more times in PBS solution. After that, each film was moved to an empty well in the TCPS well plate. All the wells, including the TCPS control wells, were then filled with the substrate solution containing OPD (800L). The absorbance at 492 nm was measured using Gen5 1.07 software after the well plate was placed in a Cytation 5, BioTek multi-well plate reader for 30 minutes at a set-point temperature of 25 °C (BioTek). The films

were extracted from the wells after 30 minutes, and the well plate was reinserted into the plate reader for a single test point absorbance measurement at 492 nm, free of interference from the zeolite substrate. The ELISA assay findings were standardized to the TCPS control wells' absorbance, and the lysozyme sorption for each experimental condition was quantified from at least three independently generated samples, with the results provided as the average of these trials (n 3).

4.3.6 Cell Viability (WST-1)

The fraction of live, healthy cells in a population is called cell viability. Cell viability assays were used to assess the overall health of cells, exposed to the films. to improve culture or experimental conditions, and to assess cell survival after exposure to chemicals, such as during a drug screen. Seventy percent ethanol was used to sterilize the zeolite films. The zeolite films were then cultured with an augmented cell medium for 24 hours (horse serum and Penn strep). L929 murine fibroblast cells were seeded at a concentration of 6.0×10^4 cells/mL after the cell medium was withdrawn. For 1, 3, and 7 days, assays were done with cells in contact with the *b* – orientated. The WST reagent was applied on days 1, 3, and 7 and incubated for 4 hours. After 4 hours, the media from each well was transferred to a fresh well plate, and absorbance was measured using a spectrofluorometer plate reader at 450 nm with a reference reading at 655 nm (Cytation 5, BioTek). The positive control of fibroblast cells with no *b* – orientated films served as the baseline for 100 percent cell viability. GraphPad Prism version 4.0 was used for all statistical analysis (GraphPad Software, Inc.). Tukey's post-test and a two-way ANOVA analysis of variance with a 95 percent confidence interval were used. There was expected to be a difference between the controls and the *b* – orientated films. To see if there are major differences between the samples, a small effect size was chosen.

4.4 Results and Discussion

4.4.1 Film Characterization

To confirm the structure and orientation of the films, they were characterized. Based on the lack of detectable carbon, the findings suggested that the structure directing agent was eliminated from the pores of the pure-silica **MFI** film, resulting in open pores. The film sample's X-ray diffraction patterns, shown in **Figure 4-1**, confirmed that the films had the *b* - oriented **MFI** structure and that this structure remained intact after calcination. The calcined films' SEM micrographs (**Figure 4-2**) revealed the typical coffin-like crystal habit, as well as a surface completely covered in interconnected crystals. Typically, the films had a thick, intergrown crystalline film on top of which was a layer of partially intergrown crystals.

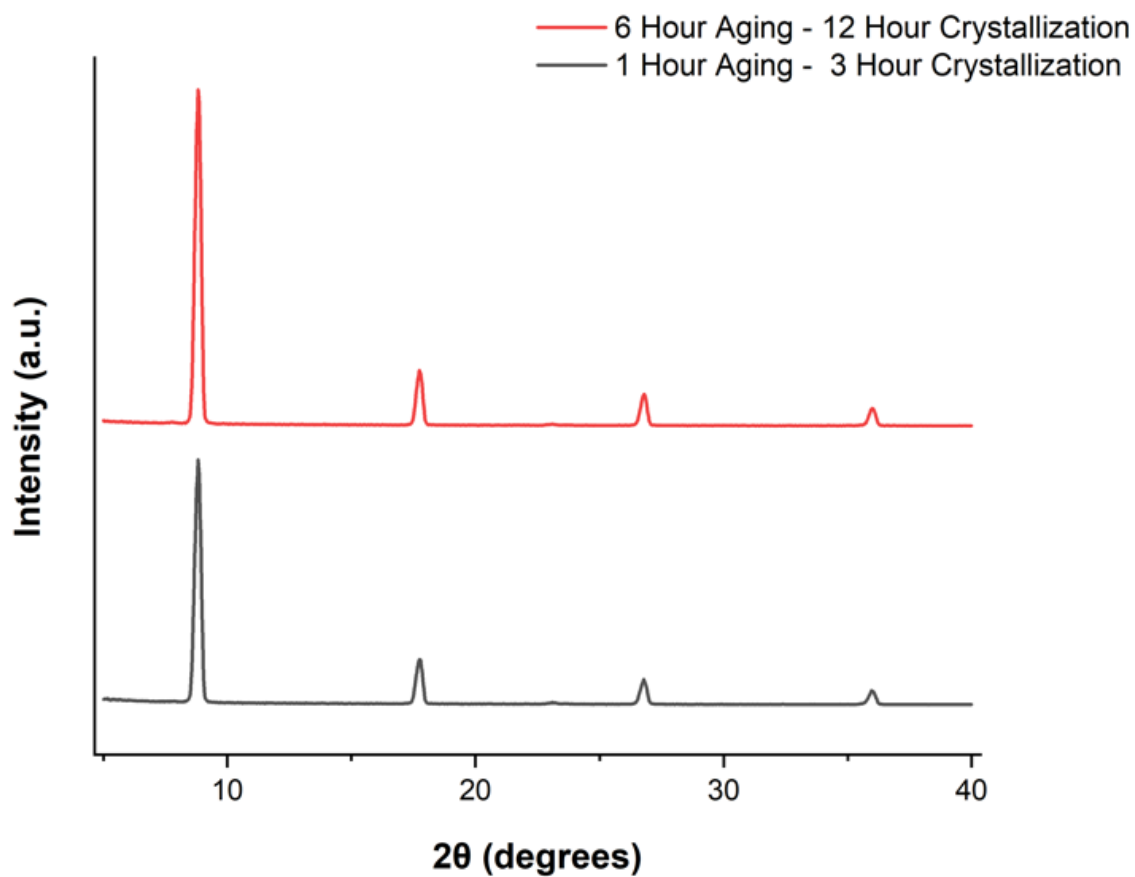


Figure 4-1. Representative X-ray diffraction patterns of *b*-oriented MFI films synthesized under 6 h aging time and 12 h crystallization time (top) and 1 h aging time and 3 h crystallization time (bottom) circumstances show that the syntheses produced the desired zeolite structure.

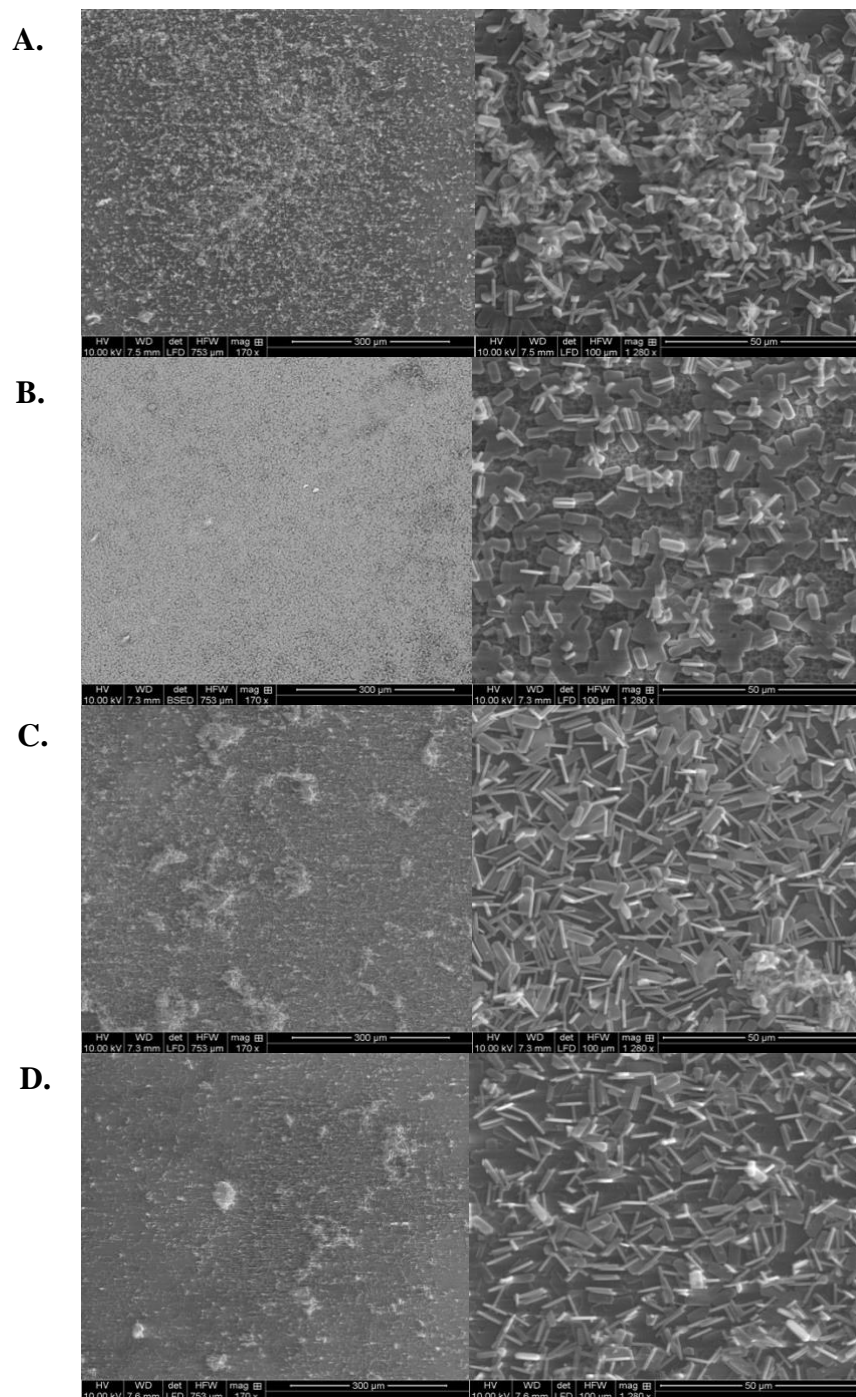


Figure 4-2. Representative SEM micrographs of *b* – oriented **MFI** films, (A) 1h – 3h – Short, (B) 1h – 3h – Long, (C) 6h – 12h – Short, and (D) 6h – 12h – Long. Surface views show characteristic, coffin-like crystals (5 – 8 μm), providing a secondary indication that **MFI** was successfully synthesized.

4.4.2 Lysozyme Sorption

One of the goals of this study was to investigate lysozyme sorption to MFI films to learn more about the potential for these materials to be used as antibacterial coatings for implantable devices. While this study did not evaluate MFI's antibacterial capabilities, as that has been explored [165, 174] elsewhere, lysozyme sorption is often a good indicator of a material's antibacterial capabilities. ELISAs and BCA tests were used to investigate the effects of crystal orientation, incubation period, and incubation volume. It is worth noting that while ELISAs allowed for comparisons of lysozyme adsorption between samples, they are not commonly employed to offer a quantitative study of the amount adsorbed. The amount of lysozyme adsorbed to a TCPS control sample from 150 L of 1 mg/mL lysozyme in PBS was used to standardize all the results reported in this investigation. The influence of zeolite synthesis parameters such as aging time, crystallization time, and the angle that the *b*-oriented crystals formed in on the adsorption of lysozyme was studied. **Figure 4-3** shows the amount of lysozyme absorbed by each sample type after an incubation of 800 μ L of solution for 1 h or 24 h after exposure. There was a significant change in the adsorbed amount of lysozyme as a function of film orientation under the majority of experimental circumstances evaluated. The sample with the synthesis condition of 1 h aging time, 3 h crystallization time, and substrate size of 1.5 cm x 0.5 cm (short) had an overall greater absorbance. Pore exposure for *b* – oriented films are known to have more pore openings facing the surrounding environment. Overall, 1 h aging time and 3 h crystallization time demonstrated a greater absorbance than 6 h aging time and 12 h crystallization time. Shortening these synthesis conditions could result in more pore openings and less crystal overgrowth.

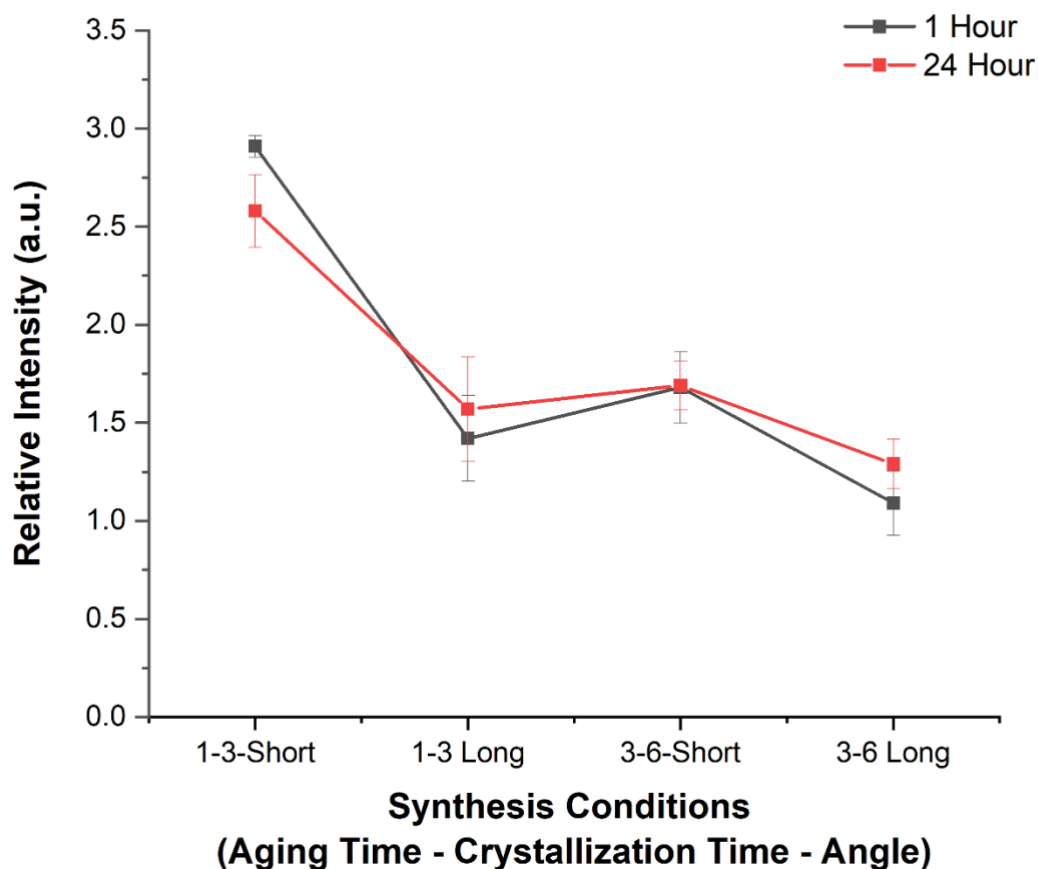


Figure 4-3. The effects of aging, crystallization, and incubation time on lysozyme adsorption on *b* - oriented, pure-silica **MFI** films. The data are presented as the average of four independent experiments' normalized absorbance.

4.4.3 Cell Viability

The interaction of L9292 murine fibroblast cells with *b* - oriented, pure-silica zeolite **MFI** films synthesized at 1 h aging, 3 h crystallization time, with a substrate size of 1.5 cm x 0.5 cm was

studied for 3 and 7 days using a WST-1 cell proliferation assay, which assesses cellular metabolic activity. Between the 3 and 7 – day the films appeared the be the most metabolically active relative on day 3 relative to day 7, shown in **Figure 4-4**. Both days maintained biocompatibility, the drop-in metabolic activity in day 7 could indicate several outcomes (1) sufficient cell adhesion to the surface of the film resulted in crowding on day 7 and/or (2) there was a higher concentration of metabolic activity at day 3 and at day 7 the cells adjusted to the environment surround the film. [175]

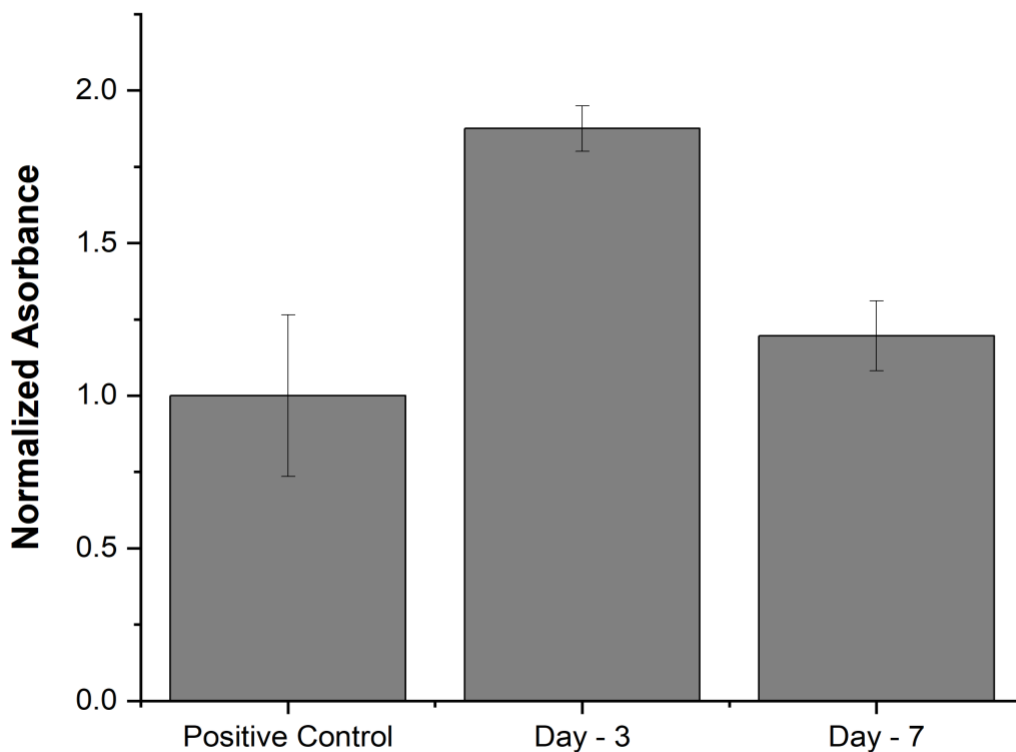


Figure 4-4. The normalized absorbance of 3 and 7 – day WST – 1 assay analyzing cellular viability of L929 fibroblast murine cells with *b*-oriented, pure-silica **MFI** films showed to increase the cell proliferation over time.

4.5 Conclusion

We successfully demonstrated that *b* – oriented, pure-silica zeolite **MFI** films are biocompatible, validated through an *in vitro* analysis of ELISA data from lysozyme sorption and WST–1 data to determine metabolic activity and cell viability of L929 murine cells. These results indicates that these films may serve as a new surface coating on implantable devices to mitigate infection.

Future studies should focus on understanding the biocompatibility of **MFI** films, through more *in vitro* analyses, such as reactive oxygen species (ROS), cell migration, and cell invasion assays.

A device coating to enhance its antimicrobial properties and its integration with the natural cell-matrix of the body to reduce infection and that has a controlled-drug delivery system can help reduce infections over a long-term time span, can greatly improve the performance and longevity of already existing biomedical applications. Future studies need to explore *b* – oriented, pure-silica zeolite MFI films further to better understand it's natural antimicrobial properties.

4.6 References

138. Colvin, J.R., *THE SIZE AND SHAPE OF LYSOZYME*. Canadian Journal of Chemistry, 1952. **30**(11): p. 831-834.
139. Den Exter, M., et al., *Stability of oriented silicalite-1 films in view of zeolite membrane preparation*. Zeolites, 1997. **19**(1): p. 13-20.
140. Hu, Y.-Y., et al., *Crystal plane-and size-dependent protein adsorption on nanozeolite*. The Journal of Physical Chemistry C, 2009. **113**(42): p. 18040-18046.
141. VanEpps, J.S. and J.G. Younger, *Implantable Device-Related Infection*. Shock (Augusta, Ga.), 2016. **46**(6): p. 597-608.

142. *Surgical Site Infections*. 2019 [cited 2022 March 25]; Available from:
<https://psnet.ahrq.gov/primer/surgical-site-infections>.
143. Donlan, R.M., *Biofilms: microbial life on surfaces*. Emerging infectious diseases, 2002. **8**(9): p. 881-890.
144. Jamal, M., et al., *Bacterial biofilm and associated infections*. J Chin Med Assoc, 2018. **81**(1): p. 7-11.
145. Vestby, L.K., et al., *Bacterial Biofilm and its Role in the Pathogenesis of Disease*. Antibiotics (Basel, Switzerland), 2020. **9**(2): p. 59.
146. Li, B. and T.J. Webster, *Bacteria antibiotic resistance: New challenges and opportunities for implant-associated orthopedic infections*. J Orthop Res, 2018. **36**(1): p. 22-32.
147. Subhadra, B., et al., *Control of Biofilm Formation in Healthcare: Recent Advances Exploiting Quorum-Sensing Interference Strategies and Multidrug Efflux Pump Inhibitors*. Materials (Basel), 2018. **11**(9).
148. Armentano, I., et al., *The interaction of bacteria with engineered nanostructured polymeric materials: a review*. TheScientificWorldJournal, 2014. **2014**: p. 410423-410423.
149. Brokesh, A.M. and A.K. Gaharwar, *Inorganic Biomaterials for Regenerative Medicine*. ACS Applied Materials & Interfaces, 2020. **12**(5): p. 5319-5344.
150. Arruebo, M., *Drug delivery from structured porous inorganic materials*. Wiley Interdiscip Rev Nanomed Nanobiotechnol, 2012. **4**(1): p. 16-30.
151. Din, F.U., et al., *Effective use of nanocarriers as drug delivery systems for the treatment of selected tumors*. International journal of nanomedicine, 2017. **12**: p. 7291-7309.

152. Patra, J.K., et al., *Nano based drug delivery systems: recent developments and future prospects*. Journal of nanobiotechnology, 2018. **16**(1): p. 71-71.
153. Trofimov, A.D., et al., *Porous Inorganic Carriers Based on Silica, Calcium Carbonate and Calcium Phosphate for Controlled/Modulated Drug Delivery: Fresh Outlook and Future Perspectives*. Pharmaceutics, 2018. **10**(4).
154. Sayed, E., et al., *Porous Inorganic Drug Delivery Systems-a Review*. AAPS PharmSciTech, 2017. **18**(5): p. 1507-1525.
155. Zhou, Y., et al., *Mesoporous silica nanoparticles for drug and gene delivery*. Acta Pharmaceutica Sinica B, 2018. **8**(2): p. 165-177.
156. Brinker, C.J., *Porous inorganic materials*. Current Opinion in Solid State and Materials Science, 1996. **1**(6): p. 798-805.
157. Corma, A., *Inorganic Solid Acids and Their Use in Acid-Catalyzed Hydrocarbon Reactions*. Chemical Reviews, 1995. **95**(3): p. 559-614.
158. Wang, Y., Y. Jiang, and M. Hunger, *Mechanism investigations of the methanol-to-olefine (MTO) process on acidic zeolite catalysts by in situ solid-state NMR spectroscopy*. Catalysis Today - CATAL TODAY, 2006. **113**.
159. Pourhajibagher, M. and A. Bahador, *Enhanced reduction of polymicrobial biofilms on the orthodontic brackets and enamel surface remineralization using zeolite-zinc oxide nanoparticles-based antimicrobial photodynamic therapy*. BMC Microbiology, 2021. **21**(1): p. 273.
160. Wang, J., et al., *Antibacterial and anti-adhesive zeolite coatings on titanium alloy surface*. Microporous and Mesoporous Materials, 2011. **146**(1): p. 216-222.

161. Milazzo, M., et al., *Biodegradable Polymeric Micro/Nano-Structures with Intrinsic Antifouling/Antimicrobial Properties: Relevance in Damaged Skin and Other Biomedical Applications*. Journal of Functional Biomaterials, 2020. **11**(3): p. 60.
162. Keskin, D., et al., *Nanogels: A novel approach in antimicrobial delivery systems and antimicrobial coatings*. Bioactive Materials, 2021. **6**(10): p. 3634-3657.
163. Wang, Y., et al., *Universal Antifouling and Photothermal Antibacterial Surfaces Based on Multifunctional Metal–Phenolic Networks for Prevention of Biofilm Formation*. ACS Applied Materials & Interfaces, 2021. **13**(41): p. 48403-48413.
164. Keskin, D., et al., *Highly Efficient Antimicrobial and Antifouling Surface Coatings with Triclosan-Loaded Nanogels*. ACS applied materials & interfaces, 2020. **12**(52): p. 57721-57731.
165. Lalueza, P., et al., *Antibacterial action of Ag-containing MFI zeolite at low Ag loadings*. Chemical Communications, 2011. **47**(2): p. 680-682.
166. Jaime-Acuña, O.E., et al., *Synthesis and Complete Antimicrobial Characterization of CEOBACTER, an Ag-Based Nanocomposite*. PLOS ONE, 2016. **11**(11): p. e0166205.
167. Zarrintaj, P., et al., *Zeolite in tissue engineering: Opportunities and challenges*. MedComm, 2020. **1**.
168. Durkee, J.B., *Chapter 11 - Stabilization of Solvents*, in *Cleaning with Solvents*, J.B. Durkee, Editor. 2014, William Andrew Publishing. p. 345-372.
169. Jia, X., et al., *Modern synthesis strategies for hierarchical zeolites: Bottom-up versus top-down strategies*. Advanced Powder Technology, 2019. **30**(3): p. 467-484.

170. Choi, S.-W., Y. Zhang, and Y. Xia, *Three-dimensional scaffolds for tissue engineering: the importance of uniformity in pore size and structure*. *Langmuir : the ACS journal of surfaces and colloids*, 2010. **26**(24): p. 19001-19006.
171. Patuwan, S.Z. and S.E. Arshad, *Important Synthesis Parameters Affecting Crystallization of Zeolite T: A Review*. *Materials (Basel, Switzerland)*, 2021. **14**(11): p. 2890.
172. Avery, K.L., et al., *Lysozyme sorption by pure-silica zeolite MFI films*. *Materials Today Communications*, 2019. **19**: p. 352-359.
173. den Exter, M.J., et al., *Stability of Oriented Silicalite-1 Films in View of Zeolite Membrane Preparation*. *Zeolites*, 1997. **19**(1): p. 13-20.
174. Peixoto, P., et al., *Metal Ion–Zeolite Materials against Resistant Bacteria, MRSA*. *Industrial & Engineering Chemistry Research*, 2021. **60**(35): p. 12883-12892.
175. Devendran, C., et al., *Cell Adhesion, Morphology, and Metabolism Variation via Acoustic Exposure within Microfluidic Cell Handling Systems*. *Advanced science (Weinheim, Baden-Wuerttemberg, Germany)*, 2019. **6**(24): p. 1902326-1902326.

Part II: Alternative Approaches for Post – Operative Infection Control Using Pre- and Pro-
Biotics: A Meta – Analysis

Chapter – 5: Meta-analysis of factors affecting probiotic establishment in pre-existing microbiomes

5.1 Abstract

Inoculation of microbial species (a.k.a. probiotics) into preexisting microbial communities is a strategy to improve the function of microbial communities and the systems they inhabit (e.g., human gastrointestinal track). Probiotics may be transient, or they may establish in the new system where they are introduced. Many factors may influence the success of probiotic establishment in preexisting microbial communities, including characteristics of the target environment, aspects of the probiotic species, and how the probiotic is delivered. However, the relative importance of factors is a critical knowledge gap that impedes microbiome engineering. To address this knowledge gap, we performed a systematic review and meta-analysis of published studies that examined the outcomes of probiotic introductions in human and animal gastrointestinal track. We found that most studies introducing probiotics introduce them daily and measure their effects on function during the application period, while few studies assess probiotic impacts in the post-delivery period. This suggests that most studies assume probiotics' presence and effects are transient. Understanding the factors that facilitate the successful establishment of inoculants is needed to improve microbiome engineering for human, animal, plant, and soil health.

5.2 Introduction

A transformative finding in biological research over the past 20 years has been the profound influence microbes may have on the functioning of the ecosystems (a.k.a hosts) in which they

reside. For example, the hundreds of microbial species tightly associated with any given plant are now conceived as an extension of the plant, expanding and modulating plant functional capabilities. [176, 177] Similarly, intestinal microbes have been linked to a plethora of human mental and physical health phenomena. [178] As a result, interest has soared in using microbial inoculants (probiotics) to steer ecosystem functioning. The number of published research articles on probiotics each year from 2002 to 2022 has increased over 6-fold, from less than 1000 to over 6000 per year according to a Scopus database search. [179] The target ecosystems for inoculation of probiotics include industrial fermenters [180], waste treatment ponds [181], algal farms [182], plants [183], agricultural soils [184], and the gastrointestinal track and skin of animals including human. [185] The performance applications are even more diverse, targeting problems in human/animal health [186], agriculture [187], energy [188], waste clean-up [189], and climate management. [190]

As the volume of probiotic research has soared, so too has the need to assess research gaps to avoid wasteful investments and to accelerate progress on neglected obstacles that limit probiotic effectiveness. [191] Numerous *qualitative* reviews of probiotic research have been published. Albright *et al.* (ibid) recently emphasized the need for *quantitative* syntheses of probiotic research, particularly meta-analyses that quantify the impact of factors that may affect the magnitude or longevity of probiotic functional effects. **To address these priorities, we performed a quantitative assessment of probiotic research focused primarily on human and animal gut microbiomes.** We restricted our assessment to research performed between 2010 and 2020 based on the rationale that studies from 2010 onwards were more likely to capitalize on technological advances (e.g., high-throughput DNA sequencing) that could provide

better measurements of microbiome composition and probiotic persistence coupled with measurements of ecosystem functioning. Microbial compositional measurements enable tracking of probiotic establishment/colonization and testing the impact of probiotics on the diversity and composition of resident microbiomes. After down-selecting an acceptable subset of 229 from a total of 1319 articles (see Methods), we performed two types of quantitative analysis. First, we performed a quantitative summarization of the fraction of articles focused on various aspects of experimental design. Second, we extracted measurement result data to quantify the magnitude of probiotic establishment, post-treatment.

We addressed the following questions:

(1) what factors do studies applying probiotics commonly test;

(2) do probiotics establish in the gut? If so, what is the magnitude of establishment, and what is the typical time frame during which the probiotics persist? and

(3) do probiotics alter resident microbial community diversity and composition? If so, does this alteration depend on the number of different types of probiotics added?

Better understanding of which factors play the largest role in the magnitude and longevity of probiotic effects is a vital step toward improving probiotic applications in human and animal health.

5.3 Methods

To survey probiotic studies related to the establishment of probiotics and their impact on microbiome composition in the gut, we performed a literature search combining results from *SCOPUS* and *Web of Science*. We limited our journal articles search dates to between 2015 and 2020 to our focus on studies more likely to contain microbial taxonomic information from high-throughput DNA sequencing. We used two sets of search strings, the first search string “community composition” and “probiotics” and “gut,” and the second search string “colonization or establishment” and “probiotics” and “gut.” Based on the abstracts, we down-selected primary research articles (reviews, perspectives were rejected) that focused on probiotic treatments and the resident microbial community. Next, we removed studies that focused on the colonization of a naïve/uncolonized gut (e.g., neonatal, gnotobiotic) because the dynamics of probiotic establishment in uncolonized guts are inherently different from dynamics in well-colonized gastrointestinal track. After merging the results from our two searches and removing duplicates across the two searches, 229 articles remained. Study subjects included humans as well as several animal types, with mice, rats, fish, and chickens being the most common animals used. For each of the 229 articles, we extracted information about experimental design that may be relevant to understanding and overcoming probiotic establishment barriers and ultimately increasing probiotic efficacy. Such factors include probiotic dose, administration frequency, administration period, and characteristics (e.g., species type and species number). In addition, we collected information regarding study outcomes to assess if probiotic addition led to functional change, microbial diversity/composition changes, and/or probiotic establishment. For the small number of studies that measured establishment and made comparisons between probiotic addition and control groups (9), we obtained data through the text and tables or used a plot

digitizer (Source Forge) to extract data from graphs. The magnitude of probiotic establishment was compared across studies by calculating the effect size $\frac{(\mu_1 - \mu_2)}{\sigma}$ (the difference between the mean of the sample and control group divided by the standard deviation of the control group).

5.4 Results and Discussion

5.4.1 What is the current focus of gut probiotics studies?

Initially, our goal was to assess factors impacting probiotic establishment and persistence. When reviewing the literature, we categorized the potential factors for manipulation into three major categories: how probiotic delivery occurs, how probiotics interact with other microbes, and how probiotics interact with the environment. Our literature survey of human/animal gut studies revealed a surprising lack of studies that routinely measured probiotic establishment and impacts more than 24 hours after the final probiotic administration; most studies completed taxonomic and functional measurements *during* probiotic administration. Our survey also revealed that most studies focused on the impacts of *presence versus absence* of probiotic additions rather than testing specific factors that might impact the probiotic success (*e.g.*, delivery dose, probiotic type, probiotic complexity) (**Figure 5-1**). Future research would likely benefit from an increased focus on the mechanisms that promote or prevent probiotic success.

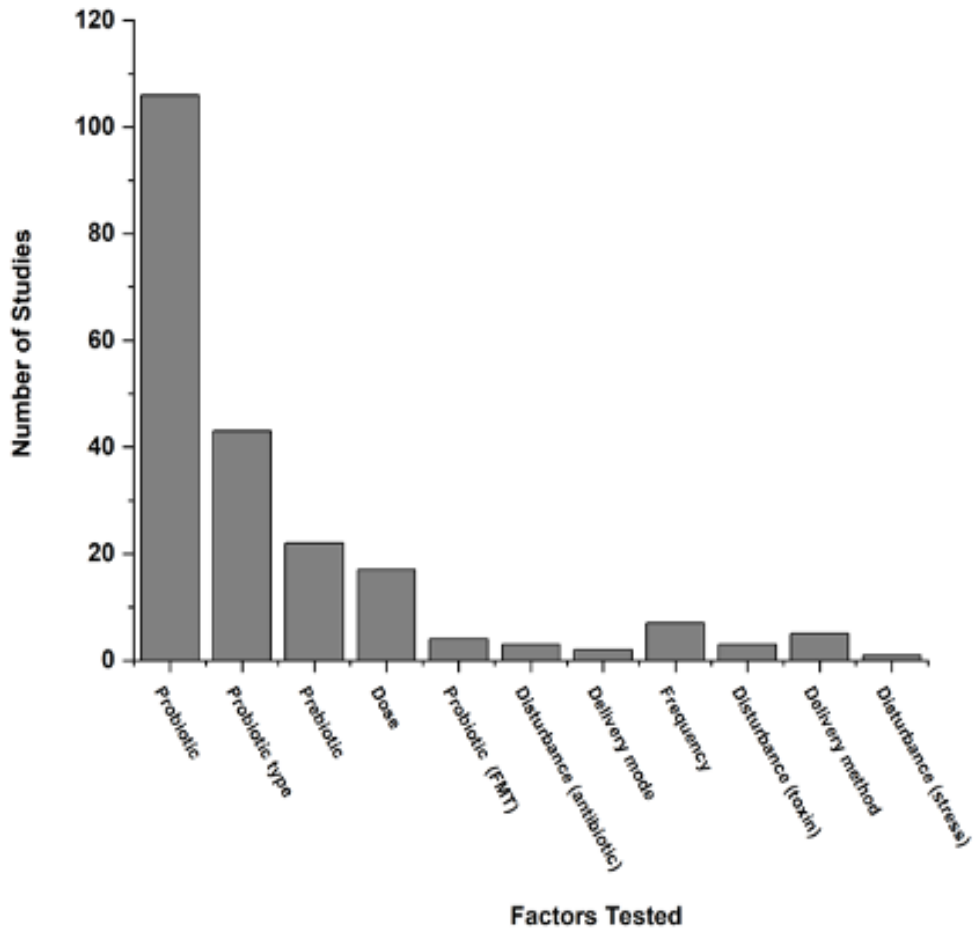
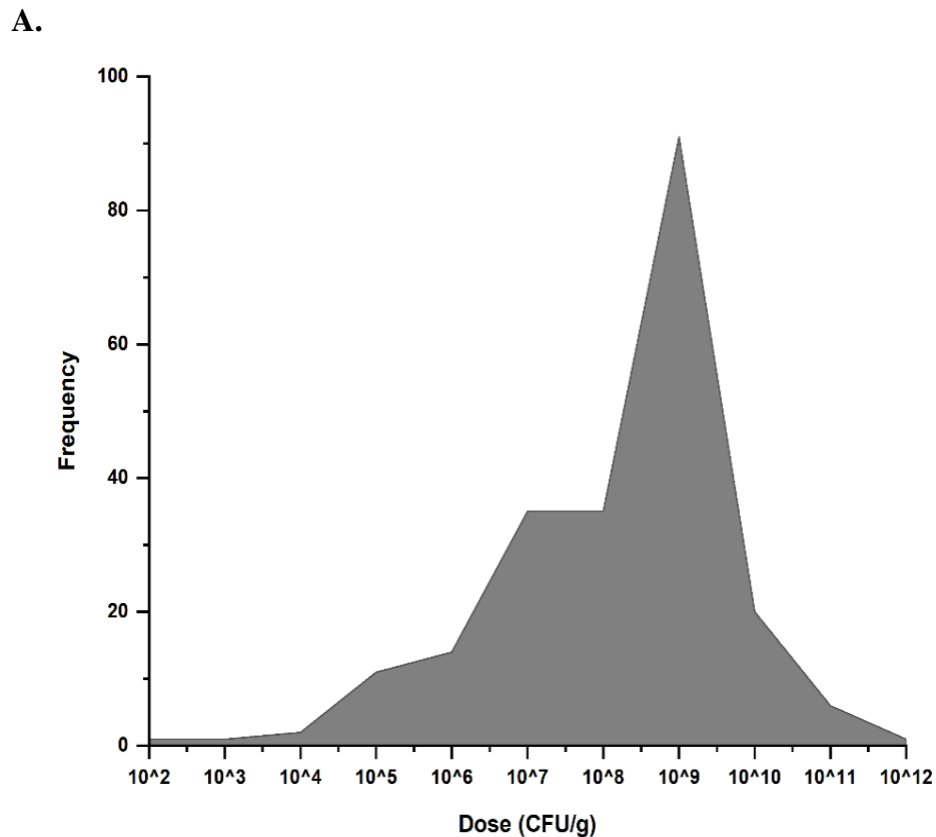
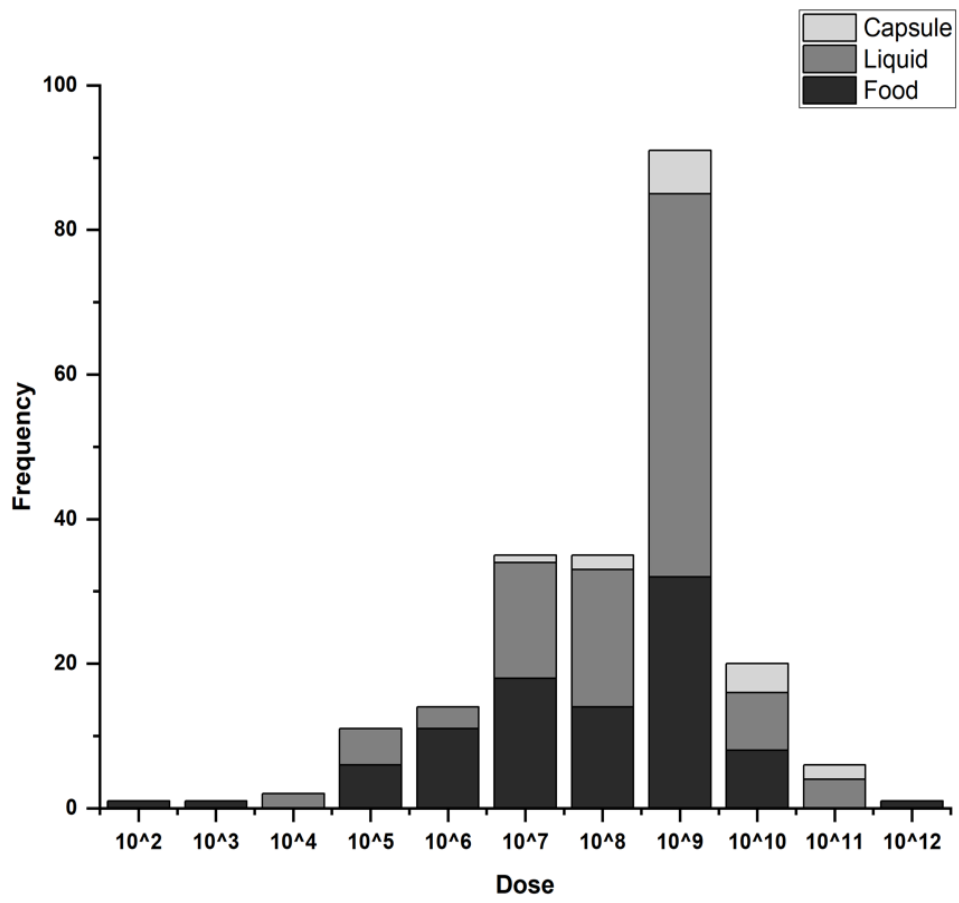


Figure 5-1. The vast majority of studies reviewed (43.7%) focused on comparing treatments with or without a probiotic, rather than factors that impact probiotic success. For studies that did assess other factors, the type and dose of probiotics were commonly explored, as well as the use of prebiotics.

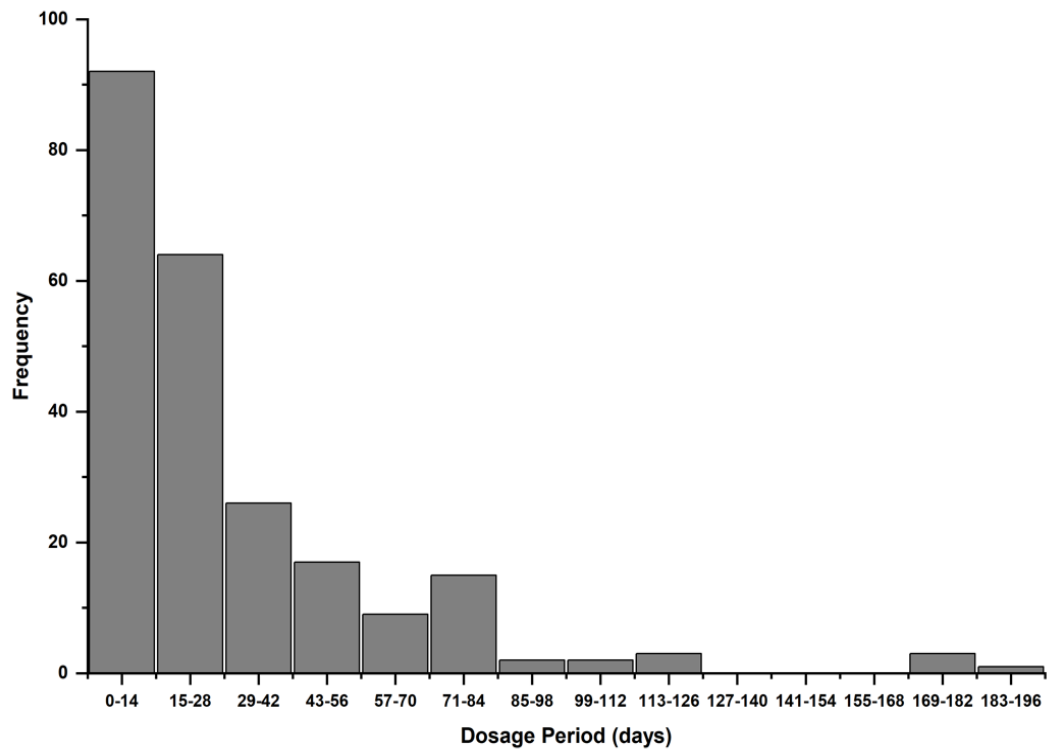
Looking more closely at the data, few studies have tested the impacts on probiotic success in terms of *how* probiotic delivery occurs, for example by manipulating the dose or frequency of probiotic additions (**Figure 5-1**). This is surprising, as propagule pressure is one of the most-tested factors in invasion biology. [192] Studies frequently administer probiotics to animals in capsule, feed, and liquid at concentrations of 10^9 CFU/g (**Figure 5-2a/2b**). Most studies occur over only a few weeks, and administration and measurement frequency are often at least once per day over 14 days. (**Figure 5-2c/2d**); again, suggesting that establishment of taxa and persistent functional effects are perhaps not expected. Microbiome samples are most frequently collected as fecal matter, although direct gut samples are also relatively common in animal studies (**Figure 5-2e**).



B.



C.



D.

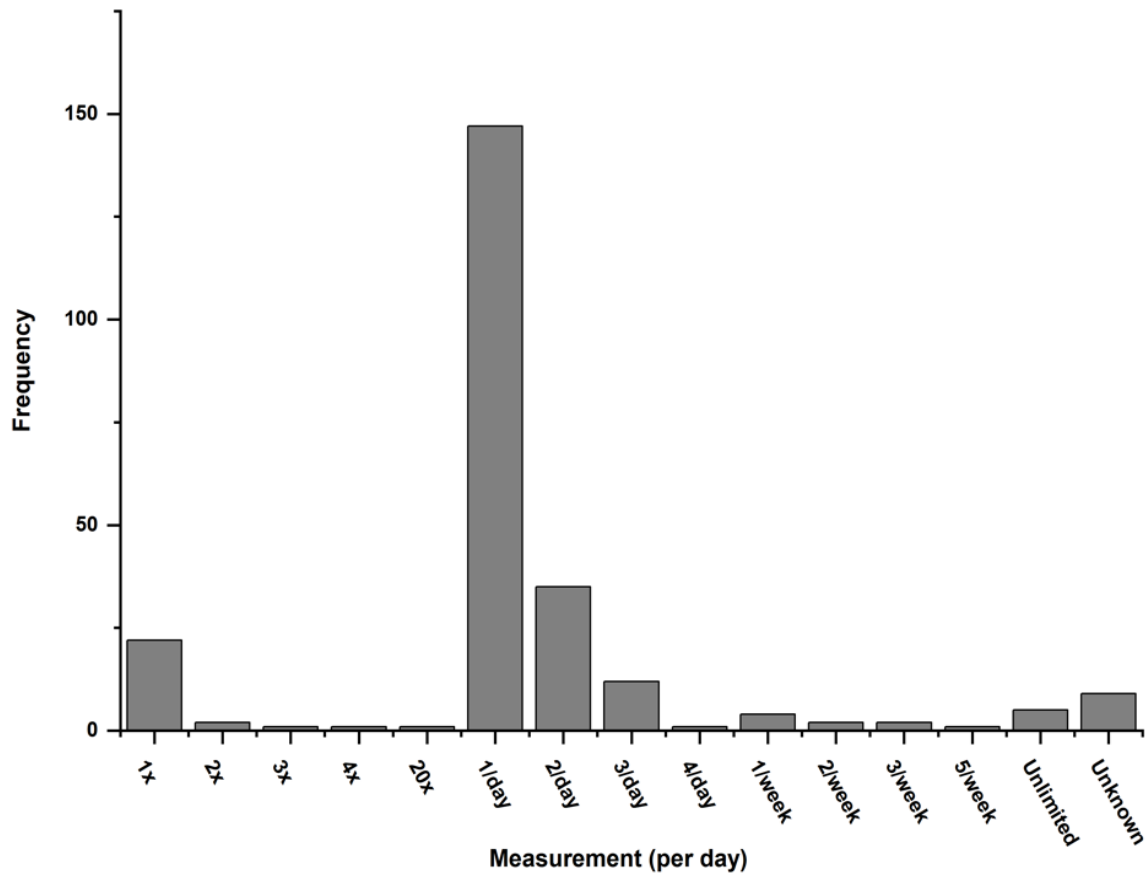


Figure 5-2. (a) Among the studies we reviewed, a dose of 10^9 CFU/g was the most frequently administered dosage, closely followed by 10^7 and 10^8 CFU/g, (b) with the doses predominantly delivered in liquid form, followed by food form, and then capsule form, (c) typically administered over a 14-day period. (d) Most studies then performed measurements daily, (e) sampling from both feces and the gut.

Following studies that focused on measuring a probiotic against a control (no-probiotic), the most common factor tested was different probiotic types (taxa). Overall, most of all probiotics included bacteria rather than fungal taxa (**Figure 5-3a**), probably because the majority of gut microbiome research is focused on the bacterial component. [193]

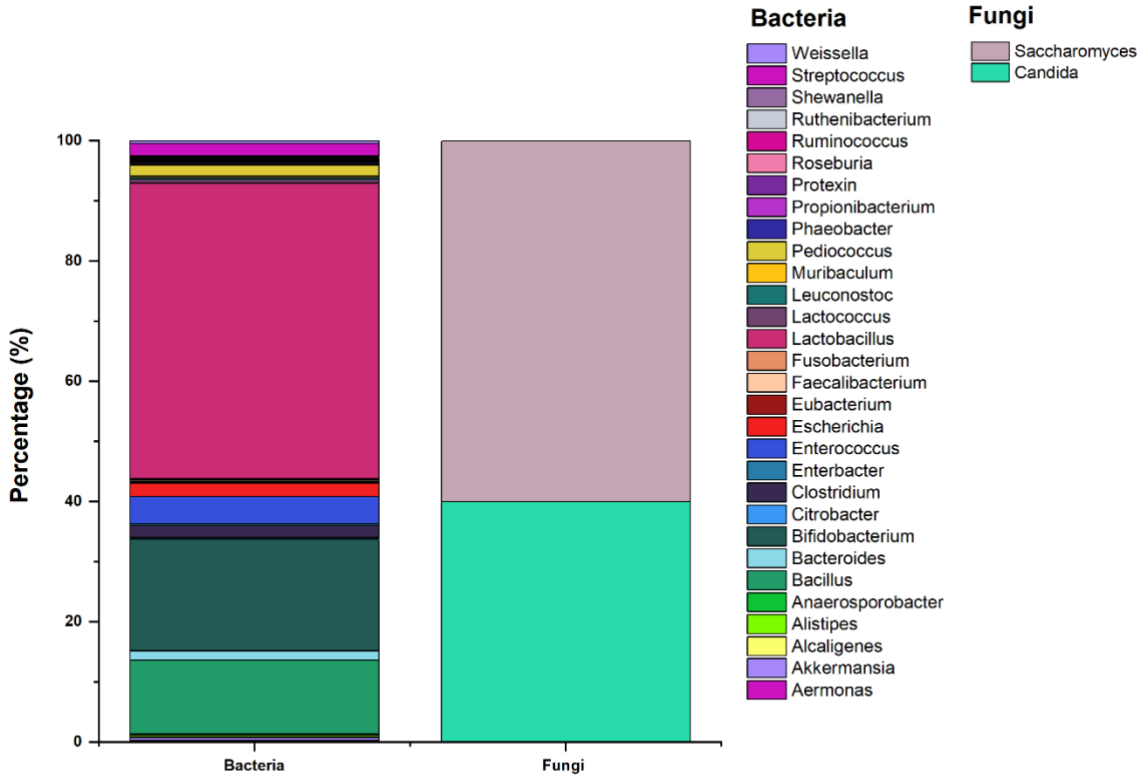


Figure 5-3a. The types of taxa used at the domain used in the probiotic mixture; bacteria were primarily used, rather than fungi.

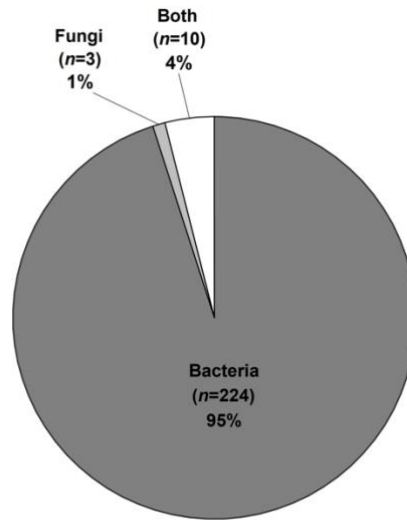


Figure 5-3b. Over 95% of studies included in our analysis included bacteria in the administered probiotics.

However, recent work has suggested that gut fungi may impact host health [194, 195], and thus we expect to see studies on fungal probiotics become more common. The bacterial genera *Lactobacillus*, *Bacillus*, *Bifidobacteria*, and *Enterococcus*, make up the majority (>80%) of probiotics tested. Given a large number of bacterial genera, it is somewhat surprising how few are targeted as probiotics. Furthermore, only a handful of studies have assessed the impacts of probiotic complexity (one taxa versus multiple taxa) on probiotic success (**Figure 5-1**). In most studies, only one or two taxa are introduced as probiotics (**Figure 5-4**). A few settings have shown the benefits of introducing complex microbial communities rather than individual taxa.

[196] Notably, fecal microbiome transplants (complex communities) have been used as probiotics to treat *Chlostridium difficile* infections. [197] Further work is warranted in broader application areas, such as reducing symptoms of lactose intolerance, irritable bowel diseases (IBD), syndrome (IBS), diarrhea, and migraines by regulating the microbiota, stimulating and developing the immune system, synthesizing and enhancing the bioavailability of nutrients, and synthesizing and enhancing the bioavailability of nutrients. [198]

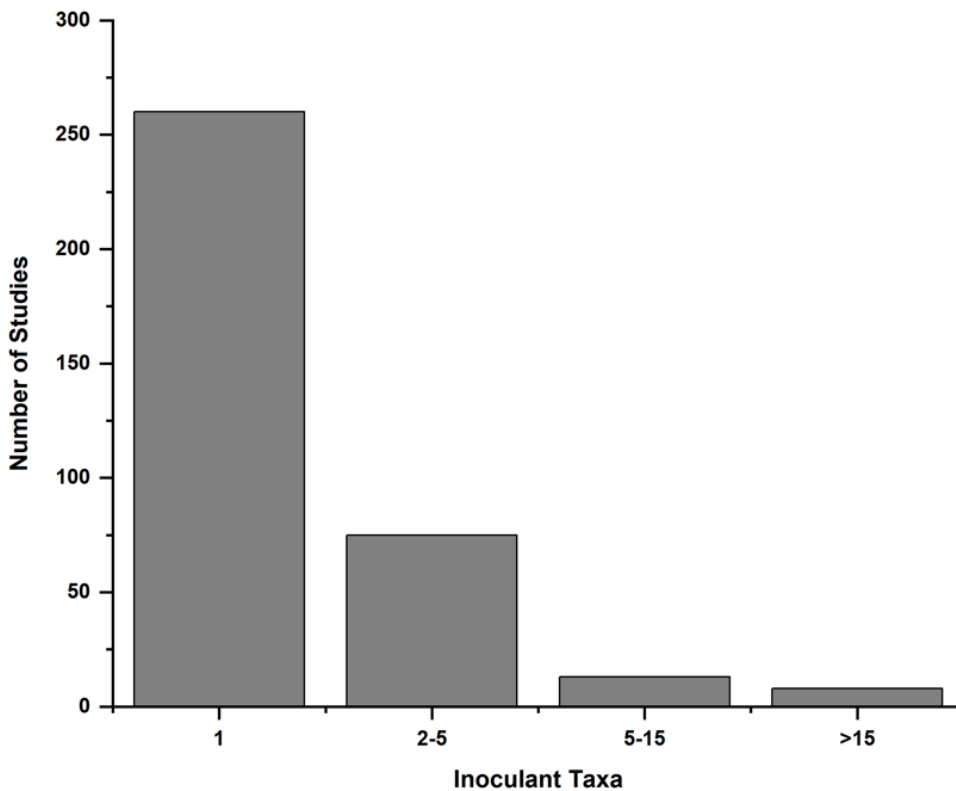


Figure 5-4. Despite a large number of available bacteria genera to be studied, most studies reviewed in our analysis focused on only 1 taxa as the inoculant. This is an interesting gap that could be explored in more detail to enrich the data set available to researchers.

Altering the abiotic environment is another way probiotic establishment/efficacy might be improved. Several studies have assessed the impacts of probiotics alone or in combination with prebiotics. Prebiotics can promote probiotic establishment either by increasing overall resource availability [199] or by adding in a specific resource that can be used by the probiotic in absence of competition from other resident taxa. [200, 201] Prebiotics alone has also been shown to alter the composition of the gut microbiota, but these changes can be difficult to predict in advance. [202] Finally, another subset of studies has assessed the impacts of disturbance before probiotic addition to enhancing establishment, for example physiological or physical stress that could influence active microbes.

5.4.2 Do probiotics impact ecosystem function and community composition of the gut?

The goals for functional outcomes (ecosystem modification) in the gut probiotic studies we surveyed included pathogen repression, disease suppression, weight control, and growth improvement, among several others (**Figure 5a**). In our survey of gut probiotic studies (**Figure 5b**), we found that, while functional outcomes were not assessed in 15% of studies, of the studies that did assess functional outcomes, most studies reported a change in function following probiotic administration (82%), while only 7% reported no difference in function. As mentioned above the caveat to this is that these studies measure function during probiotic administration and thus the persistence of the function is not guaranteed and in fact perhaps unlikely should probiotic administration cease. Furthermore, there is a known bias towards publishing positive study results which may skew this data. [203] However, in the studies that assessed changes in composition, the majority 55% reported changes in composition following probiotic additions,

while 11% saw no changes in composition. In contrast to community composition (beta-diversity), richness (alpha-diversity) was not as impacted by the probiotic addition, where 21% of studies reported changes in microbial richness following probiotic addition, while 29% reported no changes.

While far fewer studies measured probiotic presence, probiotic presence was positive and negative in approximately an equal number of studies, 16.5% and 14.4%, respectively (**Figure 5-5c**). Overall, the number of studies that reported changes in the microbial composition is striking since while often only a few taxa (**Figure 5-4**) are added to highly complex microbial communities, at least in the short term this often-had cascading effects on the microbial community. This suggests that probiotics are altering community assembly and successional patterns. Future studies assessing the persistence of these changes in composition would give further insight into the potential long-lasting impacts of probiotics on the gut microbiome.

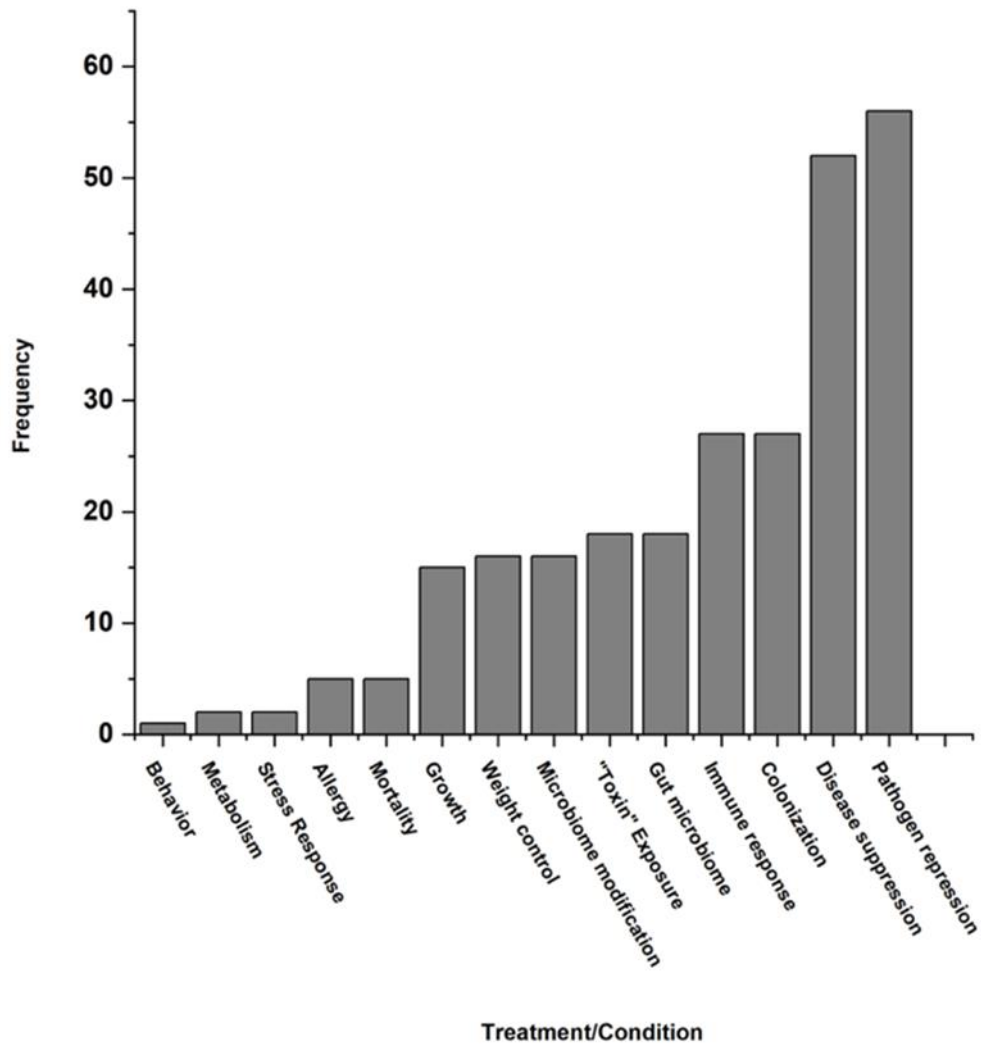


Figure 5-5a. The functional outcomes of treatments and conditions were evaluated for each study. Disease suppression and pathogen regression were the top functional outcomes observed.

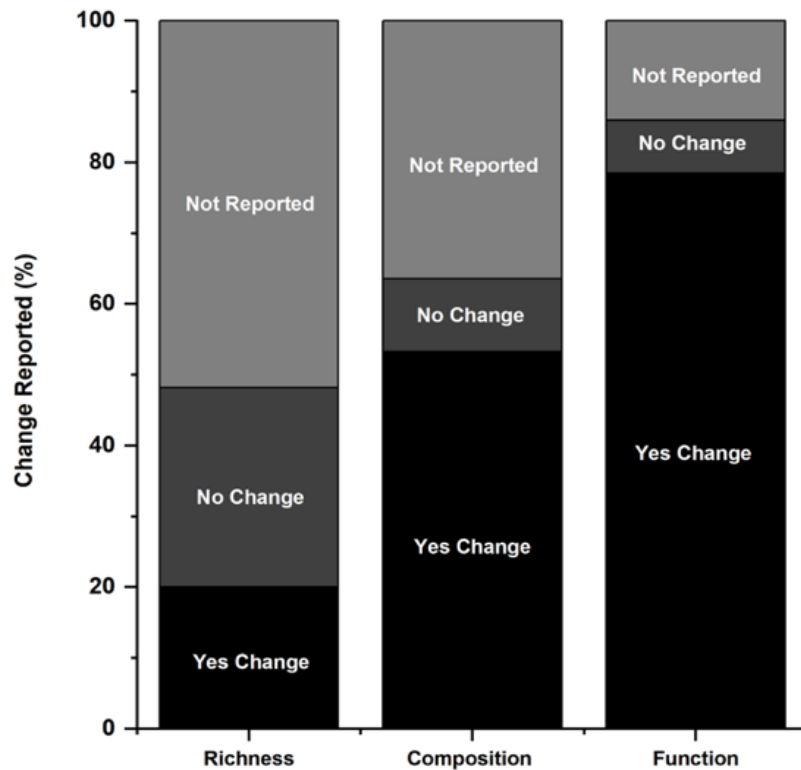


Figure 5-5b. While most studies focused on the presence/absence of probiotics, almost 85% also evaluated changes in function after the administration of probiotics. Less common was the measurement of the composition, richness, and diversity after administration. Of these factors, it is interesting that probiotic administration yielded changes in composition and function in most of the studies that evaluated these factors.

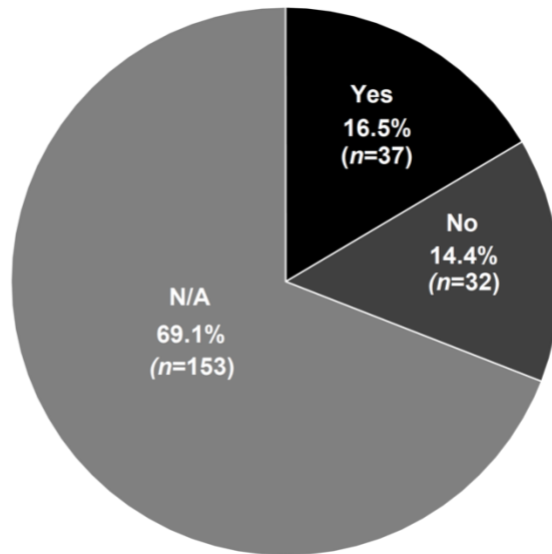


Figure 5-5c. Of the studies that we analyzed, 16.5% of studies showed establishment, 14.4% of studies did not show establishment, and 69.1% of studies did not report establishment.

Overall, few studies contained *quantitative* assessments of changes in inoculum establishment (**Figure 5-6a**). Only 35 studies out of the 229 studies we analyzed measured establishment, which here we define as the presence or absence of the probiotic in a sample greater than 24 hours after administration of the probiotic. Out of those 35 studies, only 9 had extractable data (quantitative raw data that could be extracted from studies for comparison using statistical analysis). For the 9 studies with extractable data, we calculated the magnitude of increase in the bacterial taxa in the probiotic addition treatment compared to the controls as effect size (**Figure 5-6b**). Across the studies, this included different species used, and the magnitude of increase was 1.44-fold, thus while the establishment was successful, and the probiotic taxa increased in abundance in the probiotic treatments the increase was marginal. Due to the lack of data available, this suggests that research needs to be done to improve probiotic establishment. Two

potential solutions that have been previously explored are to improve establishment by increasing adhesion potential of bacterial inoculants [204] and to use physical protection of inoculants by coating with biofilms to shield from harsh environmental conditions. [205, 206]

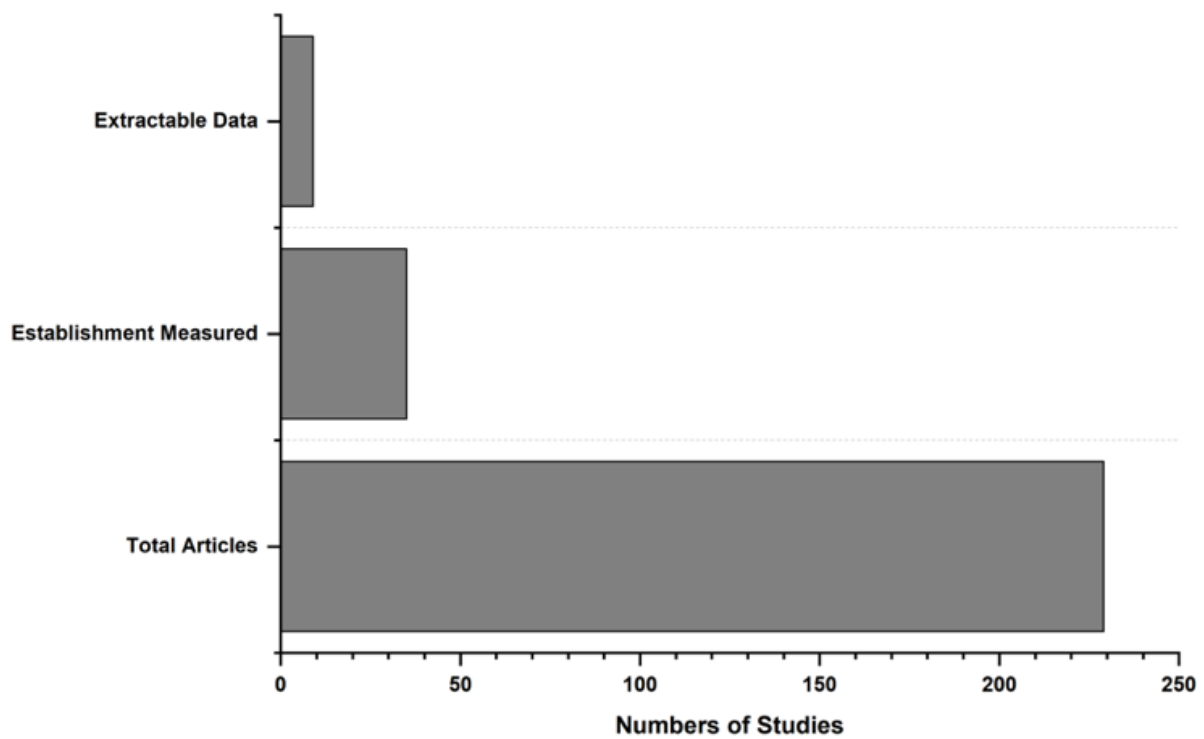


Figure 5-6a. The total number of studies vs. the studies that measure establishment and the number of studies; that had quantitative raw data that could be extracted from studies for comparison using statistical analysis.

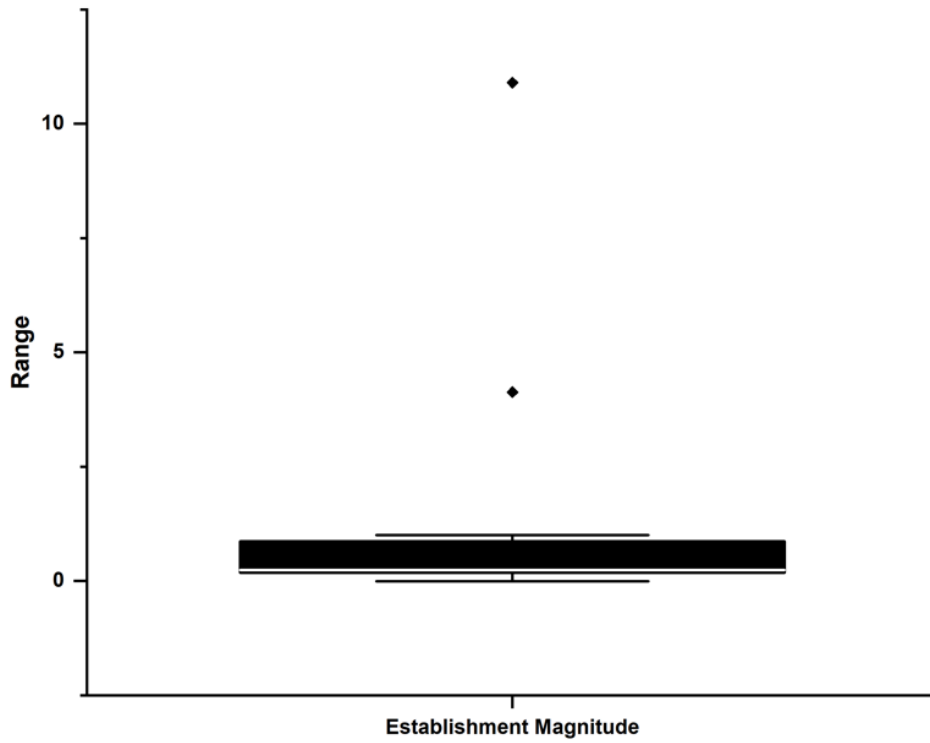


Figure 5-6b. The establishment magnitude of the data extracted to perform statistical analysis on the species used in the probiotic ($n=13$).

5.5 Conclusions

In conclusion, this meta-analysis demonstrates the factors that were assessed to determine which aspects contribute to the establishment's success in current studies. The ability to investigate the composition of complex microbial communities using advanced DNA sequencing technology has enabled researchers to get a more precise and quick taxonomic identification of individuals within those communities. However, perhaps due to this recent development of technology, there has been a lack of consistency of studies being performed to measure the microbial communities in the gut microbiome before and after the administration of probiotics. There was a lack of quantitative data to show the effectiveness of probiotics over extended time periods and a lack of studies demonstrating that probiotic establishment occurs.

5.6 References

176. Berg, G., et al., *Microbiome definition re-visited: old concepts and new challenges*. *Microbiome*, 2020. **8**(1): p. 103.
177. Bonfante, P. and A. Genre, *Mechanisms underlying beneficial plant–fungus interactions in mycorrhizal symbiosis*. *Nature Communications*, 2010. **1**(1): p. 48.
178. Clapp, M., et al., *Gut microbiota's effect on mental health: The gut-brain axis*. *Clinics and practice*, 2017. **7**(4): p. 987-987.
179. Zommiti, M., M.G.J. Feuilleley, and N. Connil, *Update of Probiotics in Human World: A Nonstop Source of Benefactions till the End of Time*. *Microorganisms*, 2020. **8**(12): p. 1907.
180. Fenster, K., et al., *The Production and Delivery of Probiotics: A Review of a Practical Approach*. *Microorganisms*, 2019. **7**(3): p. 83.

181. Verschuere, L., et al., *Probiotic bacteria as biological control agents in aquaculture*. Microbiology and molecular biology reviews : MMBR, 2000. **64**(4): p. 655-671.
182. Perković, L., et al., *Biotechnological Enhancement of Probiotics through Co-Cultivation with Algae: Future or a Trend?* Marine Drugs, 2022. **20**(2): p. 142.
183. Jiménez-Gómez, A., et al., *Plant probiotic bacteria enhance the quality of fruit and horticultural crops*. AIMS microbiology, 2017. **3**(3): p. 483-501.
184. de Souza Vandenberghe, L.P., et al., *Potential applications of plant probiotic microorganisms in agriculture and forestry*. AIMS microbiology, 2017. **3**(3): p. 629-648.
185. Tembhre M.K., C.M.K., Berthiaume F., Kumar S., *Relationship Between Probiotics and Gut-Skin Axis in Skin Wound Healing: A Recent Update*. Probiotic Research in Therapeutics, 2022.
186. Ochoa-Hueso, R., *Global Change and the Soil Microbiome: A Human-Health Perspective*. Frontiers in Ecology and Evolution, 2017. **5**.
187. Frey-Klett, P., et al., *Bacterial-fungal interactions: hyphens between agricultural, clinical, environmental, and food microbiologists*. Microbiol Mol Biol Rev, 2011. **75**(4): p. 583-609.
188. Shabat, S.K., et al., *Specific microbiome-dependent mechanisms underlie the energy harvest efficiency of ruminants*. Isme j, 2016. **10**(12): p. 2958-2972.
189. Natalia, S. and K. Olga, *Use of Probiotic Preparations in Waste Waters Cleaning of Agricultural Enterprises*. KnE Life Sciences, 2019. **4**(14).
190. Albright, M.B.N., et al., *Soil Bacterial and Fungal Richness Forecast Patterns of Early Pine Litter Decomposition*. Frontiers in Microbiology, 2020. **11**.

191. Albright, M.B.N., et al., *Solutions in microbiome engineering: prioritizing barriers to organism establishment*. The ISME Journal, 2022. **16**(2): p. 331-338.
192. Vedder, D., L. Leidinger, and J. Sarmiento Cabral, *Propagule pressure and an invasion syndrome determine invasion success in a plant community model*. Ecology and evolution, 2021. **11**(23): p. 17106-17116.
193. Marchesi, J.R., et al., *The gut microbiota and host health: a new clinical frontier*. Gut, 2016. **65**(2): p. 330.
194. Forbes, J.D., et al., *A Fungal World: Could the Gut Mycobiome Be Involved in Neurological Disease?* Frontiers in Microbiology, 2019. **9**(3249).
195. Pérez, J.C., *Fungi of the human gut microbiota: Roles and significance*. International Journal of Medical Microbiology, 2021. **311**(3): p. 151490.
196. Arnold, J.W., J. Roach, and M.A. Azcarate-Peril, *Emerging Technologies for Gut Microbiome Research*. Trends in microbiology, 2016. **24**(11): p. 887-901.
197. Khoruts, A., *Targeting the microbiome: from probiotics to fecal microbiota transplantation*. Genome medicine, 2018. **10**(1): p. 80-80.
198. Nagpal, R., et al., *Probiotics, their health benefits and applications for developing healthier foods: a review*. FEMS Microbiology Letters, 2012. **334**(1): p. 1-15.
199. Sriswasdi, S., C.-c. Yang, and W. Iwasaki, *Generalist species drive microbial dispersion and evolution*. Nature Communications, 2017. **8**(1): p. 1162.
200. Shepherd, E.S., et al., *An exclusive metabolic niche enables strain engraftment in the gut microbiota*. Nature, 2018. **557**(7705): p. 434-438.

201. Umu, Ö.C.O., K. Rudi, and D.B. Diep, *Modulation of the gut microbiota by prebiotic fibres and bacteriocins*. *Microbial ecology in health and disease*, 2017. **28**(1): p. 1348886-1348886.
202. Markowiak, P. and K. Ślizewska, *Effects of Probiotics, Prebiotics, and Synbiotics on Human Health*. *Nutrients*, 2017. **9**(9): p. 1021.
203. Mlinarić, A., M. Horvat, and V. Šupak Smolčić, *Dealing with the positive publication bias: Why you should really publish your negative results*. *Biochemia medica*, 2017. **27**(3): p. 030201-030201.
204. Zhao, L., et al., *Recent advances of mesoporous materials in sample preparation*. *Journal of Chromatography A*, 2012. **1228**: p. 193-204.
205. Wang, X., et al., *Bioinspired oral delivery of gut microbiota by self-coating with biofilms*. *Science advances*, 2020. **6**(26): p. eabb1952-eabb1952.
206. Yin, W., et al., *Biofilms: The Microbial "Protective Clothing" in Extreme Environments*. *International journal of molecular sciences*, 2019. **20**(14): p. 3423.

Chapter – 6: Summary and Conclusion

6.1 Summary and Conclusion

In this research, we explored alternative approaches to drug-based infection control. First, we discussed the need of innovation and other approaches to control and reduce infections due to antibiotic resistance. To approach this, in **Chapter 2**, we first wanted to understand the reported interactions of microbial communities in the human body and how they interact within their pre-existing communities. Then, we studied, compared, and evaluated various techniques for a materials-based approach using zeolites, and specifically, pure-silica zeolite **MFI**.

With the increased use of probiotics to help treat different medical conditions, the market has transformed into a multi-billion-dollar industry, but unfortunately, there are no standard regulations for probiotics. This is due to the lack of understanding on how probiotics are exactly beneficial and what factors are associated with that success. The meta-analysis described in **Chapter 5** can help demonstrate which factors contribute to the success of probiotics establishing in the gut microbiome. Due to the recent development of technology allowing researchers to investigate the composition of complex microbial communities using advanced DNA sequencing technology, researchers can provide a more conclusive analysis of how the individual species in the gut microbiome. This should be a primary focus of researchers in this area, as well as one of the possible bases for future regulation.

The downside to this approach is the current lack of quantitative data that can measure or determine the success of probiotics establishment. In **Chapter 3 and 4**, we wanted to explore the use of silicate-1 (**MFI**) film biocompatibility, since their antimicrobial properties have frequently

been explored. Lysozyme sorption of pure – silica **MFI** films were evaluated in **Chapter 4**. It was found that silicalite-1 (**MFI**) films were capable of lysozyme sorption, using the ELISA and BCA assays. It was shown that sorption was dependent on the incubation volume of lysozyme solution, as well as time and concentration of lysozyme. The higher the incubation volume, which was 800 μ L in our case, the absorbance increased on the surface and lysozyme was able to penetrate through the porous network of the **MFI** films. The *b* – orientation was shown to have a higher concentration of lysozyme sorption. These results showed preliminary evidence of biocompatibility of **MFI** zeolites, leading to further exploration of its biocompatibility in **Chapter 4**.

Following the initial experiments, we wanted to explore solely *b* – oriented pure-silica zeolite **MFI** films. Due to a high lysozyme sorption, we determined that this could have been achieved due to the exposure of the pores. This opened the opportunity to explore the growth of *b* – oriented crystals on the silica substrate by changing the angle (1.5 cm x 2.0 cm and 2.5 cm x 0.5 cm) in which the substrate is tilted in the Teflon liner. Furthermore, we want to see if varying the synthesis conditions of aging (1 h and 6 h) and crystallization time (3 h and 12 h) would impact the crystalline growth. Through the *in vitro* analysis of ELISA, we were able to demonstrate that lysozyme sorption was higher in samples that were aged for 1 hour and crystallized at 6 hours, with an angle of 1.5 cm x 0.5 cm. This could have been due to short crystallization time, exposing more pores and less crystalline growth.

Using these data to inform next steps, we decided to introduce L929 murine fibroblast cells to *b* – oriented **MFI** films and explore the metabolic activity and cell viability of L9292 murine cells.

An *in vitro* analysis of WST-1 data showed that on day 3 and 7, L929 murine cells and metabolic activity and cell proliferation. This further confirmed the compatibility of **MFI** films and provided preliminary evidence that these films could be used for device coatings to hopefully reduce infection for implantable devices.

6.2 Future Direction

Based on our data in **Part I**, it is clear that pure-silica zeolite **MFI** films could have potential as a coating for implantable medical devices to help reduce the infection, but there are still more studies to be done.

(1) Surface characterization analysis to understand the behavior of **MFI** films and how it interacts with biological species can be performed. Contact angle measure can be used to study the wettability of **MFI** films. Optical profilometry can be used to look at surface topography or roughness.

(2) More *in vitro* cell studies can be done to measure inflammatory response using reactive oxygen species (ROS) assays. This would determine how zeolite films would possibly contribute to the body's natural healing process.

(3) Cell migration and invasion assays could be examined using to standardized, high-throughput approach for measuring the degree to which invasive cells pass a basement membrane barrier in response to chemoattractant and/or inhibitory chemicals.

(4) Bacteria viability assay and measuring biofilm production, to understand how antimicrobial **MFI** zeolites are? Ultimately, we would want to see that **MFI** films can reduce the formation of biofilms but also can reduce adhesive pathogenic bacteria to its surface. Understanding the in-depth antimicrobial activity of **MFI** films can help us understand their appropriate use.

(5) Growing **MFI** zeolites onto flexible medical devices such as catheters or tracheostomy tubes to better understand the performance of zeolites.

Based on our data in **Part II**, probiotics do establish in the pre-existing gut microbiome, but there are still more studies to be done:

(1) Establishing a standard for researchers give more precise and quick taxonomic identification of individual bacterial species within those microbial communities.

(2) Extending studies to one week or longer after the administration of probiotics to determine the effectiveness of establishment.

(3) Identify the best protocol to study probiotic effectiveness based on disease or disorder to better help treat patients.

Due to the complications of treating post – operative infections and it being common, it is important to explore an effective multi-prolonged approach to combat this challenge. By

controlling bacteria adhesion and mitigating the formation of biofilms on the surface of the indwelling device, it may be possible to increase the effectiveness of implant infection control.

